

Copyright

by

Feng Wang

2014

**The Dissertation Committee for Feng Wang Certifies that this is the approved
version of the following dissertation:**

**A Co-translational Ubiquitination Pathway for Quality Control of
Newly Synthesized Proteins**

Committee:

Jon Huibregtse, Supervisor

Jaquelin Dudley

Arlen Johnson

Tanya Paull

Rick Russell

**A Co-translational Ubiquitination Pathway for Quality Control of
Newly Synthesized Proteins**

by

Feng Wang, B.S.; M.S.

Dissertation

Presented to the Faculty of the Graduate School of
The University of Texas at Austin
in Partial Fulfillment
of the Requirements
for the Degree of

Doctor of Philosophy

The University of Texas at Austin

August, 2014

Dedication

To my family (Fuqiang, Jinyu and Gang) and Jingjie for their love and support.

Acknowledgements

I would like to express my deepest gratitude to Dr. Jon Huibregtse, for his encouragement, guidance, patience, and enthusiasm for science. I could not ask for a better mentor. I am also grateful to the members of my committee, Drs. Jaquelin Dudley, Arlen Johnson, Tanya Paull, and Rick Russell, for their constructive criticism, great suggestions, and helpful advice. I also would like to thank all the past and present members of the Huibregtse lab: Dr. Larissa Canadeo, Dr. Hazel O'Connor, Nancy Lyon, Nicholas Maskalenko, Caleb Swaim, Dr. Hyung Cheol Kim, Aaron Charlson, Amanda Vaughn and Kyungwoon Seo, for their friendship and support throughout the years. Finally, I would like to thank my family, Jingjie, and my friends, for their love and support during graduate school.

A Co-translational Ubiquitination Pathway for Quality Control of Newly Synthesized Proteins

Feng Wang, Ph.D.

The University of Texas at Austin, 2014

Supervisor: Jon M. Huibregtse

Previous studies indicated that 6%-30% of newly synthesized proteins are rapidly degraded by the ubiquitin-proteasome system. This has generally been assumed to occur post-translationally, following failure of chaperone-assisted folding mechanisms. However, the extent and significance of co-translational quality control remains largely unknown. In investigations of ISG15, an interferon-induced ubiquitin-like protein, our lab found that ISG15 is conjugated to a very broad spectrum of newly synthesized proteins. The major ligase for ISG15, Herc5, co-fractionated with polysomes, and further studies indicated that the processes of translation and ISGylation were closely coupled. Here, I employ an *in vitro* run-off translation system and puromycin labeling experiments to demonstrate that nascent polypeptides are ISGylated within active translation complexes, providing direct support for the co-translational mechanism for ISG15 conjugation.

Approaches developed for studying co-translational ISGylation were subsequently used to examine co-translational ubiquitination (CTU), which we hypothesized might be

important in quality control of newly synthesized proteins. Consistent with this, I found that the pathway for degradation of newly synthesized proteins was initiated while proteins were being translated, with ubiquitination of actively translating nascent polypeptides. CTU is a conserved and robust pathway from yeast to mammals, with 5-6% of total nascent polypeptides being ubiquitinated in *S. cerevisiae*, and 12-15% in human cells. CTU products contained primarily K48-linked polyubiquitin chains, consistent with a proteasomal targeting function. Although nascent chains previously have been shown to be ubiquitinated within stalled and defective translation complexes (referred to here as CTU^S), nascent chain ubiquitination also occurred within active translation complexes (CTU^A). CTU^A accounted for approximately two-thirds of total CTU (CTU^T) in human cells and approximately half of CTU^T in yeast cells. CTU^A was increased in response to agents that induce protein misfolding, whereas CTU^S was increased in response to agents that led to translational misreading or stalling. These results indicate that ubiquitination of nascent chains occurs in two contexts and define CTU^A as a component of a quality control system that marks proteins for destruction before their synthesis is complete.

Finally, decreased translation fidelity is thought to lead to the accumulation of misfolded proteins and hasten the aging process. As CTU is a pathway for quality control of newly synthesized proteins, I explored whether CTU plays a protective role during the replicative aging process in budding yeast. Consistent with previous reports using human cells, I found that newly synthesized proteins are a major source of proteasome substrates under non-stressed conditions. Transient proteasome inhibition (using MG132) led to a decrease of yeast replicative life span (RLS), whereas simultaneous treatment with

cycloheximide, a translation inhibitor, suppressed this effect. Deletion of Ltn1, the major E3 ligase of the CTU^S pathway, also shortened the RLS of yeast. Together, these results provide a preliminary set of evidence supporting the hypothesis that the quality of newly synthesized proteins is an important determinant of aging.

Table of Contents

List of Tables	xii
List of Figures	xiii
Chapter 1: Introduction	1
1.1 A brief overview of the ubiquitin-proteasome system (UPS).....	1
1.1.1 Ubiquitin.....	2
1.1.2 Ubiquitin activating enzymes (E1s).....	6
1.1.3 Ubiquitin conjugating enzymes (E2s).....	7
1.1.4 Ubiquitin ligases (E3s).....	8
1.1.5 Deubiquitinating enzymes (DUBs).....	12
1.1.6 The proteasome.....	13
1.2 ISG15: An anti-viral ubiquitin-like protein	14
1.2.1 Ubiquitin-like proteins	14
1.2.2 ISG15 and its pathway enzymes.....	17
1.2.3 Anti-viral function of ISG15	18
1.2.4 ISG15 targets a broad range of newly synthesized proteins	21
1.3 Cellular proteostasis and its linkage with aging.....	23
1.3.1 Challenges of protein folding in vivo	24
1.3.2 Strategies to facilitate protein folding in vivo	25
1.3.3 Strategies for clearance of misfolded proteins	28
1.3.4 Classic model for quality control of newly synthesized proteins	32
1.3.5 Aging is linked to a gradual loss of cellular proteostasis.....	34
1.4 Goals of my doctoral work	41
Chapter 2: ISG15 is co-translationally conjugated to ribosome-associated nascent polypeptides	43
2.1 Introduction.....	43
2.2 Materials and methods.....	45
2.3 Results.....	49

2.3.1 Establishment of in vitro run-off translation and biotin-puromycin conjugation reactions	49
2.3.2 Polysome-associated nascent chains are ISGylated.....	54
2.3.3 ISGylation of nascent polypeptides of individual target proteins	60
2.4 Discussion	62
Chapter 3: A co-translational ubiquitination pathway for quality control of newly synthesized proteins	64
3.1 Introduction.....	64
3.2 Materials and methods.....	67
3.3 Results.....	72
3.3.1 CTU is a robust process in mammalian cells	72
3.3.2 CTU predominantly occurs on cytosolic rather than ER-associated polysomes.....	77
3.3.3 CTU targets are polyubiquitinated with K48 and K11 chains	79
3.3.4 CTU occurs within both stalled and active translation complexes.....	85
3.3.5 CTU is enhanced under conditions that promote protein misfolding or translational errors	90
3.4 Discussion	95
Chapter 4: Potential role of CTU in against aging	104
4.1 Introduction.....	104
4.2 Materials and methods.....	107
4.3 Results.....	109
4.3.1 Reduction of global protein translation leads to decreased CTU	109
4.3.2 Newly synthesized proteins are a major source of proteasome substrates	113
4.3.3 Transient proteasome inhibition decrease replicative life span (RLS), and this is suppressed by inhibition of translation	115
4.3.4 CTU is increased in aged yeast.....	117
4.3.5 Deletion of Ltn1, the major E3 ligase for CTUS, decreases RLS	119
4.4 Discussion	121

Chapter 5: Conclusion and future directions	124
5.1 Characterization of the CTU pathway	124
5.2 Protein translation and CTU in longevity and aging	129
References	132
Vita	153

List of Tables

Table 3.1:	Plasmids and antibodies used in chapter 3	70
Table 3.2:	siRNAs used in chapter 3	71
Table 3.3:	Identified CTU targets 3.....	100

List of Figures

Figure 1.1: The ubiquitin-proteasome system (UPS)	5
Figure 1.2: The structures of ubiquitin-like proteins resemble the structure of ubiquitin.....	16
Figure 1.3: Co-translational model for ISG15 conjugation.....	23
Figure 1.4: Three major strategies to clear misfolded proteins	29
Figure 1.5: Classic post-translational model for quality control of newly synthesized proteins	33
Figure 1.6: The hallmarks of aging.....	35
Figure 1.7: Loss of proteostasis is a hallmark of aging	37
Figure 2.1: <i>In vitro</i> run-off translation reactions	51
Figure 2.2: Validation of in vitro biotin-puromycin (Bio-Puro) conjugation reaction	53
Figure 2.3: Polysome-associated nascent chains are ISGylated.....	55
Figure 2.4: ISGylation does not occur in the run-off reaction	57
Figure 2.5: Incorporation of biotin-conjugated puromycin (Bio-Puro) into ISG15-containing nascent chains	59
Figure 2.6: ISGylation of nascent polypeptides of individual target proteins....	61
Figure 3.1: Co-translational ubiquitination (CTU) in human cells.....	73
Figure 3.2: Polysome-associated nascent polypeptides are conjugated to endogenous ubiquitin in human and yeast cells.....	74
Figure 3.3: Quantitation of CTU in different cell types.....	76
Figure 3.4: CTU occurs predominantly on cytosolic rather than ER-associated polysomes	78

Figure 3.5: CTU products contain primarily K48-linked polyubiquitin chains .	81
Figure 3.6: Identification of CTU target proteins.....	82
Figure 3.7: CTU products were subject to proteasomal degradation	84
Figure 3.8: CTU occurs within active translation complexes	86
Figure 3.9: CTU ^A accounts for the majority of the total ubiquitination activity against nascent chains	89
Figure 3.10: CTU was enhanced under conditions that promoted translational errors or protein misfolding.....	92
Figure 3.11: Cycloheximide triggers stalling and accumulation of ubiquitinated nascent chains	93
Figure 3.12: Depletion of NAC activity enhances CTU ^T	94
Figure 3.13: Role of specific E3 ligases in CTU ^T	98
Figure 4.1: Rapamycin and Torin1 treatments led to a decrease of global protein translation as well as CTU level in 293T cells	110
Figure 4.2: Yeast mutants with reduced protein synthesis rate show lower level of CTU.....	112
Figure 4.3: Newly synthesized proteins are the major source of proteasome substrates	114
Figure 4.4: MG132 treatment led to a decrease of yeast RLS whereas co-treatment with CHX can restore it.....	116
Figure 4.5: The CTU level is increased in old cells.....	118
Figure 4.6: Deletion of Ltn1 gene led to a decrease of RLS of yeast.....	120

Chapter 1: Introduction

1.1 A BRIEF OVERVIEW OF THE UBIQUITIN-PROTEASOME SYSTEM (UPS)

When the lysosome was discovered in the 1950s, it was assumed to be the site of all cellular protein degradation. However, between the mid-1950s and the late 1970s, accumulating lines of evidence suggested that the degradation of at least certain classes of cellular proteins must be lysosome-independent. Firstly, half-lives vary between proteins, from minutes to days. The relatively non-selective lysosomal degradation cannot explain the selective degradation of proteins with different half-lives (Goldberg & St John 1976). Secondly, inhibition of lysosomal function with its inhibitors showed distinct effects on degradation of different proteins: the degradation of endocytosed proteins was largely inhibited, whereas only a limited effect was observed on the degradation of intracellular proteins (Knowles & Ballard 1976; Poole *et al.* 1977; Neff *et al.* 1979). All these findings suggested the existence of non-lysosomal protein degradation pathway(s).

In 1975, Goldstein and colleagues reported that an 8.5 kD protein (now known as ubiquitin) found in cow thymus induced the differentiation of T lymphocytes and B lymphocytes (Goldstein *et al.* 1975). Furthermore, they found this protein was not only in the thymus, but also in all other tissues, as well as in all tested eukaryotes, including yeast, plants, and animal cells (Goldstein *et al.* 1975). In 1977, Ira Goldknopf and Harris Busch reported that histone H2A was a branched protein, with two amino termini and one carboxy terminus (Goldknopf & Busch 1977). In the same year, Lois Hunt and Margaret

Dayhoff revealed that one of the N-termini of H2A was identical to the N-terminus of ubiquitin, suggesting that ubiquitin could be conjugated to other proteins (Hunt & Dayhoff, 1977). Also in 1977, Etlinger and Goldberg developed a cell-free, non-lysosomal, and ATP-dependent protein degradation system using rabbit reticulocytes (Etlinger & Goldberg 1977). Using this cell-free proteolytic system, Hershko, Ciechanover, and colleagues published a series of elegant papers describing a three-step ubiquitin conjugation cascade, which is catalyzed by E1, E2 and E3 enzymes (Ciechanover *et al.* 1978; Ciechanover *et al.* 1980; Hershko *et al.* 1980; Ciechanover *et al.* 1981; Hershko *et al.* 1981; Haas *et al.* 1982; Hershko *et al.* 1983). However, it soon became clear that ubiquitin conjugation cannot fully explain the ATP requirement for intracellular protein degradation, as ATP is still necessary for breakdown of ubiquitinated proteins (Tanaka *et al.* 1983; Hershko *et al.* 1984). Several years later, two different groups identified a very large ATP-dependent proteolytic complex, the 26S proteasome (Hough *et al.* 1987; Waxman *et al.* 1987). We now know that ATP is used by the proteasome to unfold and translocate proteins into its internal proteolytic chamber for degradation (Benaroudj *et al.* 2003). The contribution of Aaron Ciechanover, Avram Hershko and Irwin Rose to the discovery of ubiquitin-proteasome system leads to the 2004 Nobel Prize in Chemistry.

1.1.1 Ubiquitin

Ubiquitin is a small protein present in all eukaryotic organisms. It is highly conserved; there are only 3 amino acids differences out of its total 76 amino acids between human and yeast ubiquitin. Ubiquitin can be covalently conjugated to target

proteins by isopeptide bond formation between its C-terminal carboxyl group and an ϵ -amino group of a lysine residue. This conjugation process, known as ubiquitination, requires three types of enzymes: ubiquitin activating enzymes (E1s), ubiquitin conjugating enzymes (E2s), and ubiquitin ligases (E3s) (Figure 1.1) (Pickart 2001; Passmore & Barford 2004). In human cells, there are two E1s (Uba1 and Uba6), approximately 60 E2s, and over 600 E3s (Rape 2009).

Ubiquitin can be linked to a target protein as one molecule at either a single site (monoubiquitination) or multiple sites (multi-monoubiquitination). Its seven internal lysine residues (K6, K11, K27, K29, K33, K48, K63) and N-terminal amino group (M1) can also be linked to other ubiquitin molecules to form polyubiquitin chains (polyubiquitination). Different types of polyubiquitin chains are associated with different cellular functions, although our understanding of this remains incomplete. K48-linked polyubiquitin chains are the main chain type involved in proteasomal degradation, whereas K63-linked chains function in various non-proteolytic cellular events, including endocytosis, DNA repair, and immune signaling (Bennett & Harper 2008; Hayden & Ghosh 2008; Zeng *et al.* 2010). The functions of other chain types are largely unknown, although all of them have been demonstrated *in vivo*. It has been proposed that all non-K63 chains might work as protein degradation signals, based on the observation that proteasome inhibition increases the level of all non-K63 chains (Xu *et al.* 2009; Kim *et al.* 2011b). K11 chains are suggested to function as a degradation signal in ERAD (ER-associated degradation) and APC/C (anaphase promoting complex/cyclosome)-mediated cell cycle regulation (Haas & Wilkinson 2008; Jin *et al.* 2008; Xu *et al.* 2009). In

Drosophila, K29 chains have been reported to mediate the lysosomal degradation of Deltex, a positive regulator of Notch signalling (Chastagner *et al.* 2006). In addition, linear polyubiquitin chain (M1 chain) is reported to play an important role in NF- κ B activation (Iwai & Tokunaga 2009).

Ubiquitin is encoded by multiple genes. The yeast ubiquitin encoding genes are UBI1 (RPL40A), UBI2 (RPL40B), UBI3 (RPS31), and UBI4. The human ubiquitin encoding genes are RPS27A, UBA52, UBB, and UBC (Kimura & Tanaka 2010). All ubiquitin proteins are translated as inactive precursors, as fusion proteins to a ribosomal protein or as a linear fusion of multiple ubiquitin moieties. Prior to being conjugated to substrates, ubiquitin precursors must be processed by de-ubiquitinating enzymes (DUBs) to expose its Gly-Gly motif at the C-terminus (Passmore & Barford 2004). Ubiquitin expressed artificially in a pre-processed form functions normally, ruling out a maturation requirement for expression as fusion proteins. Another possibility is that fusion of ubiquitin to highly expressed ribosomal proteins allows ubiquitin to be expressed at similarly high levels (Kimura & Tanaka 2010). While ubiquitin could conceivably play a chaperone function toward the ribosomal proteins to which it is fused, this is clearly not a necessity as yeast strains that are engineered to lack the ubiquitin fusion proteins show no abnormalities (Finley *et al.* 1989).

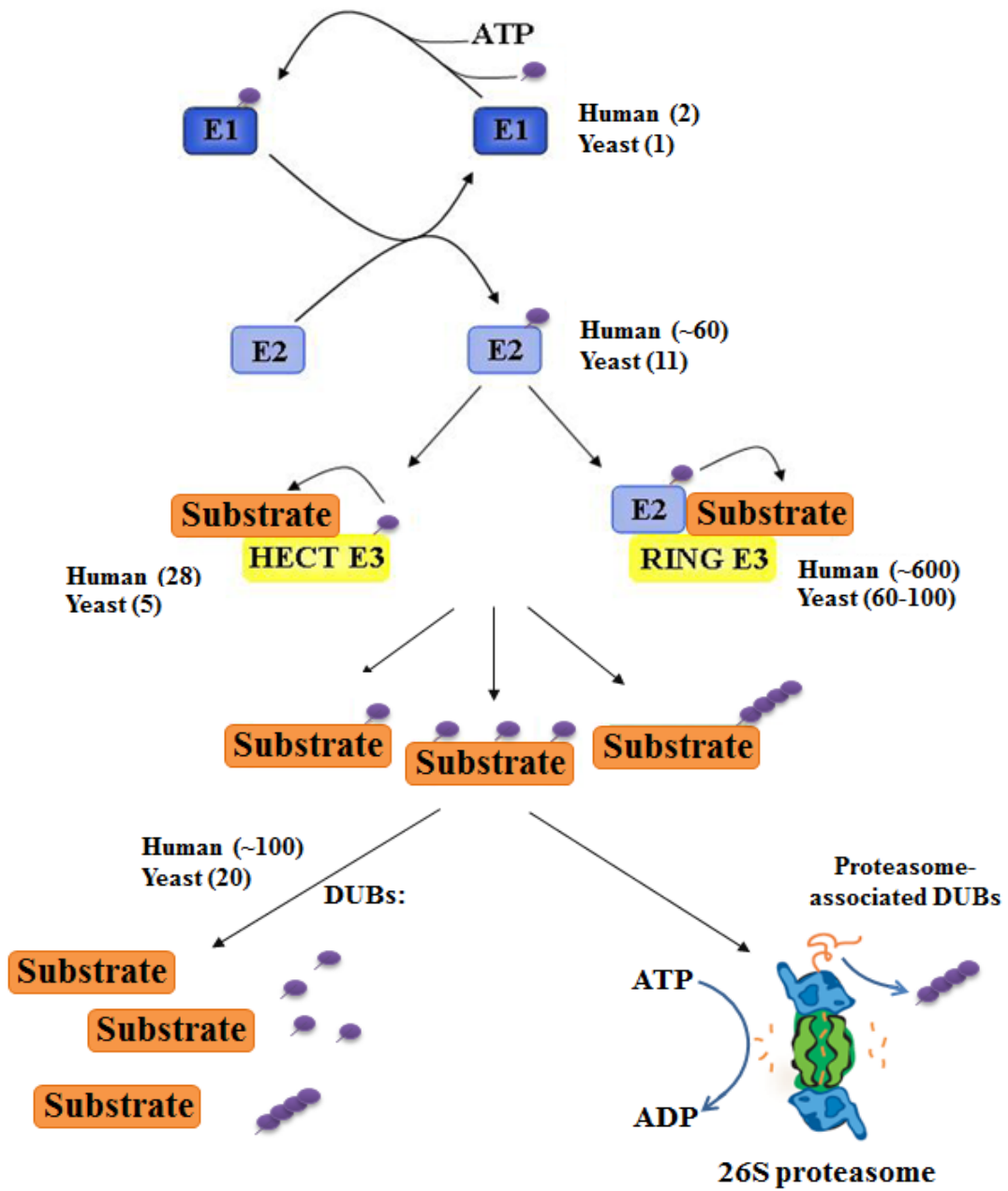


Figure 1.1: The ubiquitin-proteasome system (UPS)

1.1.2 Ubiquitin activating enzymes (E1s)

A single yeast (Uba1) and two human (Ube1, Uba6) ubiquitin E1 enzymes have been reported (Figure 1.1) (Jin *et al.* 2007; Rape 2009). Ubiquitin E1 contains three functional domains: an adenylation domain, a catalytic Cys domain, and a ubiquitin folding domain (UFD) (Schulman & Harper 2009). The adenylation domain is responsible for the activation of ubiquitin molecules. It simultaneously binds a ubiquitin molecule (Ub) and a molecule of ATP and catalyzes the formation of Ub~AMP with the release of pyrophosphate. The active site thiolate of the catalytic domain attacks the Ub~AMP to form E1~Ub. This charging of E1 with ubiquitin induces a profound conformational change in the E1 protein, leading to the exposure of the C-terminal ubiquitin fold domain (UFD), which is responsible for recruiting E2 proteins. The activated ubiquitin is then transferred from the active site cysteine of E1 to the active site cysteine of recruited E2 through a transthiolation reaction, leading to the formation of E2~Ub (Ye & Rape 2009).

In addition to ubiquitin, sixteen human ubiquitin-like proteins (UBLs) have been reported (Schulman & Harper 2009). In general, all UBLs are structurally similar, but different UBLs have their own E1 activating enzymes. E1 enzymes for specific UBLs can be monomeric (UBA1, UBA6 and UBE1L), heterodimeric (SAE1–UBA2 and NAE1–UBA3), or homodimeric (UBA4, UBA5 and ATG7) (Schulman & Harper 2009). UBLs and their E1s are believed to have originated from prokaryotic biosynthetic pathways. The bacterial proteins MoaD (molybdopterin-converting factor subunit 1) and ThiS (thiamine biosynthesis protein S), which share the UBL fold, can be activated by C-

terminal acyl-adenylation. This reaction is catalyzed by MoeB (molybdopterin biosynthetic enzyme B) and ThiF (thiamine biosynthesis protein F) respectively, whose sequences are homologous to the domain of E1s that is responsible for UBL binding and adenylation. MoeD and ThiS cannot be conjugated to other proteins, rather they are involved in sulfur transfer reactions in the molybdopterin and thiamine biosynthesis pathway, respectively (Taylor *et al.* 1998; Lake *et al.* 2001; Leimkuhler *et al.* 2001).

1.1.3 Ubiquitin conjugating enzymes (E2s)

11 yeast and around 60 human E2 enzymes have been reported (Figure 1.1) (Rape 2009; Finley *et al.* 2012). All E2 enzymes share a conserved ubiquitin-conjugating domain (UBC domain, ~150 amino acids), containing the catalytic cysteine (Pickart 2001). Since E2 enzymes are in the center of the ubiquitin conjugation cascade, they must interact with both the E1 and E3 enzymes. The interactions of the E2 with E1 and E3 enzymes are generally mutually exclusive, because the E1 and E3 interaction regions overlap extensively (Eletr *et al.* 2005; Eletr & Kuhlman 2007). Two studies reported that E1 enzymes preferentially bind to free E2 enzymes, rather than ubiquitin-charged E2s (Bencsath *et al.* 2002; Huang *et al.* 2005). In addition to the UBC domain, some E2 enzymes have unique N- and/or C-terminal extensions, which are believed to mediate specific interactions and regulations (van Wijk & Timmers 2010). Although E3 ligases determine substrate specificity of ubiquitin conjugation, E2 enzymes determine the polyubiquitin chain types in RING-E3 mediated ubiquitination (van Wijk & Timmers 2010). For instance, yeast Ubc6 and human Ube2C/UbcH10 are responsible for the formation of K11 chains in ERAD and cell cycle regulation, respectively (Haas &

Wilkinson 2008; Jin *et al.* 2008). As discussed below, E2 enzymes do not determine chain type specificity when they function with another class of E3s, HECT E3s.

1.1.4 Ubiquitin ligases (E3s)

E3 enzymes catalyze the transfer of the E2 charged ubiquitin to substrate lysine residues. There are two major groups of E3 ligases: RING E3s and HECT (Homologous to E6AP C-Terminus) E3s. The RING E3s function as scaffold proteins that bind activated E2 and substrate simultaneously, facilitating the transfer of ubiquitin directly from E2 to substrate. In the case of HECT E3 ligases, ubiquitin is transferred from the charged E2 to the active site cysteine of HECT E3. More recently, a third class of E3-ligases was identified, the RBR (RING-in-between-RING) E3-ligases, which catalyze ubiquitin conjugation by using both RING and HECT-like mechanisms. There are 28 HECT E3 ligases (5 in yeast), 14 RBR E3 ligases (2 in yeast), and over 600 RING E3 ligases in humans (60-100 in yeast). This large pool of E3 ligases defines the substrate specificity of the ubiquitin conjugation pathway.

RING E3 ligases

The RING domain was first discovered in a DNA-binding protein, Ring1. Although the RING domain was originally thought to be involved in DNA binding, we now know most RING domain proteins mediate ubiquitin transfer. The first linkage between RING domains and ubiquitination was established by the discovery of a RING domain protein, Rad18, which can promote ubiquitination of histones (Bailly *et al.* 1997). The RING domain is a type of zinc finger motif containing 6-7 cysteines and 1-2 histidines arranged as the following order: Cys-X₂-Cys-X₍₉₋₃₉₎-Cys-X₍₁₋₃₎-His-X₍₂₋₃₎-Cys-X₂-Cys-X₍₄₋₄₈₎-Cys-

X₂-Cys (X could be any amino acid) (Deshaies & Joazeiro 2009). Structure studies of the RING domain revealed that its conserved cysteines and histidines are buried inside the core domain and are important for stabilizing the three-dimensional structure of the domain through interaction with two atoms of zinc.

The RING domain mediates the interaction with E2-conjugating enzymes, whereas the substrate recognition is mediated by other portions of the RING E3 ligase. For example, a monomeric RING E3 ligase, Cbl, recognizes tyrosine-phosphorylated target proteins through its phosphotyrosine-binding domain (PTB) (Joazeiro *et al.* 1999). The U-Box domain is another E2 binding domain, called a RING-like domain. Although lack of conserved cysteine and histidine residues and no requirement of zinc atoms for structural stabilization, the three-dimensional structure of the U-Box domain is still similar to the RING domain. Mechanistically, both RING E3s and U-box E3s act as scaffold proteins which bind to a ubiquitin-activated E2 enzyme and a substrate, promoting transfer of ubiquitin from E2 to a substrate (Deshaies & Joazeiro 2009).

Many RING E3 ligases are multimeric protein complexes, such as the SCF complex, containing Skp1, Cull1, Rbx1/Roc1 and an F-box protein. Skp1 and Cull1 are the backbone of the SCF complex, whereas F-box proteins and Rbx1/Roc1 are responsible for substrate recognition and E2 recruitment, respectively. Besides F-box proteins, many alternative substrate binding proteins, including SOCS box, VHL box, or BTB domain-containing proteins, could be incorporated into cullin-RING E3 ligase (CRL) complexes, allowing this type of E3 ligases to target a wide range of substrates (Petroski & Deshaies 2005).

HECT E3 ligases

The first discovered HECT E3 ligase was E6AP, which is hijacked by the human papillomavirus (HPV) E6 protein to promote the ubiquitination and degradation of p53 (Huibregtse *et al.* 1991; Scheffner *et al.* 1993). When purified E6AP is used for an *in vitro* ubiquitination assay, it accepts ubiquitin from E2 and forms a thioester with ubiquitin as an intermediate step in E6AP-dependent ubiquitination (Scheffner *et al.* 1995). Sequence analysis revealed that a group of proteins containing a similar C-terminal domain (~350 residues) as E6AP were also capable of thioester formation, defining a new group of ubiquitin E3 ligases, the HECT E3 ligases (Homologous to E6AP Carboxyl-Terminus) (Huibregtse *et al.* 1995).

Structural studies have shown that the HECT domain consists of a ~250-amino-acid N-lobe and a ~100-amino-acid C-lobe, connected by a 4-amino-acid flexible hinge. The N-lobe is the site for recruitment of ubiquitin-charged E2s, and the C-lobe contains the active site cysteine that accepts ubiquitin from the E2 through a transthioesterification reaction (Huang *et al.* 1999). Although the C-terminal domains of HECT E3s are highly conserved, their substrate specificity is determined by their variant N-terminal regions (Scheffner & Kumar 2014). The Huibregtse lab reported that the C-lobe determines the polyubiquitin chain type specificity among HECT E3 ligases. Kim *et al.* showed that swapping the C lobe of Rsp5, a K63-specific HECT E3, with the C lobe of E6AP, a K48-specific HECT E3, resulted in Rsp5 preferentially catalyzing K48-linked chains formation (Kim & Huibregtse 2009). In addition, Kim *et al.* reported that a non-covalent ubiquitin binding site (UBS) within the N-lobe of the Rsp5 HECT domain is important

for ubiquitin chain elongation, with the proposed function being to localize and orient the distal end of the ubiquitin chain to promote the addition of the next ubiquitin molecule (Kim *et al.* 2011a).

RBR E3 ligases

The RBR (RING-in-between-RING) E3 ligases were first described by two different groups in 1999 (Morett & Bork 1999; van der Reijden *et al.* 1999). This class of proteins is characterized by the RBR signature, which consists of two RING finger domains (RING1 and RING2 domain), with an IBR domain (in-between RING domain) in the middle (Smit & Sixma 2014). RBR E3 ligases follow a two-step mechanism to mediate the transfer of ubiquitin molecule from the E2 to substrates. The ubiquitin transfer is initiated by the interaction of a ubiquitin-charged E2 with RING1 domain, similar to the interaction of E2s with classical RING E3-ligases. However, instead of facilitating the transfer of ubiquitin to substrates directly, this interaction in RBR proteins is used to promote the transfer of ubiquitin to the active site cysteine on RING2, to form a HECT-like thioester intermediate prior to the transfer of ubiquitin to its target protein (Smit & Sixma 2014).

This RING/HECT-hybrid mechanism was first uncovered in the study of the reactivity profile of UBCH7, a human E2 enzyme (Wenzel *et al.* 2011). UBCH7 exhibits broad specificity for HECT E3 ligases, but often fails to function with RING E3 ligases (Anan *et al.* 1998; Zheng *et al.* 2000). Wenzel and colleagues found that unlike many E2s that can function with RING E3s, UBCH7 lacks intrinsic E3-independent reactivity with lysines, explaining its preference for HECT E3s. Meanwhile, they also found that

UBCH7 shows activity with RBR E3 ligases, including Parkin and HHAR1, and the successful transfer of ubiquitin requires a conserved cysteine residue in RING2 domains. Moreover, *in vitro* assays showed that HHAR1 can form a β -ME (β -mercaptoethanol) sensitive intermediate with ubiquitin, indicating that RBR proteins function like RING/HECT hybrids (Wenzel *et al.* 2011).

1.1.5 Deubiquitinating enzymes (DUBs)

Deubiquitinases are a group of proteases that can hydrolyze isopeptide bonds between ubiquitin and the substrate. The human genome encodes around 79 deubiquitinases, which are classified into five families: ubiquitin C-terminal hydrolases (UCHs), ubiquitin-specific proteases (USPs), ovarian tumor proteases (OTUs), Josephins and JAB1/MPN+ metalloenzymes. Most DUBs are Cys proteases, except for JAB1/MPN+ family members, which are zinc metalloproteases (Komander *et al.* 2009).

DUBs have three major functions in cellular pathways. First, as mentioned above, ubiquitins are translated as inactive precursors either fused to ribosomal proteins or as a linear fusion of multiple ubiquitin moieties. DUB activity is required to process these precursors and generate active monomeric ubiquitin molecules with exposed C-termini. UCH family members are believed to be the major players in processing ubiquitin precursors, based on their preference for linear ubiquitin fusion proteins as substrates. Second, DUBs are important for recycling ubiquitin and maintaining ubiquitin homeostasis in cells. Some DUBs are normally associated with proteasomes and endocytic vesicles to release ubiquitin prior to substrate degradation. Third, DUBs are

important regulators of protein stability. They act as antagonists of ubiquitin signaling to rescue mis-conjugated proteins (Komander *et al.* 2009).

1.1.6 The proteasome

The 26S proteasome is the location for the degradation of most ubiquitinated proteins. It consists of two multi-subunit components: the 20S core particle and the 19S regulatory particle. The core particle is made up of 28 subunits which are arranged into four seven-subunit rings (two α -subunit rings and two β -subunit rings). The four rings are stacked to form a hollow barrel-like structure, with two β -subunit rings in the center and two α -subunit rings at each end. The core particle contains six proteolytic sites which are all located inside the chamber. As these six proteolytic sites show relatively low preference for specific amino acids, together they can digest almost any amino acid sequence (Nussbaum *et al.* 1998; Kisselev *et al.* 1999). The entrances to the proteasome core particle at both ends are so narrow that folded proteins cannot pass through, therefore preventing the unspecific degradation of folded native cellular proteins by the 20S particle (Lowe *et al.* 1995; Groll *et al.* 1997).

The 19S regulatory particle is responsible for recognizing ubiquitinated proteasome substrates, removing ubiquitin chains, and unfolding target proteins for entering the core particle. These distinct functions are performed by its different subunits: Firstly, two intrinsic ubiquitin receptors (Rpn10 and Rpn13), together with several detachable ubiquitin receptors are essential for recognition of ubiquitinated proteins. Several recent structural studies showed that Rpn10 and Rpn13 are about 9 nm apart from each other, which is closely matched to the length of the K48 chain with four ubiquitin moieties. This

may account for why proteasome substrates need a polyubiquitin chain equal to or longer than four ubiquitin molecules for tight binding to the proteasome (Beck *et al.* 2012; da Fonseca *et al.* 2012; Lander *et al.* 2012). Secondly, Rpn11 is a proteasome-associated deubiquitinase whose function is to remove the entire polyubiquitin chain from proteasome substrates for recycling (Verma *et al.* 2002; Yao & Cohen 2002). Thirdly, the 19S particle contains six ATPases (Rpt1-6) that form a ring-like structure and dock onto the core particle. They unfold the proteasome substrates and promote the translocation of unfolded proteins into the core particle by hydrolyzing ATPs (Hanson & Whiteheart 2005; Sauer & Baker 2011). With the concerted effort of these different subunits, the 19S particle promotes the degradation of ubiquitinated proteasome substrates by the core particle.

1.2 ISG15: AN ANTI-VIRAL UBIQUITIN-LIKE PROTEIN

1.2.1 Ubiquitin-like proteins

Ubiquitin-like proteins (UBLs) are a group of proteins, whose structures resemble the β -grasp fold of ubiquitin (Figure 1.2). So far, seventeen ubiquitin-like proteins have been identified, including SUMO1-4, Nedd8, FAT10, URM1, and ISG15 (Schulman & Harper 2009). Similar to ubiquitin conjugation, ubiquitin-like proteins are covalently linked to substrate proteins through the formation of isopeptide bond between their C-terminal glycine and a substrate amino group (normally a lysine side chain). Conjugation of ubiquitin-like proteins to substrates requires the E1-E2-E3 enzymatic cascade similar to that of ubiquitin. Meanwhile, many UBL-specific proteases have been identified,

which function to process UBL precursors and remove UBLs from target proteins. Although structurally related, very little evidence suggests that UBLs signal target proteins for proteasomal degradation, with the exception of FAT10, which can target its conjugated proteins for degradation with the assistance of NUM1L (NEDD8 ultimate buster-1 long) (Hipp *et al.* 2005; Schmidtke *et al.* 2009; Rani *et al.* 2012). In contrast, most of UBLs have critical regulatory roles in many cellular processes, including nuclear transport, translation, autophagy and antiviral pathways (van der Veen & Ploegh 2012). In some cases, protein conjugation activity is not necessary for certain UBLs to perform their particular biological functions. For example, Urm1 can function as a sulphur carrier in thiolation of tRNAs (Leidel *et al.* 2009; Noma *et al.* 2009). Recently, Bogunovic and colleagues reported that ISG15 can act as an extracellular cytokine to promote IFN- γ production for the control of mycobacterial disease (Bogunovic *et al.* 2012). They found that although ISG15 has no detectable signal peptide sequence, it can still be secreted by human neutrophils, monocytes and lymphocytes. Secreted ISG15 can act on T and natural killer (NK) lymphocytes to induce IFN- γ production. Interestingly, a synergistic effect on IFN- γ induction was observed when the cells were simultaneously treated with ISG15 and interleukin 12 (IL-12), another cytokine well-known to induce IFN- γ production. In addition, they found that inherited ISG15 deficiency is associated with severe mycobacterial disease in both mice and humans, providing supportive evidence of the essential role of ISG15 in the control of mycobacteria infection (Bogunovic *et al.* 2012).

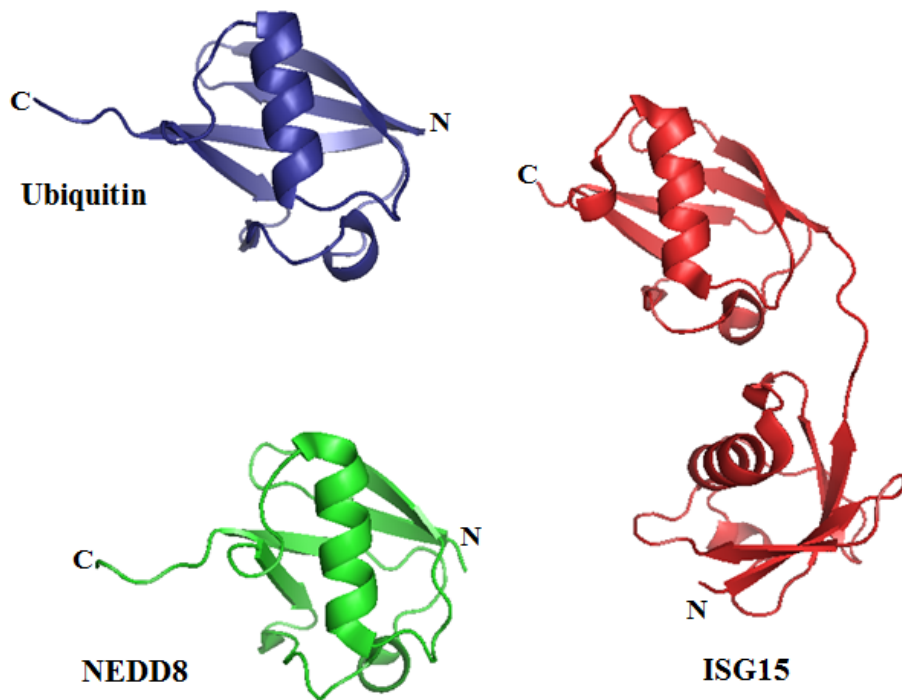


Figure 1.2: The structures of ubiquitin-like proteins resemble the structure of ubiquitin

ISG15 (red) and NEDD8 (green) structurally resemble ubiquitin (blue). Structures are adapted from (Durfee 2010) (PDB files 1Z2M, 2KO3, and 1UBQ).

1.2.2 ISG15 and its pathway enzymes

ISG15 is a 17 kD IFN- α/β -induced UBL consisting of two ubiquitin-like domains that are connected via a six-residue linker (Figure 1.2) (Narasimhan *et al.* 2005). The N-terminal domain of ISG15 is 32% identical to ubiquitin, whereas the C-terminal domain is 37% identical. ISG15 was the first identified UBL (Farrell *et al.* 1979), only 4 years later than the discovery of ubiquitin. Many years passed before the enzymes for ISG15 conjugations were identified, beginning with the ISG15 E1 enzyme (Ube1L/UBA7) in 2001 (Yuan & Krug 2001). UbcH8/Ube2L6 and Herc5 were subsequently identified as the major E2 and E3 enzymes for ISG15 conjugation, respectively (Yuan & Krug 2001; Zhao *et al.* 2004; Dastur *et al.* 2006). Similar to ISG15, all these enzymes are IFN- α/β -induced. Although several other IFN-induced E3 ligases have been identified by microarray analysis (Nakasato *et al.* 2006; Zou & Zhang 2006), Dastur *et al.* showed that depletion of Herc5 by siRNA eliminated nearly all ISG15 conjugated products in interferon treated cells, suggesting Herc5 is the major E3 ligase for ISG15 conjugation (Dastur *et al.* 2006). In addition, ISGylation could be broadly reconstituted by co-expression of Ube1L, UbcH8, ISG15, and Herc5 in non-interferon treated cells, suggesting that these represent the core enzymes for ISG15 conjugation. One of the IFN-induced E3 ligases is Herc6, the closest relative of Herc5 in human cells. Interestingly, human Herc6 does not support ISG15 conjugation but mouse Herc6 does support conjugation (Ketscher *et al.* 2012; Oudshoorn *et al.* 2012).

Like ubiquitin and many other UBLs, ISG15 is translated as an inactive precursor, so that an ISG15-specific protease is required to process its C-terminus for exposing the LRLRGG motif. Ubp43 was reported as a deconjugating enzyme of ISG15 (Malakhov *et al.* 2002); however it is not responsible for ISG15 precursor processing, as ISG15 conjugation still occurred in Ubp43^{-/-} mice (Knobeloch *et al.* 2005). Several non-catalytic functions of Ubp43 have been reported recently. For example, Ubp43 negatively regulates IFN signaling by binding to the IFNAR2 receptor subunit and blocking the interaction between JAK and the IFN receptor (Malakhova *et al.* 2006). In addition, Ubp43 was identified as an important repressor of IFN- α and drug-induced apoptosis, and this anti-apoptotic function is also independent of its ISG15 isopeptidase activity (Potu *et al.* 2010).

1.2.3 Anti-viral function of ISG15

Type 1 interferons are a component of the innate immune response. When viruses or bacteria infect cells, cells rapidly detect infected pathogens based on pathogen-associated molecular patterns (PAMPs) present on bacteria or viruses. Pattern recognition receptor proteins (PRRs) can recognize PAMPs and trigger the activation of multiple downstream signaling cascades, including interferon-regulatory factors (IRFs), leading to the production of type I interferon (IFN- α/β) (Mogensen 2009). IFN- α/β is then secreted in an autocrine and paracrine manner, and induces the expression of over a hundred interferon stimulated genes (ISGs), including MxA, PKR, p56, OAS1, APOBEC3G, many TRIM ubiquitin ligases, and the ISG15 conjugation machinery (Schoggins & Rice 2011).

Expression of ISGs facilitates the establishment of an anti-viral state; however, the biochemical mechanism of the anti-viral effects are understood for only a handful of ISGs. MxA has been shown to accumulate at the ER membrane where it can recognize and trap viral nucleocapsid-like structures, preventing these trapped viral components from being used for the generation of new virus particles (Haller *et al.* 2007). TRIM5 α is a retrovirus-specific restriction factor. It can interfere with the capsid uncoating process of the retrovirus, therefore preventing the subsequent reverse transcription and delivery of viral genome into the nucleus. The RING domain of TRIM5 α is not absolutely required for retrovirus restriction (Stremlau *et al.* 2004). Consistent with this, proteasome inhibition did not significantly affect the restriction of retrovirus infection by TRIM5 α (Stremlau *et al.* 2004; Sebastian & Luban 2005; Stremlau *et al.* 2006).

ISG15 has been reported to have anti-viral activity against several types of RNA and DNA viruses, including influenza, Sindbis, herpes, Human Immunodeficiency Virus (HIV), and Ebola (Lenschow *et al.* 2005; Okumura *et al.* 2006; Okumura *et al.* 2008; Hsiang *et al.* 2009). In most cases examined, ISG15 conjugation is essential for the antiviral activity, as the mice lacking the ISG15 E1 activating enzyme, Ube1L, showed more viral susceptibility (Giannakopoulos *et al.* 2009; Lai *et al.* 2009). It has been shown that unconjugated ISG15 molecules also have anti-viral activity. For example, the ubiquitination-induced interaction of viral Gag protein and the host's Tsg101 protein (a central component of the endosomal sorting complex (ESCRT-1)) is required for the release of HIV virions. Free ISG15 is reported to block the release of HIV-1 virions from

infected tissue culture cells by inhibition of the ubiquitination of Gag and Tsg101 proteins. Similarly, Nedd4-mediated ubiquitination of Ebola VP40 matrix protein is also required for the efficient release of VP40 virus-like particles (VLPs). Okumura *et al.* showed that ISG15 interacts with Nedd4 ubiquitin ligase and inhibits ubiquitination of VP40 to prevent efficient release of VLPs (Okumura *et al.* 2006; Okumura *et al.* 2008). In addition, free ISG15 is critical for the control of Chikungunya virus (CHIKV) infection. There is an increase in lethality in ISG15^{-/-} mice but not Ube1L^{-/-} mice following CHIKV infection. Interestingly, no differences in viral loads were observed between wild-type and ISG15^{-/-} mice; however, a dramatic increase in proinflammatory cytokines and chemokines was observed in ISG15^{-/-} mice, suggesting that the cytokine storm contributes to the lethality of ISG15^{-/-} mice after CHIKV infection (Werneke *et al.* 2011).

Several recent studies have begun to unravel the molecular mechanism of the antiviral role of ISG15 conjugation. Influenza A NS1 protein (NS1A) was identified as an ISG15 target in virus-infected cells. Chen *et al.* showed that ISGylation of NS1A protein blocks its binding to importin- α , impairing the nuclear import of NS1A protein. Meanwhile, mutation of ISGylation sites of NS1A dramatically enhances viral replication in interferon-treated cells (Zhao *et al.* 2010). ISG15 modification of a certain cellular protein is critical for the antiviral activity. ISGylation of interferon regulatory factor-3 (IRF-3) was found to increase its stability by antagonizing its ubiquitination. As a consequence, IRF-3 mediated transcription was enhanced, promoting the production of IFN- β (Lu *et al.* 2006).

Consistent with the anti-viral role of ISG15, viruses have developed different mechanisms to antagonize ISG15 and its conjugation pathway (Zhao *et al.* 2013). Influenza B NS1 protein (NS1B) has been shown to bind ISG15 and block its conjugation (Yuan & Krug 2001). Similarly, Vaccinia virus protein, E3, is also able to bind ISG15 and repress the conjugation of ISG15 (Guerra *et al.* 2008). Moreover, several viruses, including SARS Coronavirus, human Coronavirus NL63, Nairoviruses and Arteriviruses, encode proteases to remove ISG15 from target proteins (Frias-Staheli *et al.* 2007; Lindner *et al.* 2007; Clementz *et al.* 2010).

1.2.4 ISG15 targets a broad range of newly synthesized proteins

As discussed previously, the ubiquitin system contains over 600 E3 ligases to facilitate the transfer of ubiquitin to specific targets. Generally, E3 ligases recognize substrates through protein-protein interaction motifs. As a result, one E3 ligase generally recognizes only a small group of proteins sharing a common protein-protein interaction motif. Currently, more than 300 cellular proteins have been identified as ISG15 targets (Giannakopoulos *et al.* 2005; Zhao *et al.* 2005; Takeuchi *et al.* 2006). These identified ISG15 targets are involved in various cellular pathways, including cytoskeletal organization, stress responses, translation, transcription, RNA splicing, and general metabolism. In addition, no common primary sequence motif was identified within the ISG15 target proteins. Given that Herc5 is the only major E3 ligase for ISG15 conjugation, this raises a very important question: how can a single E3 ligase recognize and target such a large number of substrates?

In addressing this question, Durfee *et al.* found that: 1) the range of ISG15 substrates extends even further and includes exogenously expressed bacterial, viral, and non-naturally occurring proteins, 2) only newly synthesized proteins can be targeted for ISGylation, and 3) Herc5 co-fractionation with polysomes through interaction with the 60S ribosomal subunit (Durfee *et al.* 2010). These findings suggested a co-translational model for ISG15 conjugation: Herc5 associates with ribosomes and stochastically transfers ISG15 to newly synthesized proteins, while they are being translated. This model implies that in the context of virally infected cells, newly translated viral proteins may be an important class of ISG15 substrates (Figure 1.3).

One major issue of the anti-viral activity of ISG15 conjugation is that only a very small fraction of the total pool of any target protein was ISGylated and therefore, it is unclear how modification of a small fraction of viral protein might have a significant reduction on overall viral infectivity. Durfee *et al.* proposed a dominant negative effect model for explaining the antiviral activity of ISGylation. This model has been tested in a human papillomavirus 16 (HPV16) pseudovirus system. As predicted, only a small fraction of HPV16 L1 capsid protein was ISGylated and incorporated into mature pseudovirus. However, given that each HPV pseudovirion has 360 molecules of L1 protein, almost every pseudovirion contains multiple copies of ISGylated L1 protein. As a result, the overall viral infectivity was largely inhibited (Durfee *et al.* 2010).

Although our previous data was consistent with the co-translational model of ISG15 conjugation, direct evidence was still lacking. The goal of chapter 2 of my thesis is to rigorously test this co-translational model.

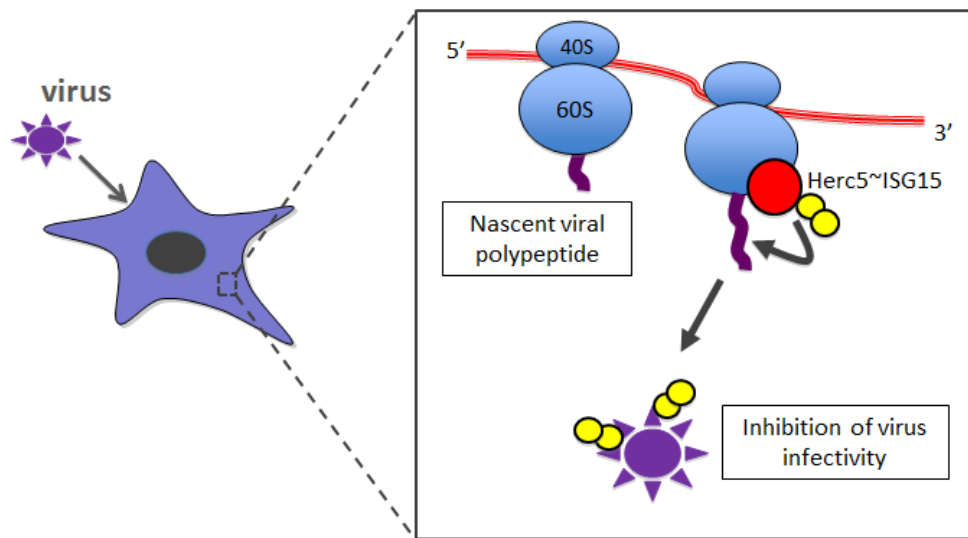


Figure 1.3: Co-translational model for ISG15 conjugation. (Adapted from Durfee *et al.* 2010)

1.3 CELLULAR PROTEOSTASIS AND ITS LINKAGE WITH AGING

Every human cell contains several billion protein molecules, ranging in size from 3 kDa to 3700 kDa (Wolff *et al.* 2014). These proteins must fold into specific three-dimensional conformations to obtain their functional activities. Inappropriately folded proteins need to be disposed of immediately and efficiently to maintain protein homeostasis. Deficiencies in protein folding or eliminating aberrant proteins are associated with many age-related diseases, such as Alzheimer's disease, Parkinson's disease, and cataracts (Balch *et al.* 2008; Douglas & Dillin 2010; Lopez-Otin *et al.* 2013). Understanding the mechanisms of protein folding, quality control and disposal of misfolded proteins is therefore crucial for therapeutic intervention in these disease states.

1.3.1 Challenges of protein folding *in vivo*

The earliest studies of protein folding were performed *in vitro*, by examining the refolding of denatured proteins in the absence of any other component or energy source. These studies found that small proteins with only a single domain could fold spontaneously *in vitro* very rapidly, demonstrating that the primary amino acid sequence of a protein contains all the necessary information for its correct protein folding (Anfinsen 1973; Chan & Dill 1998). However, large and multi-domain proteins often failed to reach their native structures during *in vitro* experiments. Considering the average number of protein domains per human protein is 3.7, human cells must have ways to ensure the efficient folding of proteins (Wolff *et al.* 2014).

Protein folding in the cell is believed to be more complicated and challenging than folding *in vitro*. First, the cellular environment is a very crowded environment, with the protein concentration up to 300-400 mg/ml, approaching the saturation point for protein crystallization (Asherie 2004). This crowded environment increases the tendency of non-native, partially folded proteins to form protein aggregates (Ellis & Minton 2006). Second, a nascent polypeptide cannot fold into a stable native structure until the complete protein has been synthesized and released from ribosome (Cabrita *et al.* 2009; Eichmann *et al.* 2010). As protein translation is relatively slow, with an elongation rate around 5 amino acids per second in human cell, nascent chains are therefore exposed as partially folded and aggregation-prone intermediates for relatively long periods of time (synthesis of a protein with an average length of 550 amino acids requires ~110 seconds). Generally, a single mRNA molecule is occupied and translated by multiple ribosomes

simultaneously, forming a polyribosome (or polysome). In the context of polysomes, the local concentration of nascent polypeptides is very high, further increasing the probability of interactions between partially folded nascent chains on adjacent ribosomes. Moreover, many proteins require certain post-translational modifications, interaction with specific ligands or binding partners, or a specific location for proper folding (Dunker *et al.* 2008; Kim *et al.* 2013).

1.3.2 Strategies to facilitate protein folding *in vivo*

Due to such challenges, cells have developed several strategies to ensure efficient and correct protein folding *in vivo*. The core strategy is the development of chaperone systems. Molecular chaperones are defined as proteins that interact with, stabilize, or help other proteins to reach their functional conformation, but they are not present in the final structure of their client proteins (Hartl & Hayer-Hartl 2009; Kim *et al.* 2013). Chaperone proteins are often referred to as heat-shock proteins (HSPs), as certain chaperones are heat- or stress-induced. Cells contain several different classes of chaperones, which are normally classified based on their molecular weight (e.g., HSP40, HSP60, HSP70, HSP90, HSP100, and several small HSPs). Chaperones are highly abundant proteins in cells, with multiple essential functions in maintaining proteome homeostasis, including *de novo* protein folding, refolding of denatured proteins, protein trafficking, and promoting the degradation of misfolded proteins (Hartl *et al.* 2011).

The central role of constitutively expressed chaperones is to facilitate *de novo* protein folding. Chaperones involved in *de novo* folding can be further divided into two groups based on whether or not they interact with ribosomes (Preissler & Deuerling

2012). The first group includes chaperones that associate with ribosomes and bind to nascent chains as soon as they emerge from the ribosomal exit tunnel. These proteins assist the early steps of *de novo* folding during translation. Eukaryotic cells contain two ribosome-associated chaperone systems, the nascent chain-associated complex (NAC) and the HSP70-based triad system (Rospert *et al.* 2002; Kampinga & Craig 2010; Jaiswal *et al.* 2011). The second group of chaperone proteins do not interact with the ribosome, including cytosolic HSP70/40, HSP60/10 (chaperonins) and prefoldin (Preissler & Deuerling 2012). They act downstream of the ribosome-associated chaperones, controlling the late *de novo* folding steps. Binding of chaperones to nascent polypeptides could prevent their premature folding and keep nascent chains in a soluble and folding-competent state. In addition, chaperonins provide an enclosed space for substrate protein folding. Most of chaperonin substrates are between 20 to 60 kDa and contain complex α/β or $\alpha+\beta$ structures (Fujiwara *et al.* 2010), and they are free to fold in the enclosed environment for approximately 10 seconds (Kerner *et al.* 2005; Horwich & Fenton 2009).

In addition to the chaperones described above, another class of chaperones in cells is linked to the stress response, assisting the re-folding of stress-denatured proteins (Albanese *et al.* 2006). In yeast, the stress-linked chaperones include HSP104, Sti1 and Ssa4. The expression of stress-linked chaperones is induced under stress conditions, controlled by the heat shock factors (HSFs) (Akerfelt *et al.* 2010). Rapid repression of global protein translation is observed under stress conditions, primarily due to inhibition of translation initiation as well as elongation pausing (Spriggs *et al.* 2010; Liu *et al.* 2013; Shalgi *et al.* 2013). These findings showed that the protein synthesis machinery can

control protein production by sensing the intracellular folding environment, preventing the production of proteins in a hostile environment and reducing the burden on chaperone systems under stress conditions (Holcik & Sonenberg 2005).

In addition to chaperone systems, cells also have several other strategies to facilitate correct protein folding. For example, many mRNAs are simultaneously translated by multiple ribosomes, forming the polyribosome structure. To avoid misinteractions between the nascent chains on two adjacent ribosomes, polysomes are organized in a pseudohelical arrangement *in vivo* to maximize the distance between nascent chains on adjacent ribosomes (Brandt *et al.* 2009). Denatured full length multi-domain proteins are normally unable to refold correctly, due to non-native inter-domain interactions. To avoid these non-native contacts, eukaryotic cells evolved a domain-wise co-translational folding strategy (Netzer & Hartl 1997; Frydman *et al.* 1999). Relatively slow elongation rates (~5 amino acid per sec in eukaryotes versus ~20 amino acids per sec in bacteria) in concert with translational pausing at rare codons prevents later domains from emerging from the ribosome until the folding of the previous domain is completed (Zhang & Ignatova 2009). The sequential domain folding strategy may have allowed for the explosive evolution of complex multi-domain proteins in eukaryotes (Agashe *et al.* 2004).

1.3.3 Strategies for clearance of misfolded proteins

Protein synthesis is a complicated process, with the participation of approximately 400 proteins (Kim *et al.* 2013). Errors occurring in each step, including transcription, mRNA processing, and translation, can have large adverse effects on the stability of the

protein (DePristo *et al.* 2005; Levine *et al.* 2005; Ogle & Ramakrishnan 2005; Pickrell *et al.* 2010). Although the error rate of protein synthesis is kept at a relatively low level, huge numbers of aberrant proteins are still produced. For example, the rate of amino acid mis-incorporation is only one in every 5,000-10,000 amino acids, but given the average length of a protein is approximate 550 amino acids, this means that 5%-10% of proteins of average length contain at least one mis-incorporated amino acid (Wolff *et al.* 2014). As a result, a significant fraction of newly synthesized proteins never attain their functional state, even with the help of molecular chaperones. Consistent with this, 6%-30% of all newly synthesized proteins are rapidly degraded in eukaryotic cells (Schubert *et al.* 2000; Vabulas & Hartl 2005; Qian *et al.* 2006). In addition to this continuous stream of misfolded proteins from newly synthesized proteins under normal conditions, a number of abnormal conditions can enhance the production of misfolded proteins, such as elevated temperature, exposure to chemicals or heavy metals, and bacteria or viral infections (Voisine *et al.* 2010).

Given that misfolded proteins are toxic, cells have elaborate strategies to monitor and clear misfolded proteins. The three major parallel strategies are: 1) refolding of misfolded proteins with the assistance of chaperones, 2) degradation of misfolded proteins through UPS and autophagy systems, and 3) sequestration of misfolded proteins into specialized quality control compartments (Figure 1.4) (Chen *et al.* 2011). Each strategy has its own advantages and drawbacks. Protein refolding is a fast and energy-efficient way to deal with deleterious proteins, and misfolded proteins can be recovered via this strategy. However, as discussed above, many multi-domain proteins are not able

to correctly refold due to non-native inter-domain interactions (Netzer & Hartl 1997). Degradation is a permanent way to clear misfolded proteins. Sequestration is a way to mitigate the burden on quality control systems when they are overloaded with misfolded proteins (Kaganovich *et al.* 2008), but inclusions are difficult to clear and some normal proteins may also be sequestered due to the relatively low specificity of this process (Olzscha *et al.* 2011).

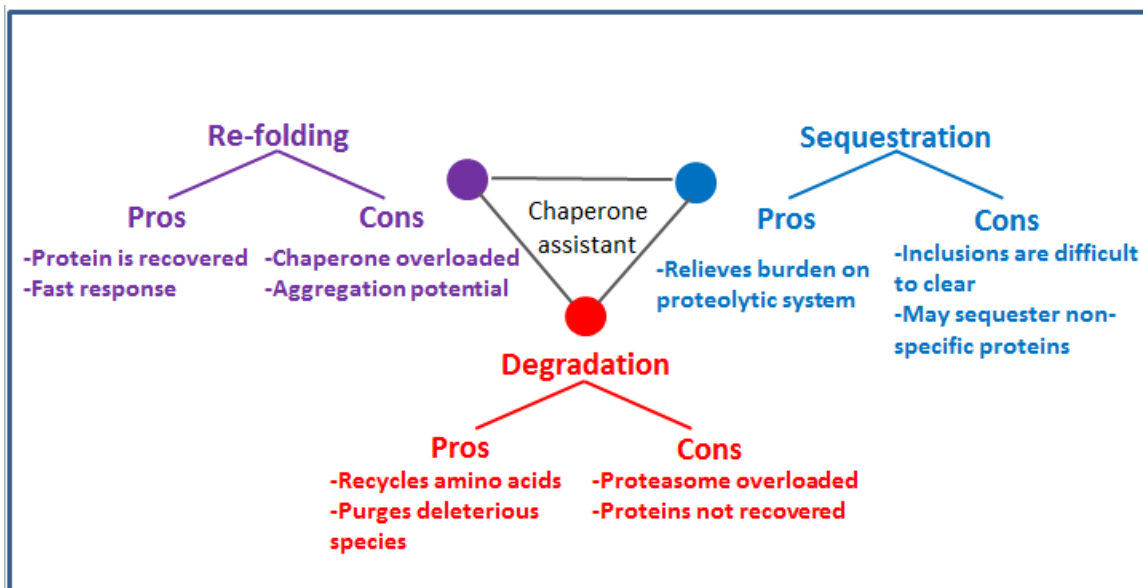


Figure 1.4: Three major strategies to clear misfolded proteins. (Adapted from Chen *et al.* 2011)

Degradation of misfolded proteins via proteolytic pathways

Eukaryotic cells have two proteolytic pathways: the ubiquitin-proteasome (UPS) system and the autophagy/lysosome system. Most of the soluble misfolded and damaged proteins are degraded by the UPS, the major degradation pathway in eukaryotes, which

corresponds to 80%-90% of total intracellular protein degradation (Goll *et al.* 2008). Recognition of misfolded proteins by ubiquitin E3 ligases may need the assistance of chaperones. For example, CHIP (carboxy-terminal HSP70 interacting protein) E3 ligase interacts with HSP70 and targets HSP70-bound misfolded proteins for proteasomal degradation (Arndt *et al.* 2007). Ubiquitination of misfolded endoplasmic reticulum (ER) proteins also requires the participation of chaperones. Two ubiquitin E3 ligases, Hrd1 and Doa10, are anchored to the ER membrane and mediate ubiquitination of misfolded ER proteins in a HSP70-dependent manner (Hirsch *et al.* 2009). Degradation of ubiquitinated proteins may also require other factors, such as p97/Cdc48-Ufd1-Npl4 complex and its cofactors. P97/Cdc48 is an AAA ATPase (ATPases associated with diverse cellular activities) with intrinsic ubiquitin binding affinity (Jentsch & Rumpf 2007). Cdc48/p97 is believed to function as a 'segregase' to extract ubiquitinated protein from its original complex by using the energy from ATP hydrolysis (Ye 2006), ensuring the specific degradation of ubiquitinated substrates but not their normal interaction partners.

Protein aggregates are too big to be degraded by the proteasome; therefore most protein aggregates are disposed of by the autophagy pathway. Autophagy is a relatively unspecific degradation pathway that is used to clear the unnecessary or dysfunctional cellular components or organelles, such as malfunctioned mitochondria and deficient ribosomes. This is done by engulfing the substrates and ultimately delivering the substrates to the lysosome (Klionsky *et al.* 2011; Murrow & Debnath 2013). At least three different forms of autophagy have been described: macroautophagy, microautophagy and chaperone-mediated autophagy (CMA) (Lee *et al.* 2012; Murrow &

Debnath 2013). Unlike the other two forms of autophagy, CMA is a relatively specific pathway, which requires an HSC70-containing complex for substrate selection and delivery into the lysosome (Arias & Cuervo 2011). Several studies revealed functional interactions between UPS and autophagy pathways. For instance, when the UPS function was blocked, autophagy was induced as a compensatory degradation pathway (Pandey *et al.* 2007). Similarly, inhibition of the autophagy pathway resulted in accumulation of proteasomal substrates in the cell (Komatsu *et al.* 2005).

Sequestration of misfolded proteins to quality control compartments

Sequestration of misfolded proteins into inclusions was initially thought as a backup strategy to manage toxic materials when quality control failed, as inclusions were often formed when chaperones and proteolytic systems were overwhelmed (Chen *et al.* 2011). A growing amount of evidence reveals that sequestration of misfolded proteins also occurs in healthy cells under normal growth conditions, suggesting a physiological feature of protein quality control (Escusa-Toret *et al.* 2013). Misfolded proteins are sorted into different spatial compartments based on their solubility and properties. Soluble ubiquitinated misfolded proteins are sequestered into the Q-body and juxtanuclear quality control compartment (JUNQ). In contrast, insoluble amyloid aggregates are sorted into the insoluble protein deposit (IPOD) compartment that is next to the vacuole (Kaganovich *et al.* 2008; Sontag *et al.* 2014). Sorting of misfolded proteins with different properties to specific compartments is believed to enhance the efficiency of protein quality control. JUNQ co-localizes with high level of chaperones and proteasomes,

suggesting that the protein refolding and degradation are highly promoted in this compartment. IPOD is associated with autophagy-related protein Atg8, which may facilitate degradation of the sequestered insoluble aggregates by lysosomes (Kaganovich *et al.* 2008). Sequestration of misfolded proteins is also thought to be important for rejuvenation of daughter cells. During asymmetric cell division, sequestered misfolded and damaged proteins were all inherited by the mother cell, giving the daughter cell clean components as well as full replicative potential (Aguilaniu *et al.* 2003; Ouellet & Barral 2012).

1.3.4 Classic model for quality control of newly synthesized proteins

In the 1970's, many studies of protein degradation in pre-labelled mammalian cells revealed that a large fraction of newly synthesized proteins (6% - 30%) was removed at a very fast rate within the first hour of chase, followed by a slower subsequent rate, with an obvious discontinuity between the two rates (Poole & Wibo 1973; Bradley *et al.* 1976; Goldberg & St John 1976). This was initially attributed to the fact that cells contain two classes of proteins: short-lived and long-lived proteins (Poole & Wibo 1973). However, a subsequent study found that electrophoretic separation of samples from short pulse treatments, with and without a substantial (1hour) chase, had no obvious alteration in their protein profiles, suggesting that the two different degradation rates most likely represent degradation rates of folding failure or success, respectively, rather than two subsets of proteins with different half-lives (Wheatley *et al.* 1980). In 2000, Schubert *et al.* reported that rapid degradation of such a large fraction of newly synthesized proteins depends on proteasome activity (Schubert *et al.* 2000). Since polypeptides normally

cannot complete folding until they are fully synthesized and released from ribosomes, this rapid degradation has generally been assumed to occur post-translationally, following, for example, failure of chaperone-assisted folding mechanisms (Figure. 1.5) (Hartl *et al.* 2011).

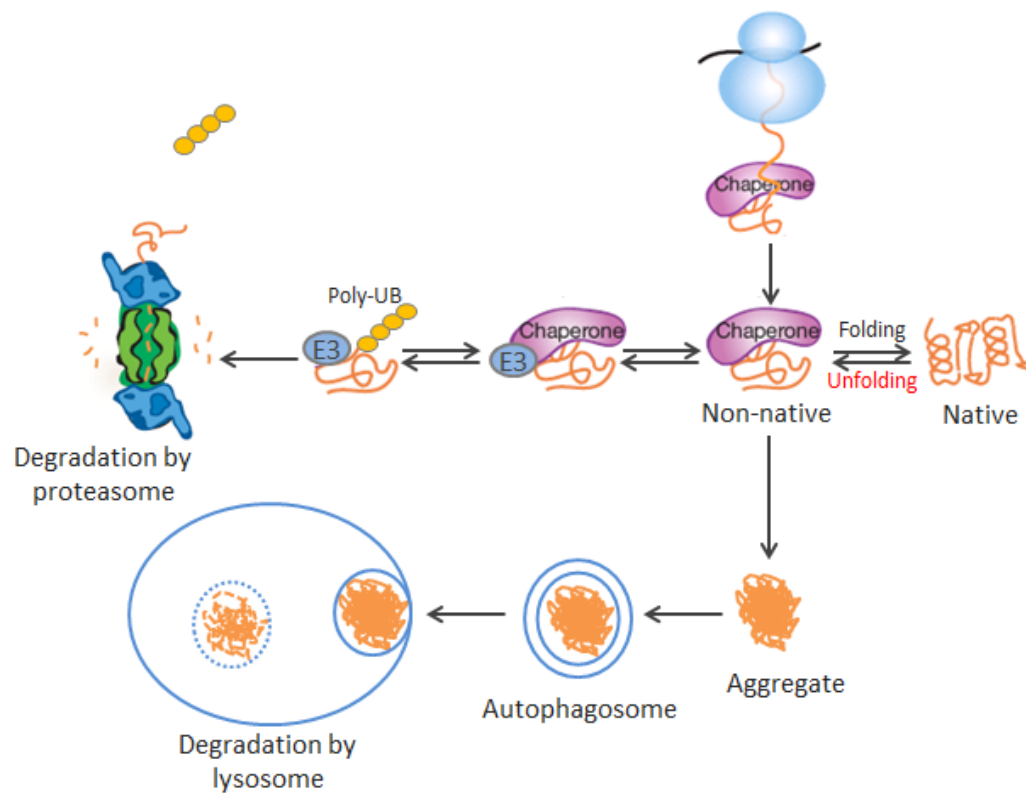


Figure 1.5: Classic post-translational model for quality control of newly synthesized proteins

In this classic model, quality control of newly synthesized proteins was generally assumed to start post-translationally, after polypeptides have been released from the ribosome. If they failed to fold into their native state even with the help of chaperones, ubiquitin E3 ligases will be recruited to target chaperone-bound misfolded proteins for proteasomal degradation. The protein aggregates are degraded by autophagy.

New evidence suggests that protein synthesis may be highly coupled with ubiquitination and degradation. Two studies observed co-translational ubiquitination of the cystic fibrosis transmembrane conductance regulator (CFTR), a very large protein prone to misfolding, and the secretory protein ApoB (Apolipoprotein B100) upon *in vitro* translation using rabbit reticulocyte lysates (Sato *et al.* 1998; Zhou *et al.* 1998). In addition, proteasomes were found to associate with the translation machinery (Sha *et al.* 2009). Furthermore, an elegant study using the ubiquitin sandwich technique showed that an engineered protein bearing an amino-terminal (N-end) degradation signal could be degraded co-translationally in *S. cerevisiae* (Turner & Varshavsky 2000). However, the extent, specificity, and significance of co-translational protein quality control remained largely elusive. The major goal of the Chapter 3 of my thesis is to address these questions.

1.3.5 Aging is linked to a gradual loss of cellular proteostasis

Aging is defined as the time-dependent functional decline of living organisms, presenting as a progressive loss of physiological integrity and increase in vulnerability to death. The underlying cause of aging was believed to be the accumulation of cellular damage (Lopez-Otin *et al.* 2013). Aging has attracted curiosity throughout the history of humankind. The new era of aging research began 30 years ago following the isolation of the first long-lived mutant strain of *C. elegans* (Klass 1983). Since then, the aging research has accelerated rapidly. Last year, Lopez-Otin and colleagues enumerated nine hallmarks of aging (Figure 1.6), according to the following criteria: 1) hallmarks should be presented during normal aging; 2) experimental aggravation of any hallmark should

accelerate aging; 3) experimental relief of any hallmark should retard the normal aging process (Lopez-Otin *et al.* 2013).

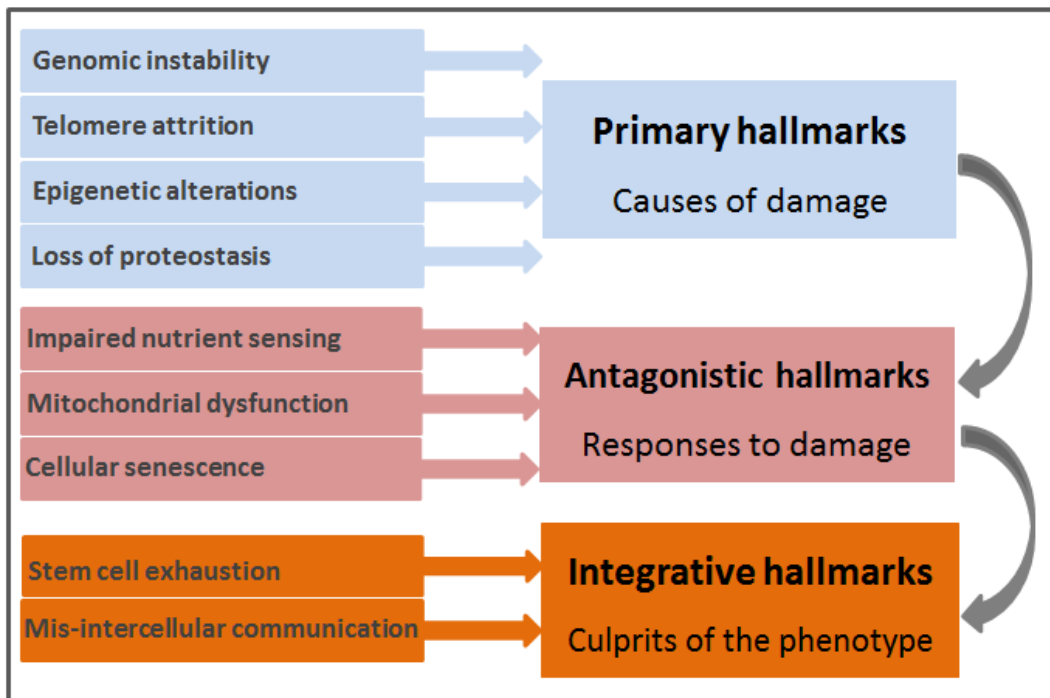


Figure 1.6: The hallmarks of aging.

Nine hallmarks of aging have been proposed by Lopez-Otin *et al.*: genomic instability, telomere attrition, epigenetic alterations, loss of proteostasis, deregulated nutrient sensing, mitochondrial dysfunction, cellular senescence, stem cell exhaustion, and altered intercellular communication. They are classified into three groups: primary hallmarks, antagonistic hallmarks, and integrative hallmarks.

Loss of proteostasis has been proposed as a hallmark of aging. Onset of many age-related diseases is connected to the accumulation of damaged proteins and/or protein aggregates, such as Alzheimer's disease, Parkinson's disease, and cataracts (Balch *et al.* 2008; Douglas & Dillin 2010; Lopez-Otin *et al.* 2013). What are the underlying reasons leading to the disruption of proteome homeostasis in aged organisms? Theoretically, both increased production of damaged proteins and functional decline of the protein quality control system could lead to the collapse of proteostasis. However, for a long time, loss of proteostasis during aging was only attributed to increased protein damage by reactive oxygen species (ROS), as proposed by the free radical theory of aging (Harman 1956). The predominant effort for anti-aging therefore, has been placed on the prevention of oxidative damage with antioxidants. In recent years, there has been increased evidence indicating that the activity of the protein quality surveillance system is essential for organisms enjoying their full life span and enhanced activity of protein quality control system can successfully extend the life span of different model organisms. Together, these establish a strong linkage between the protein quality control system and longevity (Figure 1.7) (Munoz 2003; Koga *et al.* 2011; Denzel *et al.* 2014).

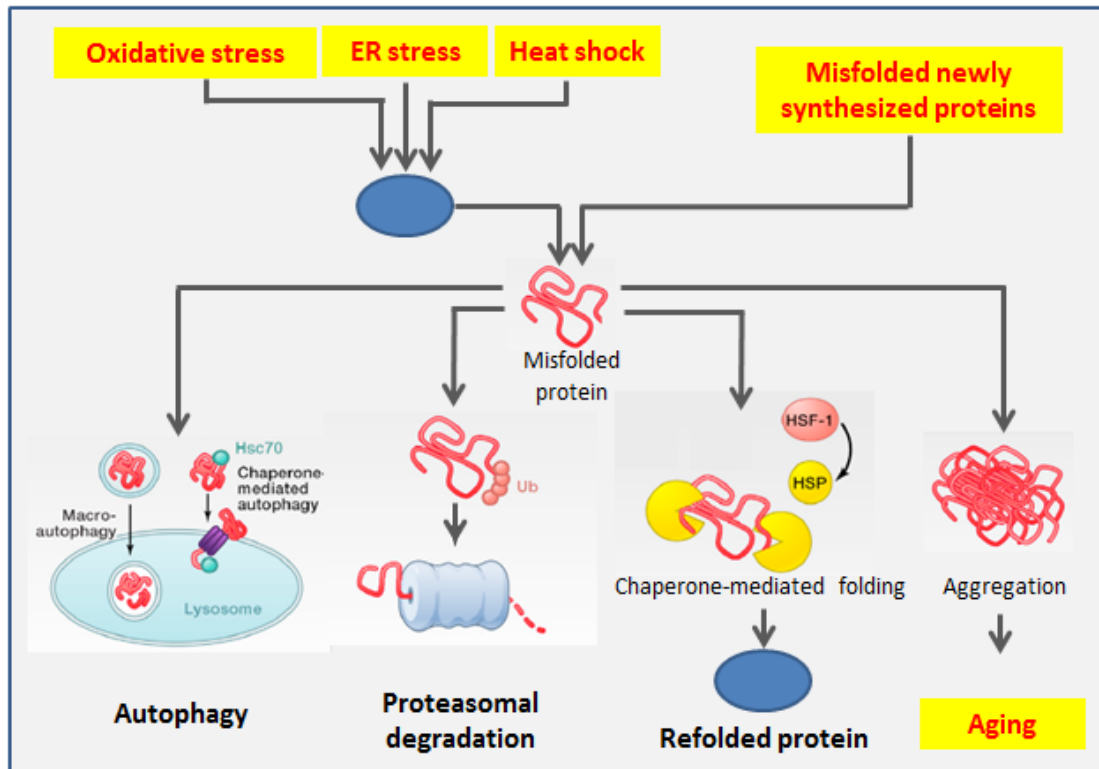


Figure 1.7: Loss of proteostasis is a hallmark of aging

Misfolded proteins may result from stress-induced unfolding of native proteins or from improperly folded newly synthesized proteins. Unfolded proteins are normally refolded by chaperones or targeted for proteasomal or lysosomal degradation. Failure to refold or degrade misfolded protein can lead to accumulation of protein aggregates and onset of some age-related diseases. Modified from Lopez-Otin *et al.* 2013.

Molecular chaperones in longevity and aging

The revelation that stress-stimulation of many heat shock proteins is impaired with aging has been shown in numerous studies. For example, stress-induced transcriptional up-regulation of HSP70 is decreased in many older organisms, including rats and monkeys (Fargnoli *et al.* 1990; Pahlavani *et al.* 1995). The reduced chaperone response can be restored by dietary restriction, successfully extending life span of various species, from yeast to human (Ehrenfried *et al.* 1996; Moore *et al.* 1998). Experimental induction of chaperones alone leads to an extended life span of most tested organisms, including both unicellular and multicellular organisms (Tatar *et al.* 1997). For instance, overexpression of heat shock factor (HSF), the transcriptional activator of chaperone proteins, successfully increased the longevity of *C. elegans*. Likewise, introducing extra copies of the HSP70 gene into flies and worms retarded their aging progress (Walker & Lithgow 2003). This phenomenon is not unique to cytosolic chaperones. Some organelle specific chaperones are also related to longevity, including ER specific chaperones, Bip, calnexin and PDI, and mitochondrial HSP70 (Kaul *et al.* 2003; Nuss *et al.* 2008). The molecular mechanism of the waning chaperone response during aging has been linked to the impaired ability of HSF to bind the heat shock element (HSE) on the promoters of chaperone genes (Heydari *et al.* 2000; Singh *et al.* 2006).

UPS in longevity and aging

The UPS system can be separated into two independent systems: 1) the ubiquitin conjugation system, containing ubiquitin, E1 activating enzymes, E2 conjugating enzymes, E3 ligases and deubiquitinases; 2) the proteasome, containing the 20S core

particle and the 19S regulatory particle. The activity of the proteasome and several ubiquitin conjugation enzymes has been shown to decrease to a certain degree with aging (Carrard *et al.* 2003; Ruotolo *et al.* 2003; Ferrington *et al.* 2005). In some aged tissues, a decreased level of free ubiquitin has been reported (Jahngen *et al.* 1990). Many reasons have been proposed to contribute to the reduction of proteasome activity: 1) unbalanced expression of α and β catalytic subunits (Chondrogianni *et al.* 2003); 2) reduced expression of proteasomal subunits (Keller *et al.* 2000); 3) incorrect posttranslational modification of critical proteasomal subunits (Bulteau *et al.* 2001); 4) decreased levels of ATP in aged cells, impairing the assembly of proteasomes (Vernace *et al.* 2007); 5) an accumulation of protein aggregates that obstruct proteasomal function (Andersson *et al.* 2013). The importance of the UPS in longevity has been further emphasized by the enhancement of proteasome activity, which can increase the life span of different model organisms (Kruegel *et al.* 2011).

Autophagy/lysosome system in longevity and aging

There are three different forms of autophagy in mammalian cells: macroautophagy, microautophagy and chaperone-mediated autophagy. Longevity is linked predominantly to macroautophagy. Macroautophagy is negatively regulated by the mTOR (mammalian target of rapamycin) signaling pathway, which is the key regulator of longevity (Kamada *et al.* 2000). Inhibition of mTOR through its inhibitor, rapamycin, successfully increases the life span of many organisms, and rapamycin-induced activation of macroautophagy is required for maximum life span extension (Bjedov *et al.* 2010; Rubinsztein *et al.* 2011). In addition to rapamycin, the microautophagy specific inducer, spermidine, was also able

to promote longevity of yeast, flies and worms (Eisenberg *et al.* 2009). Dietary supplementation of omega-6 polyunsaturated fatty acids, the fatty acids normally found in fish oil, also increased the life span of worms via induction of autophagy (O'Rourke *et al.* 2013). Consistent with its important role against aging, decreased activity of macroautophagy with age has been reported in many mammalian tissues (Cuervo *et al.* 2005; Cuervo 2008).

Protein translation and longevity

Most recently, the protein synthesis machinery has been proposed to be an important regulator of proteome homeostasis, as it functions in sensing the cellular folding environment, recruiting protein folding and translocation components, as well as adjusting elongation rate and pausing, which are essential for efficient *de novo* protein folding (Pechmann *et al.* 2013). In the last decade, a strong connection has been established between protein translation and aging. A growing pool of evidence indicates that reduced mRNA translation can significantly promote longevity in both invertebrate and vertebrate model organisms, including yeast, worms, flies, and mice (Hansen *et al.* 2007; Pan *et al.* 2007; Smith *et al.* 2008; Steffen *et al.* 2008; Selman *et al.* 2009; Zid *et al.* 2009; Johnson *et al.* 2013). However, the exact mechanism by which the reduction of protein translation could increase life span is unclear. Two major explanations have been proposed. Firstly, one piece of evidence suggests that a subset of mRNAs encoding proteins that are beneficial for longevity and stress resistance are translated more efficiently when global translation is reduced (Steffen *et al.* 2008; Zid *et al.* 2009; Rogers *et al.* 2011). Secondly, a global reduction of protein synthesis is predicted to reduce the

production of both normal and damaged proteins, which may allow the cellular protein repair and degradation system to maintain toxic proteins at lower levels. This would result in an increase in proteome homeostasis (Kaeberlein & Kennedy 2007). The goal of Chapter 4 of my thesis is to uncover the underlying mechanism of the reduced translation induced life span extension.

1.4 GOALS OF MY DOCTORAL WORK

In our 2010 paper, we demonstrated that Herc5 could ISGylate a target protein only if the target was synthesized within the same window of time that the ISG15 conjugation system was active. In addition, we found that Herc5 co-fractionated with poly-ribosomes (polysomes), strongly suggesting that ISG15 conjugation was closely coupled with protein translation. Based on these observations, we proposed a co-translational model for ISG15 conjugation: Herc5 associates with 60S ribosome subunit, and transfers ISG15 to the substrates when they are still being translated (Durfee *et al.* 2010). Although our previous data were consistent with this model, the direct evidence was still lacking. Therefore, the first part of my doctoral project was to rigorously test this co-translational model for ISG15 conjugation. Using two *in vitro* assays I developed (*in vitro* puromycin conjugation assay and run-off assay), I found that cells contain ISGylated ribosome-associated nascent chains, demonstrating that ISG15 is conjugated to the substrates in a co-translational manner.

Up to 30% of all newly synthesized proteins are rapidly degraded in eukaryotic cells in a proteasome-dependent manner. Consistent with this observation, it was recently reported that a large fraction of the total human ubiquitin-modified proteome is derived

from newly synthesized proteins. The second part of my thesis was to examine the relationship between protein translation, ubiquitination, and degradation. Using the approaches developed for studying co-translational ISGylation, I found that the pathway for degradation of newly synthesized proteins can be initiated while proteins are being actively translated, with cotranslational ubiquitination (CTU) of nascent polypeptides. This work defined CTU as a pathway for quality control of newly synthesized proteins.

Finally, a dramatic decrease of protein translation fidelity could lead to accumulation of misfolded proteins and hasten the aging process. As CTU is the pathway for quality control of newly synthesized proteins, the goal for the third part of my thesis was to explore whether CTU plays a protective role during the cellular aging process.

Chapter 2: ISG15 is co-translationally conjugated to ribosome-associated nascent polypeptides

2.1 INTRODUCTION

ISG15 is a 17 kD IFN- α/β -induced ubiquitin-like modifier consisting of two ubiquitin-like domains. ISG15 has anti-viral activity against several types of RNA and DNA viruses, including influenza, Sindbis, herpes, HIV, and Ebola virus (Lenschow *et al.* 2005; Okumura *et al.* 2006; Okumura *et al.* 2008; Giannakopoulos *et al.* 2009; Hsiang *et al.* 2009; Lai *et al.* 2009). The E1, E2, and E3 enzymes that mediate ISG15 conjugation are also IFN- α/β -induced proteins, and these are Ube1L, UbcH8, and Herc5, respectively. Herc5 is a HECT domain ligase with N-terminal RCC1 repeats, and it is the only human HECT E3 known to conjugate a modifier other than ubiquitin (the mouse homolog, Herc6, is an IFN-induced HECT E3 that plays the equivalent role in mouse cells (Versteeg *et al.* 2010)). The biochemical effect of conjugation on target proteins remains unknown, although, like most other ubiquitin-like modifiers, it does not appear to specify proteasomal degradation. The utilization of a single E1 and E2 enzyme for ISG15 conjugation is consistent with other Ubl conjugation systems (e.g., Sumo, Nedd8), although it was surprising that a single E3 enzyme was responsible for nearly all ISG15 conjugation activity, given that mass spectrometry-based target identification studies had identified approximately 300 high-confidence targets in human cells (Malakhov *et al.* 2003; Giannakopoulos *et al.* 2005; Zhao *et al.* 2005; Takeuchi *et al.* 2006). siRNA depletion of Herc5 strongly suppressed overall conjugation, as well as conjugation to all individual target proteins analyzed (Dastur *et al.* 2006). Furthermore, co-expression of ISG15, Ube1L, UbcH8, and Herc5 in non-interferon-stimulated cells effectively

reconstituted total ISG15 conjugation, indicating that these proteins represent the core IFN-induced components of this conjugation system (Dastur *et al.* 2006). The cellular targets of ISG15 belong to many functional classes of proteins, and there were no apparent common characteristics of the target proteins (e.g., intracellular localization, potential recognition motifs). Therefore, a key question was how a single E3 enzyme was capable of recognizing such a large and diverse set of target proteins.

We previously demonstrated that Herc5 could ISGylate a target protein only if the target was synthesized in the same window of time that the ISG15 conjugation system was active. In addition, Herc5 was shown to co-fractionate with polysomes and free 60S ribosomal subunits, strongly suggesting that the processes of ISGylation and protein translation were closely coupled (Durfee *et al.* 2010). We proposed a model in which Herc5 stochastically modifies proteins, with very little substrate selectivity, as they are translated. In the context of an IFN-stimulated cell, this further suggested that newly translated viral proteins may be an important class of ISG15 targets, and that the inherent lack of substrate specificity of the system might be viewed as an attempt to target the widest possible range of viral proteins. Here, we test a critical aspect of the co-translational model for conjugation of ISG15 by demonstrating that nascent polypeptides are ISGylated within active translation complexes.

2.2 MATERIALS AND METHODS

Plasmids and antibodies: Plasmids expressing Ube1L, Ube1L- Δ UFD, UbcH8, UbcH8-F62A, HA-Herc5, HA-Herc5-C994A, and 3XFLAG-ISG15 were described previously (Zhao *et al.* 2005; Dastur *et al.* 2006; Durfee *et al.* 2008). 3XFLAG-ISG15-AA was made in this study by replacing the terminal glycine residues of ISG15 with alanines. Five methionine codons were introduced at the 3' end of the ORFs encoding pcNTAP-IQA, -IQC, -p56, and FLAG-NS1A (Durfee *et al.* 2010). Anti-Ube1L and Anti-FLAG M2 antibodies were purchased from Sigma Aldrich, anti-UbcH8 antibody was purchased from Abgent, anti-HA antibody was purchased from Covance, and anti-TAP antibody was purchased from Rockland Immunochemicals. Anti-puromycin antibody was a gift from Peter Walter (University of California, San Francisco)

Cell culture, transfections, IFN- β treatment, and immunoblotting: HeLa and HEK293T cells were maintained in Dulbecco's modified Eagle's medium (DMEM) supplemented with 10% fetal bovine serum. Plasmid DNA transfections were performed with cells at 60%-80% confluence by using Lipofectamine 2000 transfection reagent (Invitrogen). For the experiment shown in figure 2.3B, HeLa cells were transfected with either 3xFLAG-ISG15 or 3xFLAG-ISG15-AA as indicated. Twenty-four hours post-transfection, ISG15 conjugation was induced by treating cells with 1000 units/ml IFN- β for another 24 hours. Cells were harvested and lysed in lysis buffer containing 1% NP-40, 100 mM Tris, pH 7.9, 100 mM NaCl, 1 mM DTT, 100 μ M phenylmethylsulfonyl fluoride (PMSF), 4 μ M leupeptin, and 0.3 μ M aprotinin.

Protein expression and purification: Purified ISG15 was obtained by expression in *E. coli* as a GST fusion protein, with an added cAMP-dependent kinase recognition motif (RRASV). Cells were collected and resuspended in phosphate-buffer saline (PBS) containing 1% Triton X-100 (Sigma) and lysed by sonication. ISG15 was

purified from total cell lysate using GST-Bind Resin (Novagen) and resuspended in 50 μ l of kinase buffer (40 mM Tris, pH 7.5, and 20 mM MgOAc). 32 P labeling of ISG15 was performed by adding 2 μ l of adenosine 5'-[γ - 32 P] triphosphate (PerkinElmer Life Sciences) and 2 μ l of cAMP-dependent protein kinase (Promega). After 1h rotation at room temperature, unincorporated adenosine 5'-[γ - 32 P] triphosphate was removed by washing beads with kinase buffer. GST-ISG15 protein was then subjected to site-specific cleavage with PreScission protease (GE Healthcare) to release ISG15 from beads. The activity of purified ISG15 was tested in an E1-E2 thioester assay (Durfee *et al.* 2008), which was performed in the presence of 25 mM Tris-HCl (pH 7.5), 50 mM NaCl, 5 mM MgCl₂, 0.1 mM DTT, 50 μ g/ml of purified ISG15, 1.25 μ g/ml of Ube1L (Boston Biochem), and 5 μ g/ml UbcH8 (Boston Biochem).

Polysome preparation and *in vitro* run-off translation assays: A single 150-mm culture dish of either HeLa or 293T cells was harvested and lysed in 3 ml ice-cold lysis buffer containing 100 mM Tris (pH 7.4), 50 mM KCl, 25 mM MgCl₂, 1 mM DTT, 100 μ M PMSF, 4 μ M leupeptin, 0.3 μ M aprotinin, 200 μ g/ml heparin, and 40 U/ml RNaseOUT RNase inhibitor (Invitrogen). Lysates were clarified by centrifugation at 16,300 x g for 10 min at 4°C, and the supernatants were loaded on top of a 2 ml 35% sucrose solution (10mM Tris, pH 7.4, 85mM KCl, 5mM MgCl₂, 35% sucrose) and centrifuged for 90 min at 60,000 rpm in a Beckman NVT 65.2 rotor at 4°C. The polysome-containing pellets were resuspended in polysome buffer (10 mM Tris pH 7.4, 10 mM NaCl, 3 mM MgCl₂, and 0.2 mM DTT) at a concentration of 30 A₂₆₀ unit/ml and stored at -80°C.

In vitro run-off translations were performed as described previously (Vayda 1995), with addition of 1 A₂₆₀ units of polysomes, 25 μ l rabbit reticulocyte lysate (RRL; Promega), 20 μ M amino acid mixture (minus methionine), 10 mCi/ml 35 S-methionine,

and 4 μ l TNT reaction buffer to each 100 μ l run-off reaction. Aurintricarboxylic acid (ATA; Sigma) was added to a final concentration of 0.1 mM to inhibit translation initiation (Stewart *et al.* 1971). After 1h incubation at 30 °C, one volume of RIPA buffer (50 mM Tris ,pH 7.4, 150 mM NaCl, 1% NP-40, 0.1% SDS) was added to terminate the reaction, and the mixtures were incubated with either Anti-FLAG M2 Affinity Gel (Sigma) or IgG-agarose (Sigma) overnight at 4 °C. The beads were washed four times with 0.1% NP-40 buffer (0.1% Nonidet P-40, 100 mM Tris, pH 7.9, 100 mM NaCl). Proteins were eluted from beads by adding SDS-PAGE loading buffer and boiling at 90°C for 5 min, and the samples were analyzed by SDS-PAGE and autoradiography. For cycloheximide (CHX) treatment, CHX was added to the reaction at a final concentration of 200 μ g/ml, and for the RNase treatment, RNase (Sigma) was added to polysome fractions at a final concentration of 10 μ g/ml. The mixture was incubated at 4 °C for 5 min before addition to the run-off translation reaction.

***In vitro* puromycin conjugation assays:** Each 100 μ l Bio-Puro conjugation assay contained the following components: 10 mM Tris, pH 7.4, 400 mM KCl, 3 mM MgCl₂, 2 A₂₆₀ units of polysomes, and 2 μ M biotin-linked puromycin (Jena Bioscience). Puromylation reactions were performed at 37°C for 90 min and post-reaction, 5% of each sample was analyzed to determine the total nascent chains labeled. For immunoprecipitation of FLAG-Ub modified nascent chains, two volumes of RIPA buffer (50 mM Tris, pH 7.4, 150 mM NaCl, 1% NP-40, 0.1% SDS) was added to equal amounts of total nascent chains, and the mixtures were incubated with anti-FLAG M2 Affinity Gel (Sigma-Aldrich) overnight at 4°C. The beads were washed four times with 0.1% NP-40 buffer (0.1% NP-40,100 mM Tris, pH 7.9, 100 mM NaCl). Proteins were eluted from beads by adding SDS-PAGE loading buffer and boiling at 90°C for 5 min, and the samples were analyzed by SDS-PAGE and probed with

fluorescently tagged streptavidin. For the experiment shown in Figure 2.2, polysomes were pretreated with either 200 $\mu\text{g/ml}$ CHX (lane 5), 0.1 mg/ml RNase (lane 6), 10 μM unlabeled puromycin (lane 7), or 10 $\mu\text{g/ml}$ biotin at 30°C for 15 min.

2.3 RESULTS

2.3.1 Establishment of *in vitro* run-off translation and biotin-puromycin conjugation reactions.

To determine whether nascent polypeptides were present in an ISGylated state within active translation complexes, we developed two *in vitro* assays to specifically probe ribosome-associated nascent chains: the *in vitro* run-off translation assay and the *in vitro* biotin-puromycin conjugation assay. *In vitro* run-off translation systems have been described previously, where polysomes are partially purified from cell extracts, and translation of the associated nascent chains is completed *in vitro* in the presence of ³⁵S-methionine, translational cofactors, and an inhibitor of translation initiation (aurintricarboxylic acid; ATA) (Stewart *et al.* 1971). The radiolabeled products of the reaction represent proteins that were initiated *in vivo* and completed *in vitro*.

To first establish parameters and requirements for run-off translation, polysomes were collected from 293T cell extracts by centrifugation through 35% sucrose and added to reactions containing rabbit reticulocyte lysate (RRL), ³⁵S-methionine, amino acids, and ATA. Figure 2.1A (lane 1) shows the complete spectrum of translation products from this reaction. Generation of the radiolabeled proteins was dependent on addition of polysomes and RRL, and all reaction products were eliminated when the polysome fraction was pre-treated with RNase or cycloheximide (Figure 2.1A). Products were not significantly altered when the reaction was performed without addition of either exogenous amino acids (presumably due to a sufficient supply in the reticulocyte lysate) or ATA (Figure 2.1A). As expected, since polysome-associated ribosomes direct translation of the run-off products, ribosome-depleted RRL supported run-off translation (Figure 2.1B), indicating that the required components contributed by the RRL were soluble translation factors and other small molecules (*e.g.*, eEF1A, eEF2, aminoacyl-tRNAs, amino acids, GTP).

To determine whether individual proteins could be detected within total run-off reactions, polysomes were isolated from cells that had been transfected with a plasmid expressing either IQ-A or IQ-C (two previously described fragments of IQGAP1(Durfee *et al.* 2010)), both of which contained an N-terminal TAP tag and a C-terminal five-methionine (5M) tag to increase incorporation of radiolabel. IgG sepharose beads were used to isolate the TAP-tagged proteins from the run-off reactions, and ³⁵S-labeled products corresponding to the predicted size of both proteins were detected (Figure 2.1C). These results indicated that the assay was sensitive enough to detect a specific protein generated from a mixture of total polysome-associated nascent polypeptides.

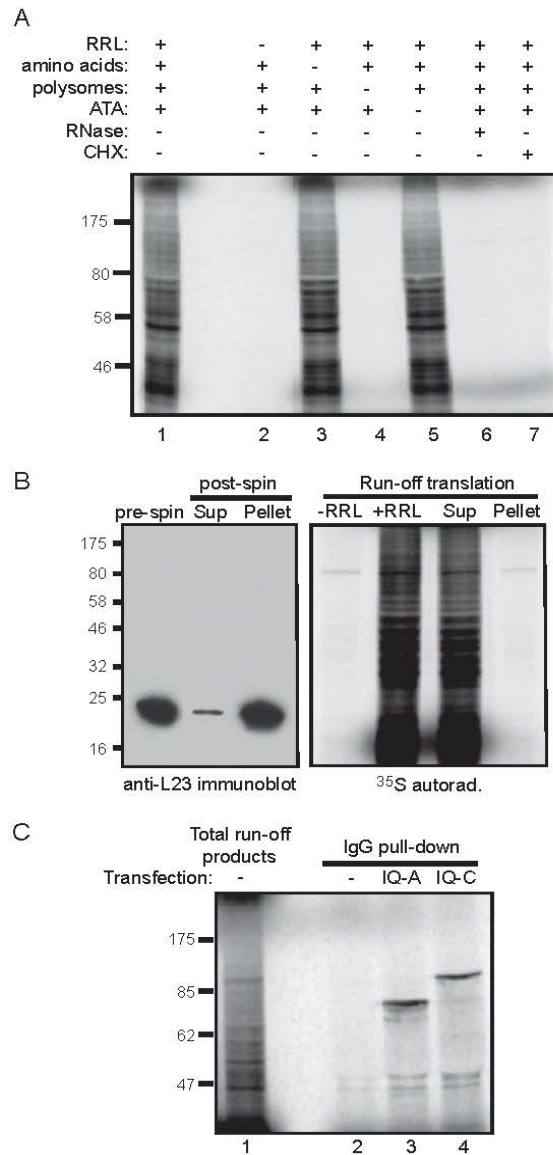


Figure 2.1: *In vitro* run-off translation reactions.

(A) Requirements for the *in vitro* run-off translation reaction. RRL: rabbit reticulocyte lysate; ATA: aurintricarboxylic acid; CHX: cycloheximide. (B) The ribosomes present in RRL are not required for the run-off reaction. Ribosomes were depleted from RRL by ultracentrifugation. The left panel shows an immunoblot for the L23a ribosomal protein in RRL (pre-spin), the supernatant from the spin (Sup), and the pellet fraction. Only a small amount of L23a was left in the supernatant, yet it supported run-off translation similarly to complete RRL (right panel). (C) Run-off translation, examining individual proteins. The total spectrum of ^{35}S -labeled run-off products generated from 293T polysomes is shown in lane 1. Lanes 2-4 show IgG sepharose pull-downs of run-off products generated from polysomes isolated from untransfected cells (lane 2), cells transfected with TAP-tagged IQ-A-5M (80 kD predicted product; lane 3), or TAP-tagged IQ-C-5M (100 kD predicted product; lane 4).

Puromycin is a structural analog of aminoacyl-tRNA that blocks translation by forming a covalent bond with the carboxyl-terminus of nascent polypeptides (Pestka 1971). We utilized biotin-conjugated puromycin (Bio-Puro) to label polysome-associated nascent polypeptides *in vitro*. To establish reaction parameters, polysomes were collected from HEK293T cell extracts by centrifugation through 35% sucrose and incubated *in vitro* with Bio-Puro. Total reaction products were resolved by SDS-PAGE, blotted to nitrocellulose, and probed with fluorescent streptavidin. Figure 2.2 (lane 2) shows the complete spectrum of reaction products. Generation of the products was dependent on addition of Bio-Puro, as opposed to either free biotin (lane 3) or unlabeled puromycin (lane 4), and products were almost completely eliminated when polysomes were pretreated with RNase or unlabeled puromycin (Figure 2.2, lanes 6 and 7). The inhibitory effect of RNase on this reaction was likely due to cleavage of the peptidyl-tRNA ester linkage, which leads to release of nascent chains (Kelkar *et al.* 2012). The prior addition of cycloheximide to polysomes *in vitro* (CHX; lane 5) had no effect on the Bio-Puro reaction, consistent with the fact that CHX inhibits ribosome translocation without affecting peptidyl transferase activity (David *et al.* 2012).

Pretreatment:	-	-	-	-	CHX	RNase	Puro	Bio
Bio-Puro:	-	+	-	-	+	+	+	+
Biotin:	-	-	+	-	-	-	-	-
Puro:	-	-	-	+	-	-	-	-

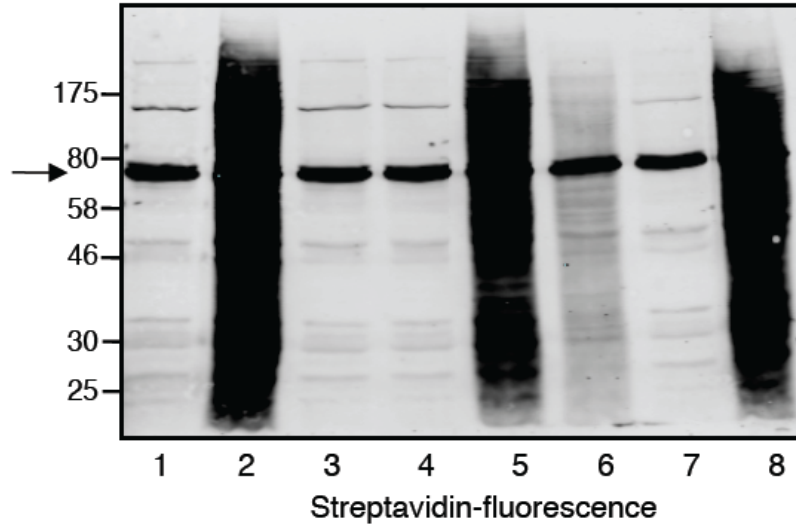


Figure 2.2: Validation of *in vitro* biotin-puromycin (Bio-Puro) conjugation reaction.

Polysomes from HEK293T cells were used in all reactions. Reaction with Bio-Puro is shown in lane 2; Bio-Puro was deleted in lane 1, and replaced by free biotin (Bio) in lane 3 or by untagged puromycin (Puro) in lane 4. Polysomes were pretreated with cycloheximide (CHX), RNase, untagged puromycin or biotin in lane 5, 6, 7, and 8 respectively. Bio-Puro was detected with fluorescently-labeled streptavidin. Background bands seen, for example, in lane 1, represent endogenous biotin-conjugated proteins (*e.g.*, arrow at 74 kD represents priopionyl-CoA carboxylase).

2.3.2 Polysome-associated nascent chains are ISGylated

The run-off translation assay was used to determine whether ISGylated nascent polypeptides were present within active translation complexes. As illustrated in Figure 2.3A, the cotranslational model for ISGylation predicts that Herc5 transfers ISG15 to nascent chains on polysomes; if so, then the *in vitro* run-off products will contain proteins that are both ISGylated and labeled with ³⁵S-methionine. In the first experiment, HeLa cells were transfected with a plasmid expressing 3XFLAG-ISG15 (3F-ISG15) or 3F-ISG15-AA, a non-conjugatable form of ISG15 with the two terminal glycine residues converted to alanines; the cells were then either treated with IFN- β , or left untreated, for 24 hours. Figure 2.3B (left) shows an anti-FLAG immunoblot of total cell extracts, demonstrating that in the presence of IFN- β treatment only 3F-ISG15, and not 3F-ISG15-AA, was conjugated to cellular proteins. Polysomes from these extracts were then used in run-off translation reactions, and Figure 2.3B (center) shows that the distribution of total radiolabeled run-off products was similar in all reactions. Figure 2.3B (right) shows the anti-FLAG-ISG15 immunoprecipitation of the run-off products, demonstrating that FLAG-ISG15-containing radiolabeled run-off products could be immunoprecipitated from the reaction programmed with polysomes from IFN-treated cells, but not with polysomes from non-IFN-treated cells or cells that expressed 3F-ISG15-AA. These results indicate that ISG15 was conjugated to nascent chains *in vivo* in the context of fully competent translation complexes.

A second experiment was performed using non-IFN-stimulated 293T cells expressing 3FISG15, Ube1L, UbcH8, and Herc5, or, as a control, 3F-ISG15 with inactive mutant forms of Ube1L (Δ UFD), UbcH8 (F62A), and Herc5 (C994A) (Durfee *et al.* 2010). Consistent with the results above, radiolabeled 3F-ISG15 conjugates were

immunoprecipitated only from reactions programmed with polysomes from cells expressing the active conjugation enzymes (Figure 2.3C).

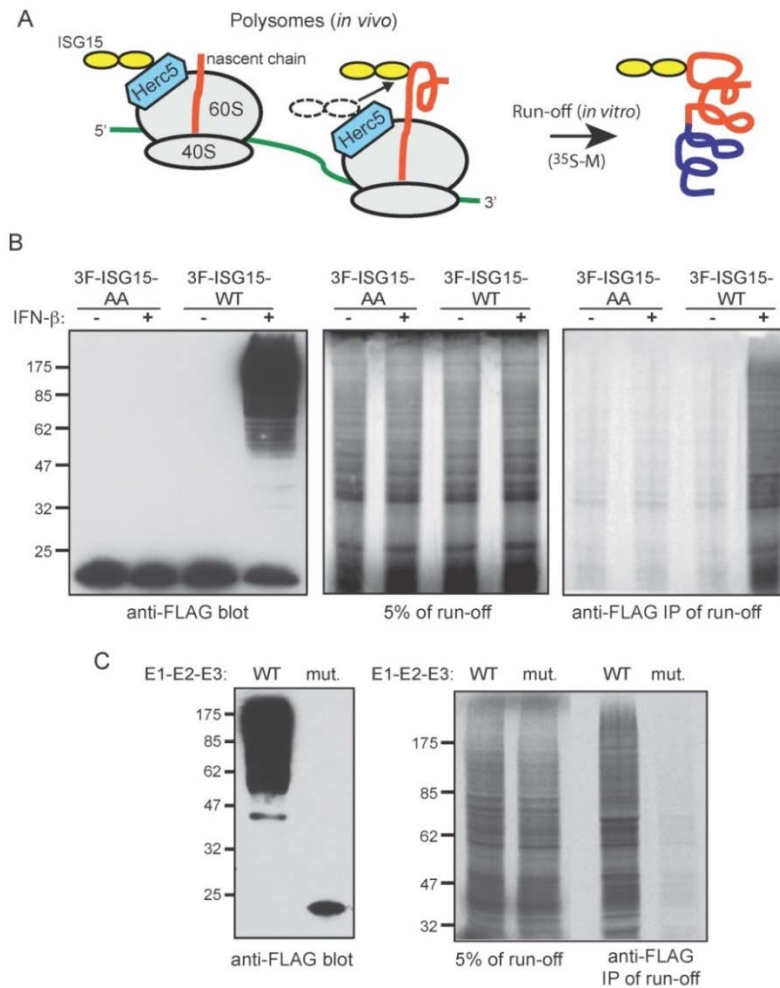


Figure 2.3: Polysome-associated nascent chains are ISGylated.

(A) Design of the run-off translation experiments. The co-translational model proposes that Herc5 modifies nascent chains on actively translating polysomes (left). The *in vitro* run-off translation products programmed with these polysomes should therefore contain proteins that were initiated and ISGylated *in vivo*, and translated to completion (in the presence of ^{35}S -methionine; ^{35}S -M) *in vitro*. (B) IFN- β -stimulated cells contain ISGylated nascent polypeptides. (C) Cells were transfected with plasmids expressing 3F-ISG15, Ube1L, UbcH8, and Herc5 (WT), or 3F-ISG15 with inactive mutant forms (mut.) of Ube1L (ΔUFD), UbcH8 (F62A), and Herc5 (C994A). Left panel shows an anti-FLAG immunoblot of total cells extracts, and right panel shows 5% of the run-off reactions and the anti-FLAG immunoprecipitates of the run-off reactions.

For the run-off experiments, it was important to demonstrate that the ISGylation of these radiolabeled proteins occurred *in vivo*, when they were nascent polypeptides, rather than in the *in vitro* run-off reaction. As shown in figure 2.4A, when ³²P-labeled ISG15 was added to complete run-off reactions, it was not detectably activated or conjugated to any proteins, even when the polysomes were derived from cells expressing the wild-type conjugating enzymes (right panel; lane 4 compared to negative controls, lanes 2 and 5). Figure 2.4A (left panel) shows that the radiolabeled ISG15 used in this experiment was fully competent in forming thioester adducts with purified recombinant Ube1L and UbcH8. In addition, there was no detectable free ISG15, Ube1L, or UbcH8 present in the polysome fractions derived from cells expressing the complete conjugation system (Figure 2.4B). Herc5, as expected, co-purified with polysomes (Figure 2.4B). We therefore conclude that the ISGylated run-off products, generated from polysomes from cells expressing ISG15, Ube1L, UbcH8, and Herc5 proteins, were ISGylated *in vivo* as nascent polypeptides.

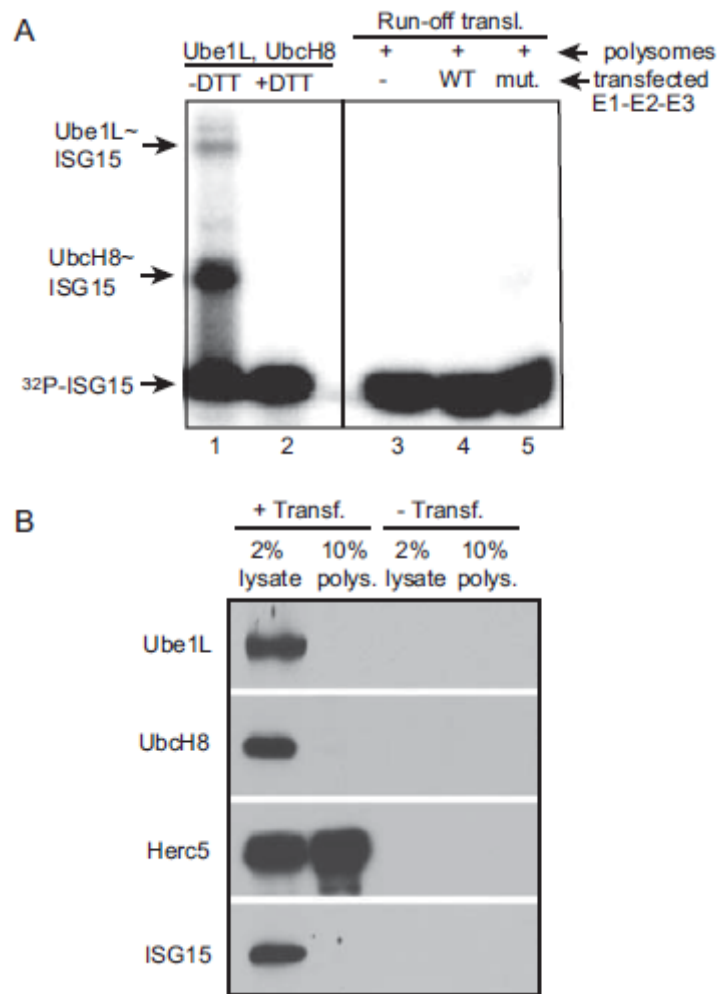


Figure 2.4: ISGylation does not occur in the run-off reaction.

(A) ³²P-labeled ISG15 was prepared and shown to be competent for conjugation in an *in vitro* Ube1L- and UbcH8-dependent thioester assay; Ube1L~ISG15 and UbcH8~ISG15 adducts are indicated in lane 1, and these adducts are disrupted in the presence of DTT. ³²P-labeled ISG15 was added to run-off translation assays programmed with polysomes from untransfected cells (lane 3), cells transfected with wild-type Ube1L, UbcH8, and Herc5 (lane 4), or cells transfected with inactive mutant versions of each enzyme (lane 5). The ³²P-labeled ISG15 was not incorporated into conjugates in any case. (B) Ube1L, UbcH8, and free ISG15 were not present in polysome fractions from cells co-transfected with ISG15, Ube1L, UbcH8, and Herc5. Herc5, as expected, was the only component that co-fractionated with polysomes. Control immunoblots from untransfected cells are shown in the right two lanes.

We also utilized Bio-Puro, a translation terminator, in an alternative test of the co-translational model. Puromycin terminates translation by being covalently incorporated into the C-terminus of nascent polypeptides. As above, polysomes were first isolated from cells in the absence or presence of active ISGylation components (3F-ISG15, Ube1L, UbcH8, Herc5). However, rather than adding rabbit reticulocyte lysate and other run-off reaction components, the polysomes were incubated only with puromycin, in the absence of any additional proteins, amino acids, or translation factors. As in the run-off reactions, the prediction was that if ISGylated nascent chains were present on polysomes, then these chains should subsequently incorporate Bio-Puro at their C-termini. Following incubation with Bio-Puro, 3F-ISG15 conjugates were immunoprecipitated with anti-FLAG antibody and then probed with fluorescent streptavidin. As shown in Figure 2.5, Bio-Puro was robustly incorporated into ISG15-containing nascent polypeptides, confirming that nascent polypeptides are substrates for ISGylation.

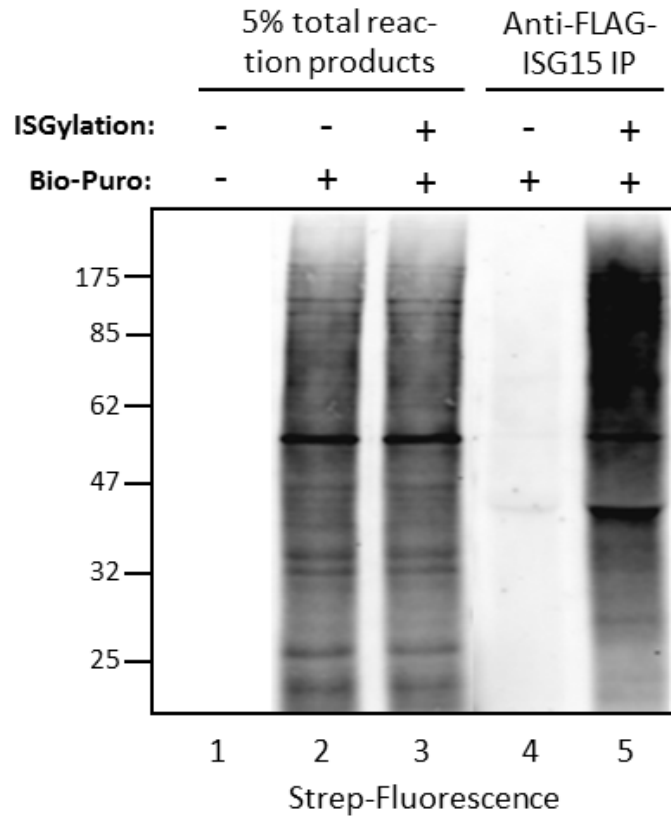


Figure 2.5: Incorporation of biotin-conjugated puromycin (Bio-Puro) into ISG15-containing nascent chains.

Cells were co-transfected with 3F-ISG15 and wild-type Ube1L, UbcH8, and Herc5 (ISGylation +) or mutant forms of the enzymes (ISGylation -), and polysomes were isolated and incubated with or without puromycin. 3F-ISG15 containing polypeptides were immunoprecipitated with anti-FLAG antibody and probed with fluorescent streptavidin (lanes 4 and 5). Lanes 1-3 represent 5% of the total puromycin-containing reaction products before immunoprecipitation.

2.3.3 ISGylation of nascent polypeptides of individual target proteins

I also examined ISGylation of individual target proteins by expressing, along with the conjugation components, target proteins with an N-terminal tag (TAP or FLAG) and a C-terminal 5M tag. Four target proteins were examined in this context: IQ-A, IQ-C, p56, and NS1A. As described above, IQ-A and C are two non-overlapping fragments of human IQGAP1, a previously identified ISG15 target protein (Zhao *et al.* 2005). p56 is a well-studied interferon-induced protein (Sen & Sarkar 2007) that was also identified as an ISG15 target (Zhao *et al.* 2005), and ISGylation of the influenza A NS1 protein (NS1A) has been shown to inhibit virus replication (Zhao *et al.* 2010). Typically, only 5-20% of the total pool of a newly synthesized protein is ISGylated (Durfee *et al.* 2010), and that run-off products are predicted to contain both unmodified and ISGylated forms of the full-length target proteins, with the unmodified form predominating. Figure 2.6 (left panels) shows Western blots of total cell extracts for the four different target proteins (TAP-IQ-A, TAP-IQ-C, TAP-p56, and FLAG-NS1A), demonstrating that all four proteins were ISGylated when co-expressed with ISG15, Ube1L, UbcH8, and Herc5. Figure 2.6 (right panels) shows the anti-TAP or anti-FLAG IPs of the corresponding run-off translation products. In all cases, full-length unmodified and ISGylated forms of the target proteins were detected in reactions programmed with polysomes from cells expressing the complete conjugation system. The higher molecular weight conjugates of p56 were not detected in the run-off immunoprecipitation, which may be due to the position of the modification sites within the protein (*i.e.*, the run-off assay has an inherent bias toward detecting more N-terminal ISGylation events).

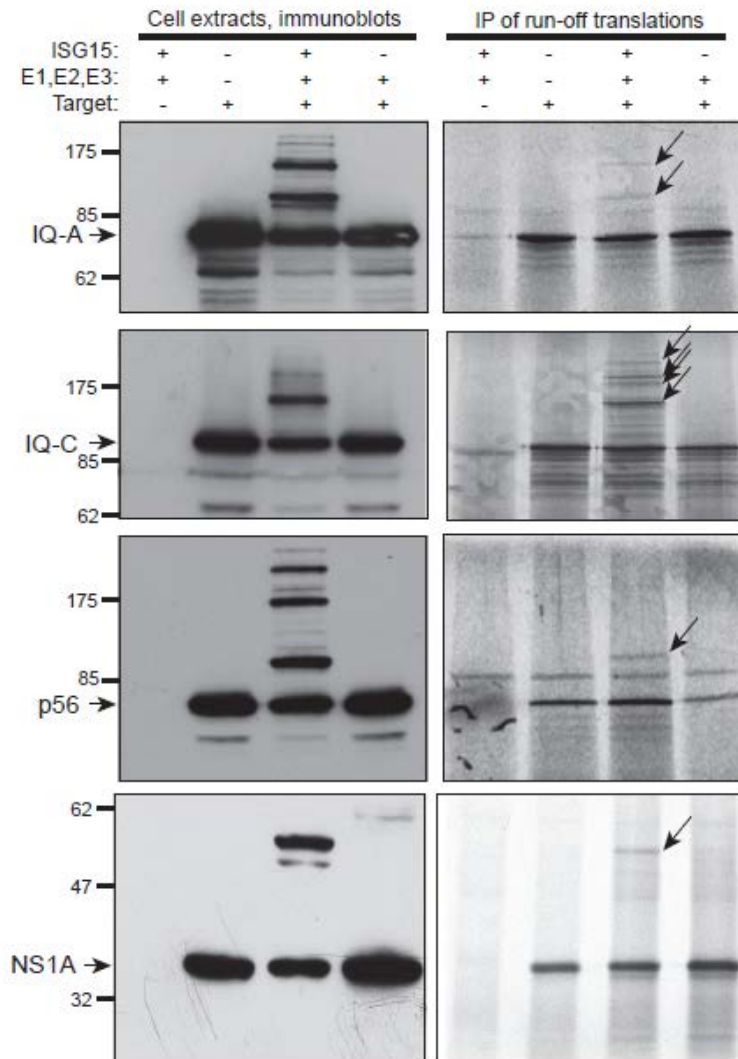


Figure 2.6: ISGylation of nascent polypeptides of individual target proteins.

Four targets were examined: TAP-tagged IQ-A, IQ-C, and p56, and FLAG-tagged influenza NS1A. The targets were expressed by transfection, either by themselves or with plasmids expressing the E1, E2, and E3 enzymes, with or without ISG15. Left panels show immunoblots of total cell extracts (either anti-TAP or anti-FLAG). Right panels show autoradiograms of the run-off translation reaction products after IgG pulldown of the TAP-targets or anti-FLAG IP of NS1A. Arrows indicate the major ISGylated run-off products for each protein.

2.4 DISCUSSION

The results presented here demonstrate that nascent ribosome-associated polypeptides are ISGylated while they are engaged in active translation complexes. This strongly supports the model that Herc5 is poised on the 60S ribosome to stochastically ISGylate a very broad spectrum of newly synthesized proteins, as they emerge from the ribosome.

The efficiency of ISGylation, even when examining newly synthesized pools of proteins, is relatively low, with typical modification levels ranging from 5-20% of a given target protein. Although the basis of the apparent inefficiency of ISGylation is unknown, I speculate that the system is tuned to be efficient enough to elicit antiviral responses (*e.g.*, through dominant-negative effects on viral structural proteins (Durfee *et al.* 2010)), yet inefficient enough to avoid extensive damage to newly translated cellular proteins. There are several possible factors that might influence ISGylation efficiency, including translation rates, co-translational folding rates, and primary or secondary structural elements that promote or interfere with ISGylation. Identifying the factors that influence the “code” for ISGylation will be important for understanding how Herc5 recognizes lysine residues within nascent chains and may have implications for the evolution of viral protein sequences (*i.e.*, have viral protein sequences been selected for evasion of ISGylation?).

The use of run-off translation assays and the reaction of puromycin with partially purified polysomes allowed us to test the co-translational model in the absence of a completely reconstituted *in vitro* ISGylation system. It is now clear that complete *in vitro* reconstitution will require, at a minimum, the complete set of conjugating enzymes and an active translation system. Purified and biochemically active ISG15, Ube1L, and

UbcH8 are available (Durfee *et al.* 2008), and future efforts will be focused on the incorporation of biochemically active Herc5 into *in vitro* translation systems.

Although Herc5 co-fractionates with 60S ribosomal subunits, the direct contact site(s) for Herc5 on this subunit are not yet known, but these could obviously be composed of rRNA and/or ribosomal proteins. Herc5 contains N-terminal RCC1 repeats, which, based on analogy to the yeast RCC1 protein, are likely to form a seven-bladed β -propeller. The RCC1 repeats of Herc5 are required for ribosome co-fractionation (Durfee *et al.* 2010), and interestingly, yeast RCC1 is a chromatin-associated protein by interaction with both nucleic acid and protein within nucleosome complexes (Makde *et al.* 2010). An attractive model is that Herc5 is positioned near the polypeptide exit tunnel on the 60S subunit, modifying nascent chains as they emerge. Interestingly, ubiquitin- and proteasome-dependent degradation of newly synthesized misfolded or damaged proteins has been described in several contexts (Schubert *et al.* 2000; Turner & Varshavsky 2000; Bengtson & Joazeiro 2010), and it will be interesting to determine whether the ligases required for these processes are related to Herc5 with respect to enzyme mechanism, recognition of nascent chains, and their physical link to the translational machinery.

Chapter 3: A co-translational ubiquitination pathway for quality control of newly synthesized proteins¹

3.1 INTRODUCTION

Newly synthesized proteins are prone to misfolding and aggregation (Ellis 2001), and this is compounded by errors in processes affecting transcription, mRNA processing, translation, and protein localization (Levine *et al.* 2005; Ogle & Ramakrishnan 2005; Pickrell *et al.* 2010). As a result, a significant fraction of newly synthesized proteins never attain their functional state. Timely and efficient clearance of misfolded proteins is crucial for maintaining cellular functions, and numerous human diseases are associated with a deficiency in eliminating aberrant proteins, including neurodegenerative diseases, type 2 diabetes, cystic fibrosis, peripheral amyloidosis, cancer, and cardiovascular disease (Hartl *et al.* ; Lenschow *et al.* 2005; Balch *et al.* 2008; Morimoto 2008; Hartl *et al.* 2011). Understanding the mechanisms of protein folding, quality control, and disposal of misfolded proteins is therefore crucial for therapeutic intervention in these disease states.

In eukaryotic cells, the ubiquitin-proteasome system (UPS) is the major pathway for elimination of misfolded proteins (Wolf & Hilt 2004; Qian *et al.* 2006). Substrates of the UPS are marked with ubiquitin via E1-E2-E3 enzyme cascades, and subsequently delivered to the 26S proteasome for degradation (Welchman *et al.* 2005). Surprisingly, between 6% and 30% of all eukaryotic newly synthesized proteins are very rapidly degraded by the UPS (Schubert *et al.* 2000; Qian *et al.* 2006), suggesting that the UPS plays an important role in quality control of newly synthesized proteins. The “DRiP”

¹ This chapter has been published in: “WANG, F., DURFEE, L.A. & HUIBREGTSE, J.M. **A cotranslational ubiquitination pathway for quality control of misfolded proteins.** 2013, *Mol Cell* 50: 368-78.”

Author Contributions: F.W. and J.H. designed and interpreted all experiments; F.W. performed most of the experiments; L.D. performed the siRNA knockdown experiments; F.W., L.D. and J.H. wrote the paper.

(Defective Ribosomal Products) hypothesis proposed that these degradation products serve an important biological function as a source of MHC class I peptides (Yewdell *et al.* 1996; Reits *et al.* 2000). Although this hypothesis has been extensively debated (Yewdell & Nicchitta 2006), there is little doubt that, for many proteins, synthesis and degradation are closely coupled, in a seemingly energetically wasteful process.

Consistent with a role for ubiquitin in the process, it was recently reported that a large fraction of the total human ubiquitin-modified proteome is derived from newly synthesized proteins (Kim *et al.* 2011b). Importantly, the relationship between protein translation, ubiquitination, and degradation has not been established. The simplest model is that newly translated proteins are targeted for ubiquitination after their release from the ribosome, perhaps after failing a quality control surveillance test or after unsuccessful attempts at chaperone-assisted folding (McClellan *et al.* 2005). Alternatively, certain protein chaperones engage nascent polypeptides as they emerge from the ribosome (Hartl *et al.* 2011; Preissler & Deuerling 2012), so it is conceivable that protein fate decisions might be made while translation is in progress. Consistent with this, Turner and Varshavsky showed that an engineered protein bearing an amino-terminal (N-end) degradation signal could be degraded co-translationally in *S. cerevisiae* (Turner & Varshavsky 2000). Although this implied that the protein was ubiquitinated co-translationally, N-end rule ligases have not been shown to target their natural substrates co-translationally. The cystic fibrosis transmembrane conductance regulator (CFTR), which is a very large protein prone to misfolding, was shown to be subject to co-translational ubiquitination in an *in vitro* rabbit reticulocyte lysate translation system (Sato *et al.* 1998), although this may have been related to the very slow translation rate in that system.

An additional aspect of initial protein quality control is the recognition and disposal of translation products produced from defective mRNAs (Shoemaker & Green 2012). For example, poly-lysine containing sequences generated from the poly-A tails of non-stop mRNAs trigger stalling of the nascent chain within the exit tunnel, and two ubiquitin ligases, Ltn1 and the CCR4/NOT complex, have been implicated in the ubiquitination and degradation of these protein products (Dimitrova *et al.* 2009; Bengtson & Joazeiro 2010; Brandman *et al.* 2012). In addition to nonstop decay (NSD), other mRNA surveillance mechanisms associated with translational stalling include no-go decay (NGD) and nonsense-mediated decay (NMD). The protein products of these stalled ribosomes, as well as those of ribosomes backed up behind stall sites, are likely to also be specifically targeted for degradation, but the mechanisms remain largely uncharacterized.

The Huibregtse lab previously demonstrated that ISG15, an interferon-induced ubiquitin-like modifier, is stochastically conjugated to newly synthesized proteins by Herc5, a ribosome-associated HECT domain ligase (Durfee *et al.*, 2010). These results suggested that ISG15 is co-translationally conjugated to nascent polypeptides, and we proposed that this is an attempt to interfere with the function of newly synthesized viral proteins (Durfee *et al.* 2010; Skaug & Chen 2010). This observation, along with the reports on degradation of newly synthesized proteins, led us to address whether ubiquitin, perhaps similarly to ISG15, is co-translationally conjugated to ribosome-associated nascent polypeptides. I report that co-translational ubiquitination (CTU) is a surprisingly robust process in human cells and that CTU occurs in at least two contexts: within stalled complexes (CTU^S) and within active translation complexes (CTU^A). The latter is remarkable in that it implies that a protein can be marked for degradation before synthesis is completed.

3.2 MATERIALS AND METHODS

Cell culture, transfections, and antibodies: *Saccharomyces cerevisiae* strain BY4741 was grown at 30°C in rich medium (yeast extract peptone). HeLa, HEK293T, and NIH 3T3 cells (ATCC), and UBR1/2^{-/-} and control MEFs (kindly provided by Yong Tae Kwon, University of Pittsburgh) were maintained in Dulbecco's modified Eagle's medium (DMEM) supplemented with 10% fetal bovine serum and 1% antibiotics mixture. Primary human keratinocytes (Lonza) were maintained in KGM-Gold™ Keratinocyte Growth Medium (Lonza). Plasmid DNA and siRNA transfections were performed with cells at 60%-80% confluence using Lipofectamine 2000 (Invitrogen). All plasmids, antibodies and siRNAs used in this study are listed in Table 3.1 and 3.2. IRDye 680RD Streptavidin was purchased from LI-COR Bioscience.

Polysome isolation: To isolate total polysomes, cells were lysed in high-salt polysome lysis buffer (100 mM Tris, pH 7.4, 50 mM KCl, 25 mM MgCl₂, 1 mM DTT, 100 μM PMSF, 4 μM leupeptin, 0.3 μM aprotinin, and 200 μg/ml heparin). Lysates were clarified by centrifugation at 16,300 x g for 10 min. at 4°C, and supernatant was loaded on a 2 ml 35% sucrose cushion (with 10 mM Tris pH 7.4, 85 mM KCl, 5 mM MgCl₂) and centrifuged for 90 min. at 316,000 x g in a Beckman NVT 65.2 rotor at 4°C. Polysome-containing pellets were resuspended in 200 μl polysome buffer (10 mM Tris, pH7.4, 10 mM NaCl, 3 mM MgCl₂, and 0.2 mM DTT) and stored at -80°C. For drug treatments prior to polysome isolation, cells were treated with 2 μM pactamycin (Sigma-Aldrich) for the indicated times (Figures 3.9-3.11) or cells were treated for 60 min. (Figure 3.10) with either 0.5 mg/ml AZC (Sigma-Aldrich), 20 μM VER155008 (Tocris Bioscience), 50 μM

Pifithrin- μ (Tocris Bioscience), 200 $\mu\text{g/ml}$ hygromycin B (Cellgro), 1000 $\mu\text{g/ml}$ geneticin (Gemini Bio Products), 20 μM Eeyarestatin 1 (Tocris Bioscience) or 20 nM 17-AAG (Selleck Chemicals).

Quantification of CTU level: Each 100 μl Puromycin conjugation assay contained the following components: 10 mM Tris, pH 7.4, 400 mM KCl, 3 mM MgCl_2 , 2 A_{260} units of polysomes, and 2 μM fluorescent puromycin (2 μM 6-FAM-dc-Puro, Jena Bioscience). Puromylation reactions were performed at 37°C for 90 min and post-reaction, two volumes of 0.1% NP40 buffer were added after the reaction, and the mixtures were spun through Microcon centrifugal filters (YM-3, Millipore) to remove unreacted 6-FAM-dc-Puro. Total reaction products (10%) were saved as input to estimate the amount of total nascent chains, and the rest was subjected to two rounds of Tandem Ubiquitin Binding Entity-Agarose (TUBE 2, LifeSensors) pull-downs to isolate ubiquitin conjugates. TUBE pull-down efficiency was evaluated by immunoblotting of pre- and post-down supernatants with anti-ubiquitin antibody. The fluorescent signal from the TUBE pull-down ubiquitin conjugates and from the input nascent polypeptides was measured with a SpectraMax-M3 Multi-mode plate reader, with the excitation wavelength at 485 nm.

Purification of CTU targets for LC-MS/MS: HEK293T (twenty 150-mm culture dishes) were transfected with 5 μg per dish of plasmid expressing FLAG-Ub. Two days post-transfection, polysomes were isolated as described above and nascent polypeptides were labeled with Bio-Puro. Two volumes of RIPA buffer were added after the reaction, and the mixtures were incubated with anti-FLAG M2 Affinity Gel overnight

at 4°C to isolate FLAG-Ub conjugates. The beads were washed four times with 0.1% NP-40 buffer, and proteins were eluted from beads by adding PBS containing 2% SDS and boiling at 90°C for 5 min. Eluted proteins were diluted with 0.1% NP40 buffer to decrease the final concentration of SDS to 0.2%, and then incubated with Avidin Agarose Resin (Thermo Scientific) overnight at 4°C to isolate FLAG-Ub conjugated nascent polypeptides. The beads were washed four times with RIPA buffer, and proteins were eluted from beads by adding SDS-PAGE loading buffer and boiling at 90°C for 5 min. The samples were analyzed by SDS-PAGE and stained with Coomassie Brilliant blue. Proteins greater than 30 kD were excised from the gel. LC-MS/MS was performed at the Taplin Mass Spectrometry Facility at Harvard Medical School.

Cytosolic and ER-associated polysome isolation: To isolate cytosolic and ER-associated polysomes, a sequential detergent extraction method was used (Jagannathan *et al.* 2011). Cells in a 150-mm culture dish were washed once with 10 ml of PBS at room temperature, and then treated with 10 ml of ice-cold PBS containing 50 mg/ml CHX for 10 min. on ice (to allow for microtubule depolymerization). Cells were then permeabilized with 2 ml of digitonin lysis buffer (110 mM KOAc, 25 mM K-HEPES, pH 7.2, 2.5 mM Mg(OAc)₂, 1 mM EGTA, 0.03% digitonin, 1 mM DTT, 50 mg/ml CHX, 100 μM PMSF, 4 μM leupeptin, 0.3 μM aprotinin, 200 μg/ml heparin, 50 μM NEM, and 40 U/ml RNaseOUT RNase inhibitor) for 5 min. on ice to release cytosolic polysomes. Permeabilized cells were washed once with the same buffer and then lysed in 3 ml ice-cold high-salt polysome lysis buffer to solubilize ER-associated polysomes. Cytosolic

and ER-associated polysomes were then collected by pelleting through a 35% sucrose cushion as described in the Experimental Procedures.

PLASMIDS	NOTES
FLAG-Ub	Plasmids expressing FLAG-Ub and all mutant forms of Ub were made by introducing the human ubiquitin ORF into the previously described pcDNA3XFlag vector (Zhao <i>et al.</i> 2005) using NotI and XbaI.
FLAG-Ub Δ GG	
FLAG-Ub-K0	
FLAG-Ub-K11/K48	
FLAG-Ub-R11/R48	
FLAG-Ub-R11	
FLAG-Ub-R48	

ANTIBODIES	NOTES
Anti-Bip	BD Biosciences - 610978
Anti-BTF3 (FL-206)	Santa Cruz Biotechnology - sc-28717
Anti-CHIP	Sigma-Aldrich - C9243
Anti-CNOT4	Abcam - ab63028
Anti-CNOT4 (O-23)	Santa Cruz Biotechnology - sc-130728
Anti-E6AP	(Talis <i>et al.</i> 1998)
Anti-FLAG M2 Monoclonal	Sigma-Aldrich - F3165
Anti-Ltn1	Sigma-Aldrich - HPA029143
Anti-RPL23a (3E11)	Novus Biologicals- H00006147-M10
Anti-RPS6 (C-8)	Santa Cruz Biotechnology - sc-74459
Anti-Tubulin	EMD Millipore - CP06
Anti-UBE3C (N1N3)	Genetex - GTX119102
Anti-Ubiquitin (VU-1)	LifeSensors - VU101

Table 3.1: Plasmids and antibodies used in chapter 3.

GENE	siRNA	NOTES
BTF3	GGAUGAUGAUGAUGAAGUU	(Kusumawidjaja <i>et al.</i> 2007)
CHIP/STUB1	GGAGCAGGGCAAUCGUCUG	(Wang <i>et al.</i> 2008)
CNOT4	GUAGAUGGCAGAACACUUA	Dharmacon: D-020323-01
CNOT4	CCAAUUCUCUCAAUAGUAC	Dharmacon: D-020323-02
CNOT4	CGUCUUUGUUGUAGGUUUA	Dharmacon: D-020323-03
CNOT4	UAACCUAUAUCCGGUCAGA	Dharmacon: D-020323-04
E6AP	CAACUCCUGCUCUGAGUA	(Kelley <i>et al.</i> 2005)
LTN1	GAUACCUUCUCACUUGGAA	Sigma-Aldrich: SASI_Hs01_00118676
NACA	CCAGUCAGUAAAGCAAACCTT	(Hotokezaka <i>et al.</i> 2009)
UBE3C (HUL5)	GAGAGUAGAUGUUCAAGAA	Dharmacon: D-007183-01
UBE3C (HUL5)	GAGAAUGCUUGAAGUAUUU	Dharmacon: D-007183-02
UBE3C (HUL5)	GAAGAAAGGCGAAGGUUGA	Dharmacon: D-007183-03
UBE3C (HUL5)	CGUUUUAACUGUUGGCGAA	Dharmacon: D-007183-04
Control	Universal siRNA Negative Control #1	Sigma-Aldrich: SIC001

Table 3.2: siRNAs used in chapter 3.

3.3 RESULTS

3.3.1 CTU is a robust process in mammalian cells

I utilized the *in vitro* Bio-Puro conjugation assay, which was developed in Chapter 2, to determine whether nascent polypeptides were ubiquitinated on polysomes isolated from cells expressing FLAG-Ub. As illustrated in Figure 3.1A, if nascent polypeptides were ubiquitinated in cells, then the *in vitro* Bio-Puro reaction would generate polypeptides modified with both FLAG-Ub and Bio-Puro. In contrast, if ubiquitination of newly synthesized proteins was strictly post-translational (*i.e.*, after release of peptides from ribosomes), then Bio-Puro-conjugated polypeptides would not contain FLAG-Ub. Polysomes were isolated from HEK293T cells expressing FLAG-Ub or FLAG-Ub- Δ GG (a non-conjugatable form of ubiquitin) and nascent chains were labeled *in vitro* with Bio-Puro. Figure 3.1B (lanes 1 and 2) shows that the distribution of total biotin-labeled nascent polypeptides was similar in both reactions. An anti-FLAG immunoprecipitation (IP) was used to isolate ubiquitinated proteins, which were then analyzed by SDS-PAGE and immunoblotting with fluorescent streptavidin. Figure 3.1B (lanes 3 and 4) shows that the FLAG-Ub IP pulled down a broad distribution of proteins conjugated to Bio-Puro, while the FLAG-Ub- Δ GG IP did not. This result indicated that polysome-associated nascent polypeptides were ubiquitinated in cells. Importantly, NEM was included in the cell lysis buffer to block any potential post-lysis ubiquitination activity, and control reactions confirmed that there was no ubiquitination activity in NEM-containing lysis buffer (Figure 3.1C).

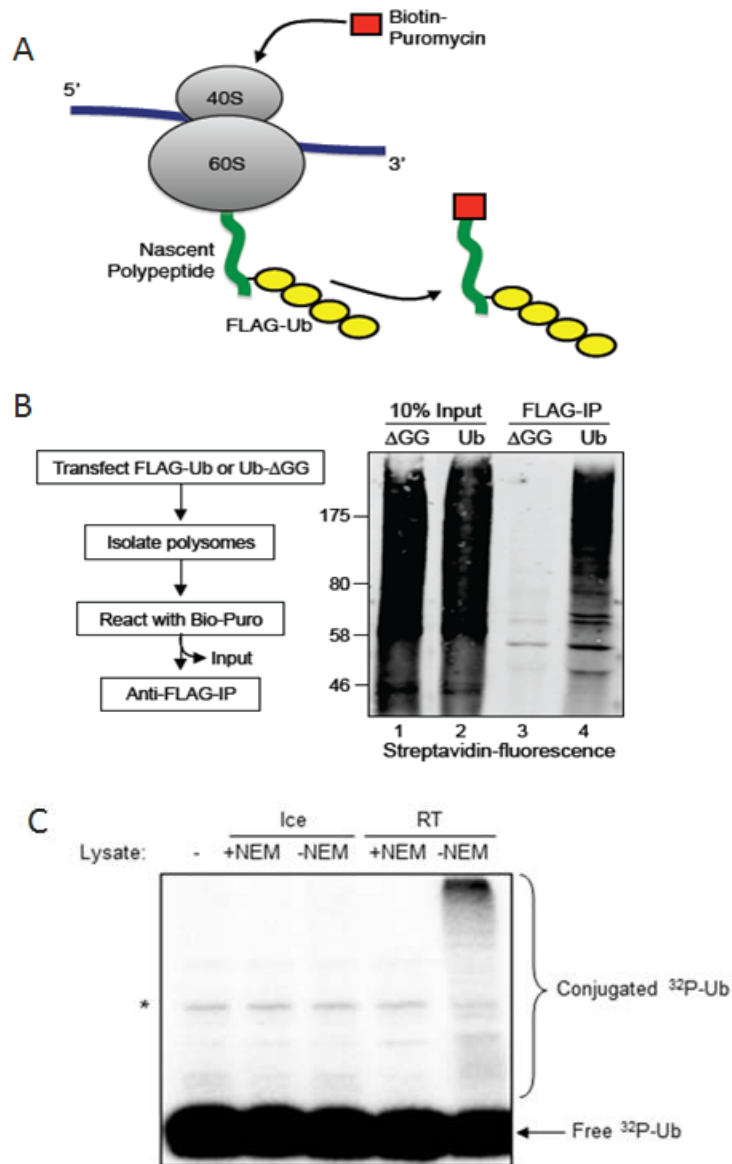


Figure 3.1: Co-translational ubiquitination (CTU) in human cells.

(A) Scheme for detection of CTU. If CTU occurs *in vivo*, polysomes should contain nascent polypeptides modified with both FLAG-ubiquitin and Bio-Puro. (B) Polysome-associated nascent polypeptides are conjugated to FLAG-Ub. Cells were transfected with plasmids expressing wild type FLAG-Ub (Ub) or FLAG-Ub- Δ GG (Δ GG). Nascent chains were labeled with Bio-Puro *in vitro*, then immunoprecipitated with anti-FLAG antibody, and blotted with fluorescent streptavidin. (C) No detectable ubiquitination occurs after cell lysis in the presence of NEM. Purified 32 P-labeled ubiquitin was included in the high salt polysome lysis buffer to evaluate potential post-lysis ubiquitination. Cell lysates with or without NEM were incubated at either room temperature or 4°C for 90 min, and then subjected to autoradiography analysis. Asterisk marks contaminating uncut GST-Ub.

To eliminate the possibility that CTU was a result of overexpression of FLAG-Ub, similar experiments were done with untransfected cells, examining conjugates to endogenous ubiquitin. Polysomes were collected from HEK293T cells and incubated *in vitro* with Bio-Puro (illustrated in Figure 3.2, left). Biotin-labeled nascent chains were isolated on neutravidin-agarose and immunoblotted with anti-ubiquitin antibody. Consistent with the results above, Figure 3.2 (middle) shows that a broad set of nascent polypeptides was modified with ubiquitin. Similar results were obtained using polysomes isolated from *Saccharomyces cerevisiae* cells expressing only endogenous ubiquitin (Figure 3.2, right).

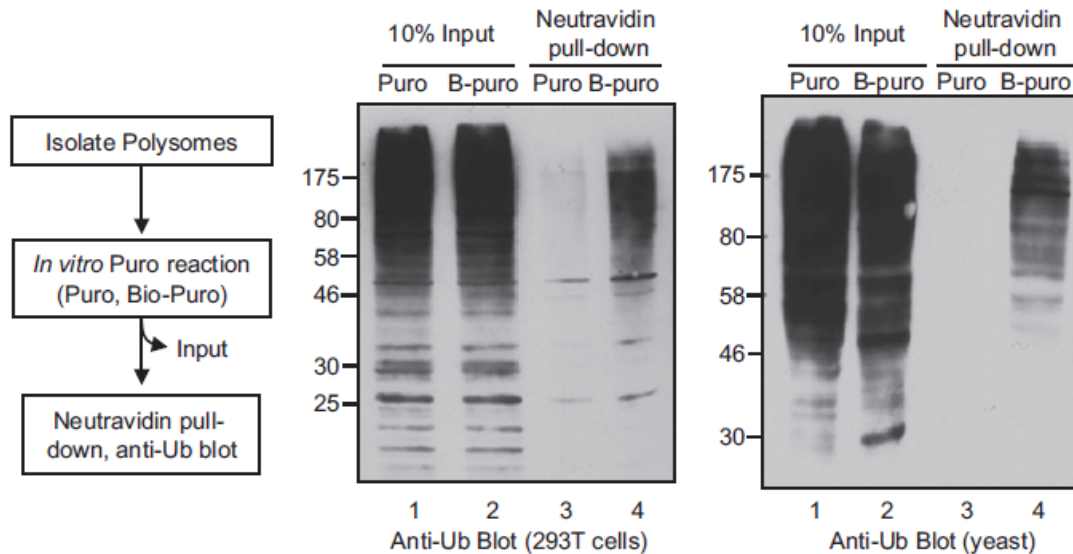


Figure 3.2: Polysome-associated nascent polypeptides are conjugated to endogenous ubiquitin in human and yeast cells.

Polysomes from untransfected HEK293T or *S. cerevisiae* cells were incubated with either Bio-Puro or untagged Puro to label associated nascent chains. Biotin labeled polypeptides were isolated by neutravidin pull down and analyzed by anti-ubiquitin immunoblotting.

The percentage of nascent chains that were ubiquitinated in cells was estimated by using fluorescently labeled puromycin (6-FAM-dC-Puro; Figure 3.3A, left). As above, polysomes were isolated from untransfected cells and total nascent polypeptides were labeled *in vitro* with 6-FAM-dC-Puro. Ubiquitinated polypeptides were then purified from the reaction on a ubiquitin-binding protein matrix (TUBE-Agarose, LifeSensors). The percentage of ubiquitinated nascent chains was determined by measuring the fluorescent signal of the TUBE pull-down compared to the fluorescent signal from the input nascent polypeptides (correcting for the efficiency of the TUBE pull-down, determined separately to be approximately 73%; Figure 3.3B). In HEK293T cells, 12-15% of the total nascent polypeptides were co-translationally ubiquitinated (Figure 3.3A, right). Similar values were obtained in other human (HeLa) and mouse (NIH3T3) cell lines, as well as primary human foreskin keratinocytes (HFKs). These results indicate that CTU is a robust process across many mammalian cell types. The fraction of ubiquitinated nascent chains was reproducibly lower in budding yeast cells, with approximately 6% of total nascent chains being ubiquitinated (Figure 3.3A).

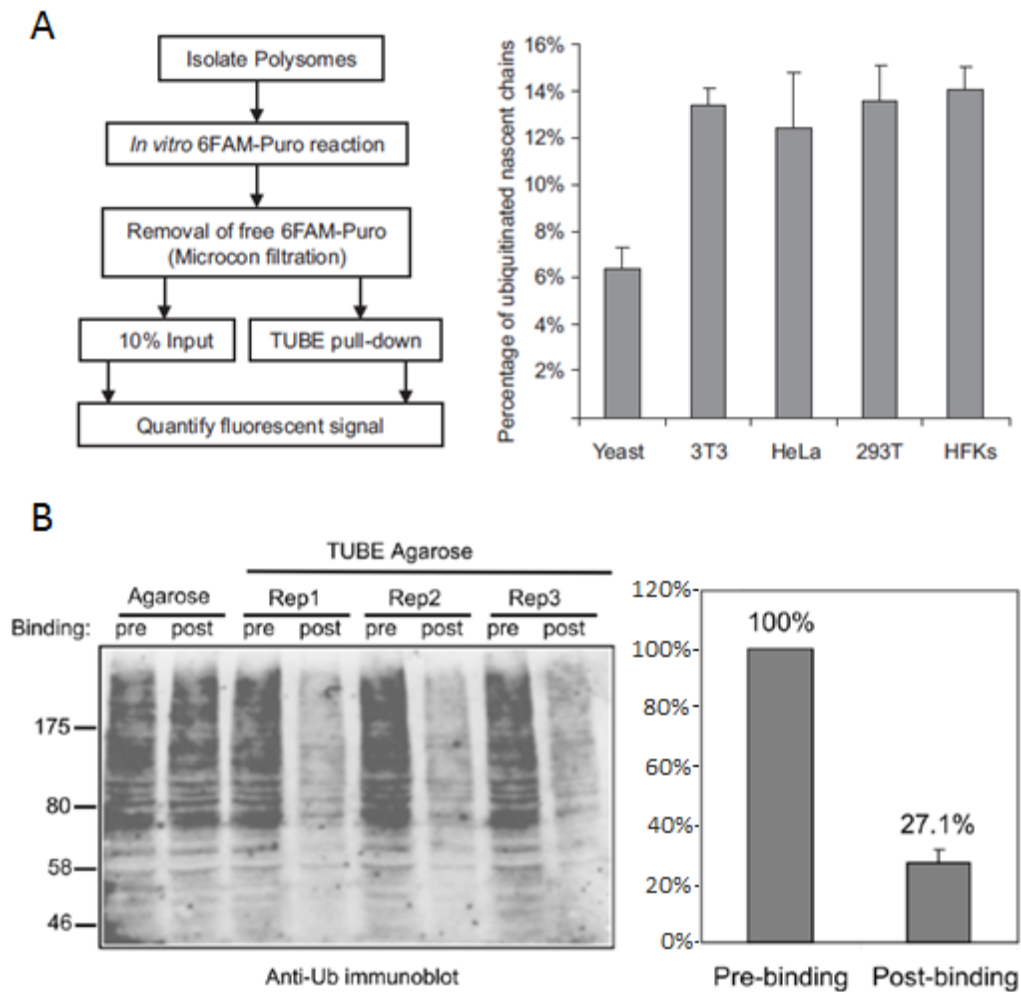


Figure 3.3: Quantitation of CTU in different cell types.

(A) Quantitation of CTU in different cell types. Polysomes were isolated from the indicated cell types, and polysome-associated nascent chains were labeled with fluorescently-tagged puromycin (6-FAM-dC-Puro). Total reactions (10%) were used to estimate the amount of total nascent chains (input); the remainder was subject to TUBE pull down to isolate ubiquitinated proteins, and fluorescence intensity was measured. Error bars indicate standard error of the mean (SEM) of three independent experiments. (B) Evaluation of TUBE pull-down efficiency. The efficiency of binding of ubiquitinated proteins by TUBE beads was determined by immunoblotting of pre- and post pull-down supernatants with anti-ubiquitin antibody, followed by IRDye 680 anti-mouse Licor secondary antibody. Error bars indicate standard error of the mean (SEM) of three independent experiments.

3.3.2 CTU predominantly occurs on cytosolic rather than ER-associated polysomes

Secreted and membrane proteins comprise approximately 30% of the eukaryotic proteome (Stevens & Arkin 2000), and these are synthesized primarily on ER-associated polysomes. I determined the relative contribution of cytosolic and ER-associated polysomes to total CTU by fractionating the two types of polysomes by sequential detergent extraction (Figure 3.4A) (Jagannathan *et al.* 2011). Digitonin was used to selectively solubilize the plasma membrane and release cytosolic polysomes from FLAG-Ub-transfected cells. The permeabilized cells were washed and ER-bound polysomes were then solubilized with Triton-X 100. The fractionation efficiency was validated via Western blot analysis with antibodies that recognize tubulin (a cytosolic protein) and BIP/GRP78 (an ER luminal protein; Figure 3.4B). Immunoblotting of a ribosomal protein (RPS6) showed that polysomes were present in both cytosolic and ER fractions. The cytosolic and ER-derived polysomes were collected by centrifugation through 35% sucrose and used in *in vitro* Bio-Puro conjugation reactions (Figure 3.4C). Nascent polypeptides on cytosolic polysomes were heavily ubiquitinated, although the signal from ER-associated polysomes was approximately 5-fold less (normalized for total nascent chains). This indicated that CTU occurs predominantly, but not exclusively, on cytosolic polysomes (Figure 3.4C, right).

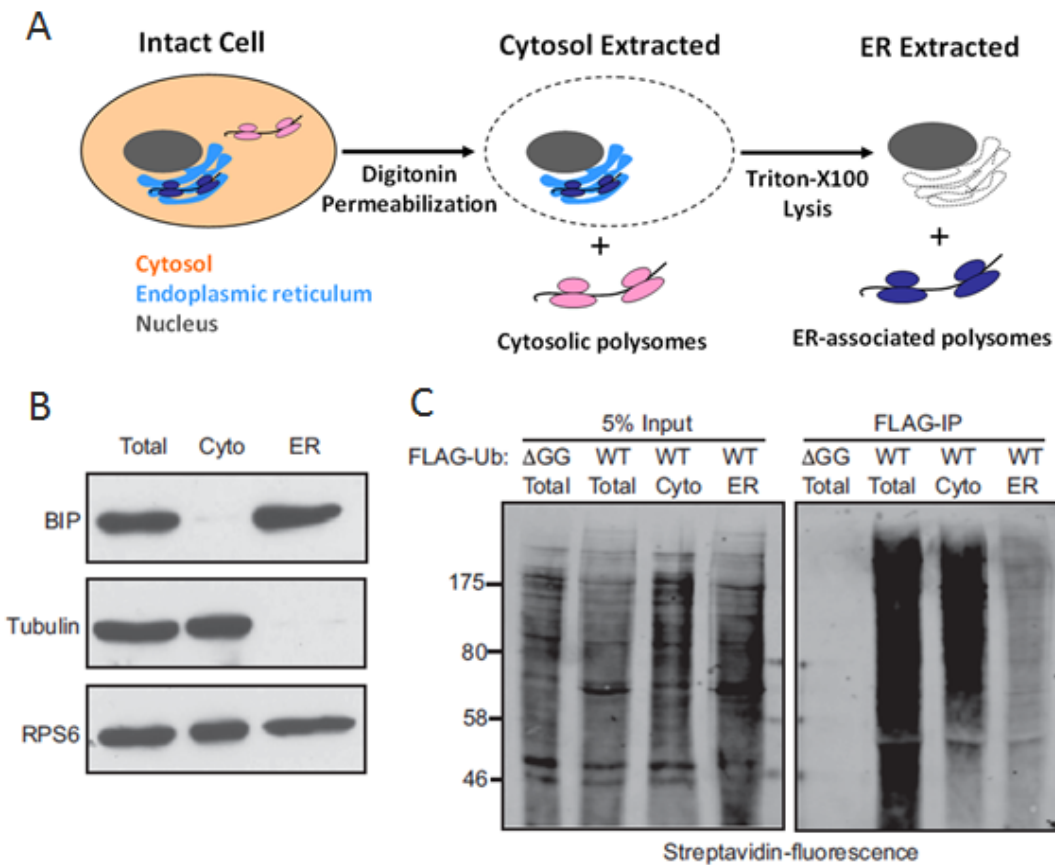


Figure 3.4: CTU occurs predominantly on cytosolic rather than ER-associated polysomes.

(A) Scheme for fractionation of free and ER-associated polysomes. (B) Fractionation of cytosolic and ER-associated polysomes was validated by immunoblotting with antibodies that recognize tubulin (cytosolic protein), Bip (ER lumenal protein) and RPS6 (small ribosomal protein). (C) Cytosolic and ER-associated polysomes were isolated from HEK293T cells expressing FLAG-Ub. Polysome-associated nascent chains were labeled with Bio-Puro and then immunoprecipitated with anti-FLAG antibody. Left panel is 5% input of total Bio-Puro conjugation products, and the right panel represents immunoprecipitation of nascent proteins that were modified with both FLAG-Ub and Bio-Puro.

3.3.3 CTU targets are polyubiquitinated with K48 and K11 chains

To determine the ubiquitin chain topology on CTU target proteins, FLAG-Ub-containing and Bio-Puro-labeled CTU products were incubated with the catalytic core of ubiquitin-specific protease 2 (USP2cc) to strip ubiquitin from target proteins. Addition of USP2cc to ubiquitinated nascent polypeptides led to a nearly complete loss of anti-FLAG-Ub immunoreactivity (Figure 3.5A, left). When the same reaction products were probed with fluorescent streptavidin, the average molecular weight of the CTU products was significantly decreased (Figure 3.5A, right), suggesting that most puromycin-labeled CTU targets were modified with multiple ubiquitin molecules.

CTU products were purified and characterized by LC-MS/MS to determine chain type linkages and to identify a preliminary set of CTU targets. Figure 3.6A shows the Coomassie blue-stained SDS-PAGE gel of purified ubiquitinated nascent chains. Proteins greater than 30 kD were excised from the gel and tryptic peptides were identified by LC-MS/MS. The mass spectrometry analysis indicated the presence of K48- and K11-linked polyubiquitin chains within the purified CTU products, with no evidence for other chain types. Both of these chain types can target proteins for proteasomal degradation (Xu *et al.* 2009; Behrends & Harper 2011). To confirm the chain topology observed by the LC-MS/MS analysis, a series of FLAG-Ub mutants (Figure 3.5B) were expressed in HEK293T cells. Polysomes were isolated, nascent chains were labeled with Bio-Puro, and FLAG-Ub-conjugates were immunoprecipitated and probed with fluorescent streptavidin. Expression of lysine-less ubiquitin (K0) led to a sharp decrease in the average apparent molecular weight distribution of CTU products (Figure 3.5C).

Expression of ubiquitin that retained only K11 and K48 (K11/K48) supported production of CTU products that appeared identical to those produced in the presence of wild-type FLAG-Ub. In contrast, expression of R11/R48 ubiquitin (with all other lysines intact) resulted in CTU products that appeared similar to those produced in the presence of K0 ubiquitin. Expression of R48 ubiquitin had a similar effect as R48/R11 on the average length of CTU products, while R11 ubiquitin had no detectable effect on conjugates. These results suggest that K48-linked chains are the predominant type of chain formed on CTU products. In addition to the identification of K48- and K11-linked chains, the mass spectrometry analysis of CTU products identified approximately 130 putative CTU target proteins (Table 3.3), all of which were previously identified in a large-scale ubiquitin proteomics study that identified ~5000 ubiquitinated human proteins (Kim *et al.* 2011b). These proteins are distributed in diverse intracellular compartments, with nuclear and cytosolic proteins predominating (Figure 3.6C). Interestingly, large proteins are highly enriched in identified CTU targets, with average length of CTU targets longer than 1000 amino acids (average length of all human proteins is around 500 amino acids) (Figure 3.6B).

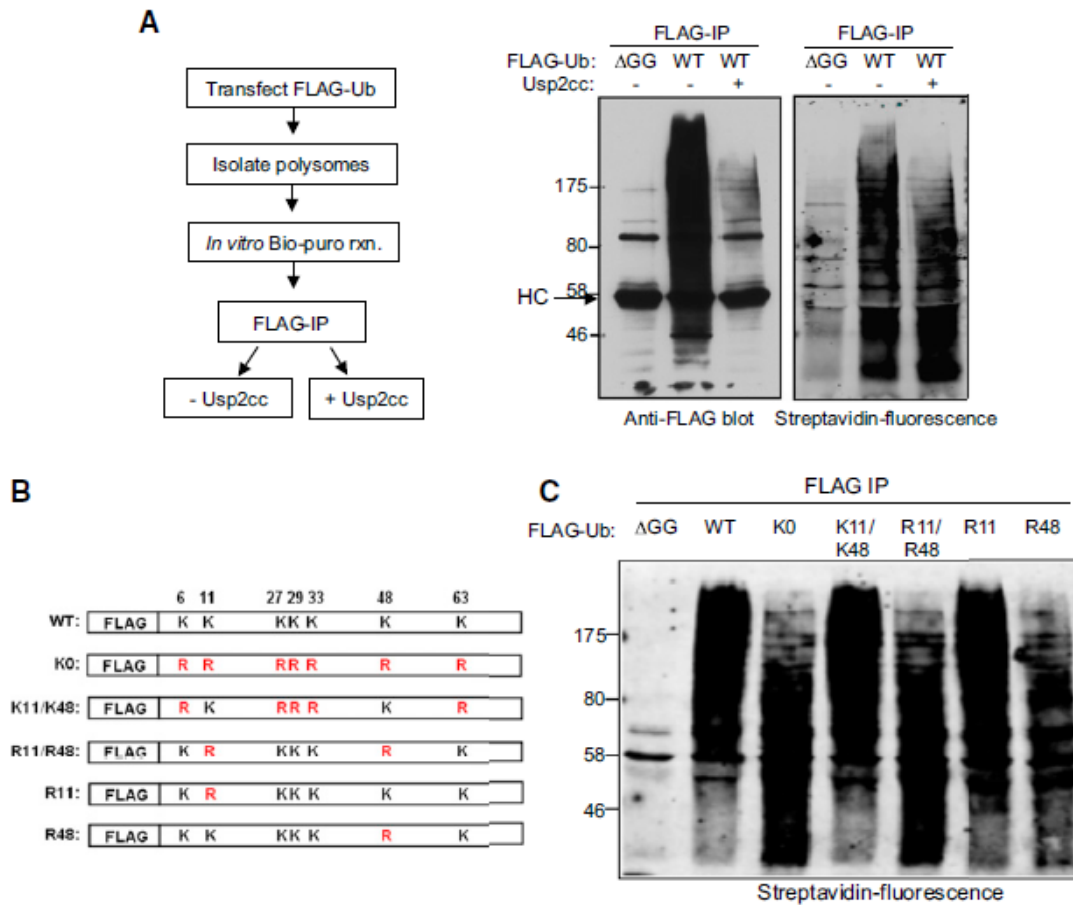


Figure 3.5: CTU products contain primarily K48-linked polyubiquitin chains.

(A) CTU target proteins are multi-ubiquitinated. Ubiquitinated nascent polypeptides were labeled with Bio-Puro, and immunoprecipitated with anti-FLAG antibody. The immunoprecipitated products were treated with the catalytic domain of ubiquitin-specific protease 2 (USP2cc) to strip ubiquitin (see schematic, left). Middle panel is the anti-FLAG-Ub blot analysis of samples before and after USP2cc treatment (HC is IgG heavy chain). Right panel shows the fluorescent-streptavidin blot of the FLAG IPs. The molecular weight change of CTU products after USP2cc treatment indicates that the majority of the CTU products contained multiple ubiquitin moieties. (B) Schematic diagram of mutant forms of FLAG-ubiquitin expressed in HEK293T cells. (C) Polysomes were isolated from cells expressing the indicated form of ubiquitin. Nascent chains were labeled with Bio-Puro *in vitro*, and then immunoprecipitated with anti-FLAG antibody. The immunoprecipitated products were subject to SDS-PAGE, and detection was with fluorescent streptavidin.

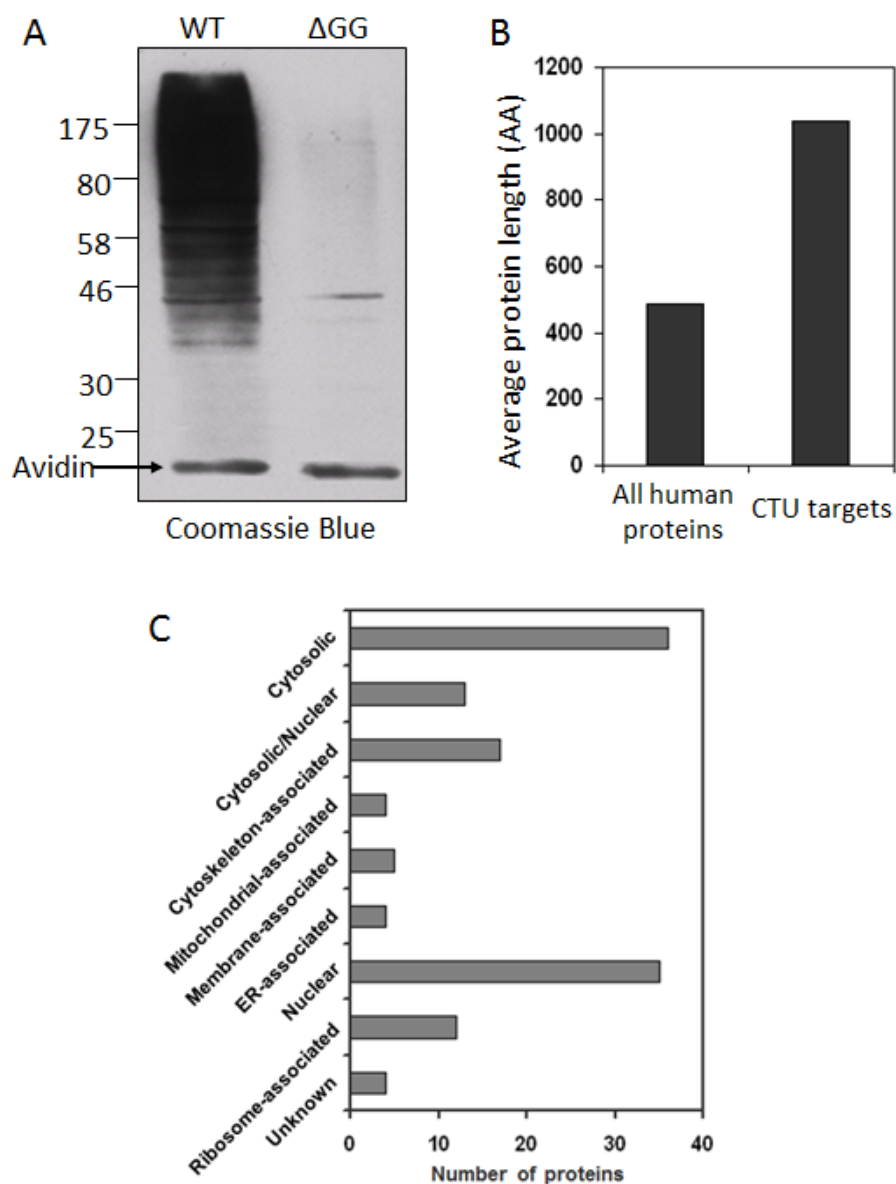


Figure 3.6: Identification of CTU target proteins.

(A) CTU products were double-affinity purified as described in the text, starting with polysomes from cells expressing with FLAG-Ub or FLAG-Ub- Δ GG. Purified proteins were subject to SDS-PAGE and stained with Coomassie Blue. All proteins >30 kD were excised from the gel and tryptic peptides were identified by LC-MS/MS. See Table 3.3 for list of identified proteins. (B) Large proteins were enriched in identified CTU products. (C) Categorization of 130 CTU targets with respect to intracellular localization (localization according to Uniprot).

To confirm that CTU products were subject to proteasomal degradation, cells were treated with cycloheximide prior to cell lysis for various periods of time to trap nascent polypeptides on polysomes. Polysomes were then isolated, nascent chains labeled with Bio-Puro, and FLAG-Ub-conjugates were immunoprecipitated and probed with fluorescent streptavidin. As shown in Figure 3.7 (top), the amount of ubiquitinated nascent chains increased after CHX treatment, reaching a peak between 5 and 10 minutes, then gradually decreased. A possible explanation for these observations was that CTU products transiently accumulated on cycloheximide-stalled polysomes and were then subject to proteasomal degradation over time. To test this, the experiment was repeated in the presence of both CHX and the proteasome inhibitor MG132. As shown in Figure 3.7 (bottom), the amount of CTU products continued to increase beyond the 10 minute time point (Figure 3.7, bottom), indicating that ubiquitinated nascent chains are subject to proteasomal degradation.

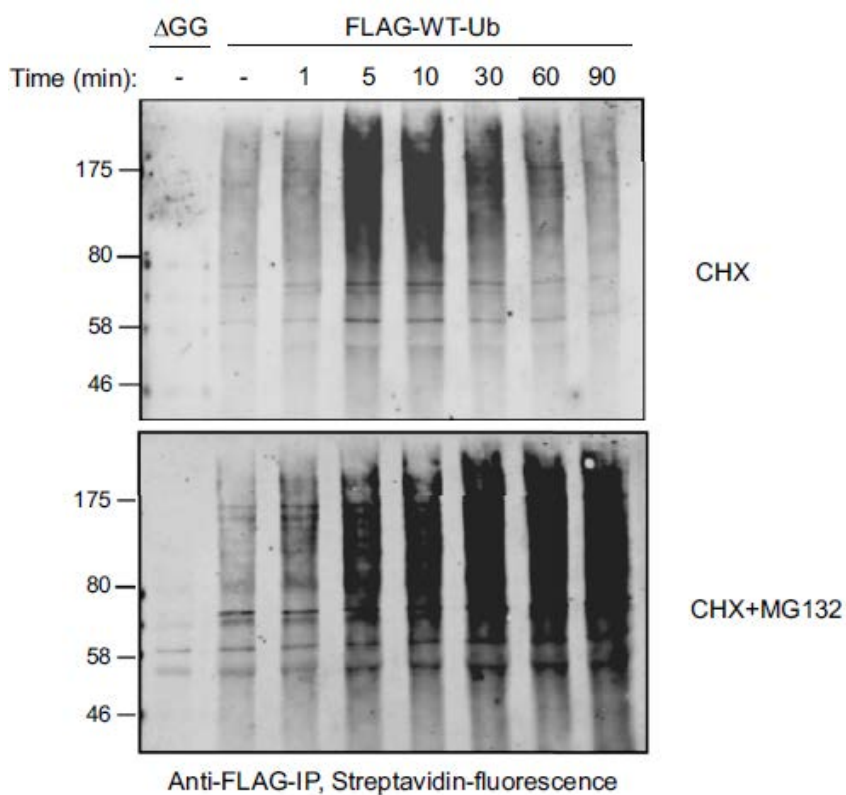


Figure 3.7: CTU products were subject to proteasomal degradation.

HEK293T cells were transfected with plasmids expressing FLAG-Ub or FLAG-Ub- Δ GG. Prior to lysis, cells were treated with CHX alone or simultaneously with CHX and MG132 for the indicated times. Polysomes were isolated from these cells and reacted with Bio-Puro. Nascent polypeptides were analyzed by anti-FLAG immunoprecipitation and detected with fluorescent streptavidin.

3.3.4 CTU occurs within both stalled and active translation complexes

In vitro run-off translation reactions developed in the last chapter were used to address whether CTU occurs within active or stalled translation complexes. Polysomes from cells transfected with FLAG-Ub or FLAG-Ub-ΔGG were collected and used in run-off translation reactions. As illustrated in Figure 3.8A, if CTU occurred in cells within translation-competent complexes, then ³⁵S-labeled run-off products should also contain FLAG-Ub. In contrast, if CTU occurred post-translationally or if CTU products were derived exclusively from irreversibly stalled polysomes, then *in vitro* run-off translation products should not yield products that contained both ³⁵S-Met and FLAG-Ub. Figure 3.8B shows ³⁵S-Met was robustly incorporated into FLAG-Ub-containing polypeptides, indicating that at least a portion of CTU products were generated within active, elongation-competent translation complexes.

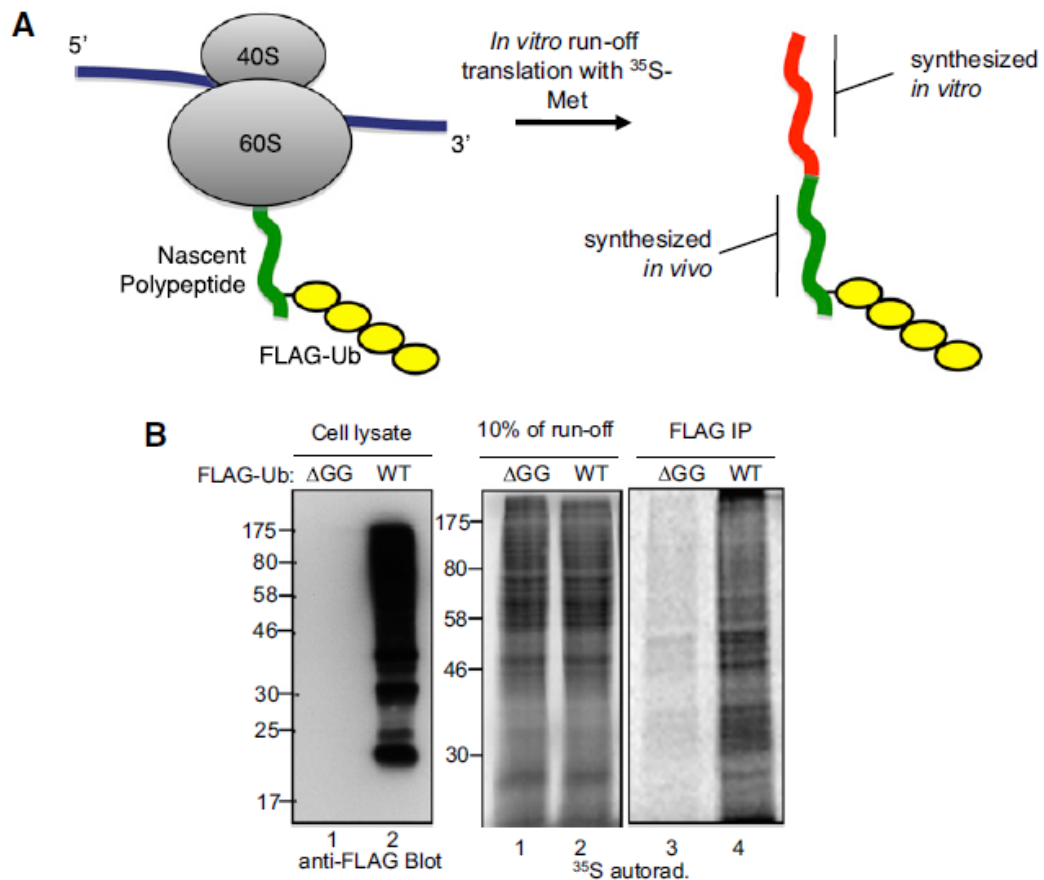


Figure 3.8: CTU occurs within active translation complexes.

(A) The CTU model predicts that if ubiquitin is conjugated to nascent chains on actively translating polysomes and translation can proceed following CTU, then *in vitro* run-off products will contain both ubiquitin and ³⁵S-methionine. Green represents the portion of the polypeptide chain translated *in vivo*, and red represents the ³⁵S-methionine-containing polypeptide translated *in vitro*. (B) Cells were transfected with plasmids expressing FLAG-Ub (WT) or FLAG-Ub-ΔGG (ΔGG), and polysomes from these cells were used in run-off reactions. Left panel shows an anti-FLAG immunoblot of total cell extracts, the center panel shows 10% of the run-off reactions, and the right panel shows the anti-FLAG immunoprecipitates of the run-off reactions.

I next sought to determine the relative proportion of total CTU products (CTU^T) that were generated from active (CTU^A) versus stalled (CTU^S) translation complexes. Before addressing this, I first determined the proportion of total nascent chains that are in stalled translation complexes in cells, regardless of their ubiquitination state. A brief treatment of cells with pactamycin (5 or 10 minutes), an inhibitor of translation initiation, was used to allow run-off of all nascent chains present within active translation complexes. At an estimated translation rate of 5-9 amino acids per second (Orlowski & Ross 1981; Ross & Orlowski 1982), five minutes of pactamycin treatment is sufficient to allow completion of translation of all but the longest proteins. Figure 3.9A shows that a 5 minute treatment of 293T cells with pactamycin was sufficient to block any detectable incorporation of ^{35}S -methionine into cellular proteins in a subsequent 5 minute metabolic pulse. Therefore nascent chains from untreated cells and from pactamycin treated cells (5 or 10 minutes) were labeled with fluorescently-labeled puromycin and the total fluorescent signal was quantitated. The fluorescent-puromycin signal from pactamycin-treated cells was approximately 27% and 22% of the untreated cells at the 5 and 10 minute time points, respectively (Figure 3.9B), indicating that nearly a quarter of all nascent chains are in stalled complexes. The slight decrease in stalled nascent chains between the 5 and 10 minute time points is likely to represent the clearing of stalled complexes over time, either by degradation mechanisms or the resumption of transiently stalled complexes.

I next determined the fraction of total CTU products (CTU^T) that were derived from stalled translation complexes (CTU^S) by quantitating the amount of doubly-tagged

(ubiquitinated and puromycylated) nascent chains that remained on polysomes after 5 or 10 minutes of pactamycin treatment. As shown in Figure 3.9C, CTU^S was approximately 36% of CTU^T at the 5 minute time point, and slightly less (32%) at the 10 minute time point. Therefore, CTU^S accounts for approximately a third of CTU^T , and CTU^A (the fraction of CTU products that ran-off during pactamycin treatment) accounts for the remaining two-thirds. Considering that ~25% of nascent chains are in stalled complexes, we infer that approximately 15-18% of stalled nascent chains are ubiquitinated, whereas 11-14% of nascent chains in active translation complexes are ubiquitinated.

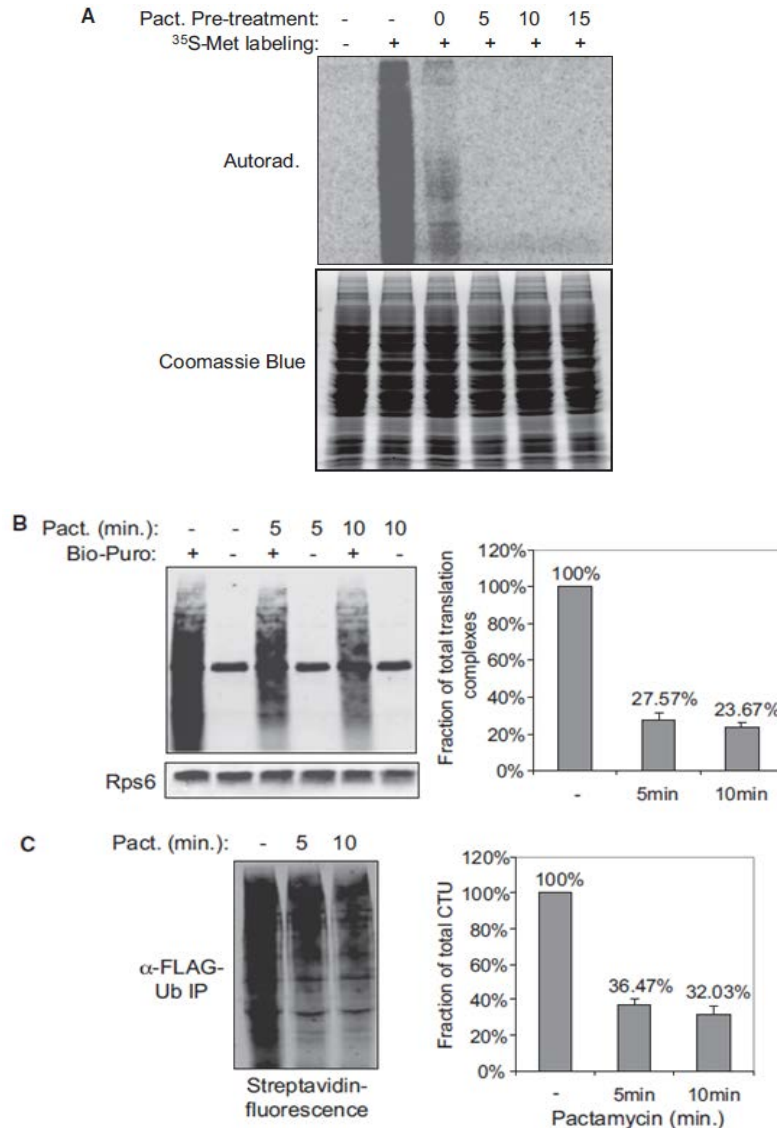


Figure 3.9: CTU^A accounts for the majority of the total ubiquitination activity against nascent chains.

(A) A brief treatment of cells with pactamycin was sufficient to allow run off of actively translating nascent chains. Cells were treated with pactamycin for the indicated times, followed by a 5 min. labeling with ³⁵S-methionine. In lane 3, pactamycin was added simultaneously with the ³⁵S-Met. Coomassie Blue staining shows proteins were loaded equally in each lane. (B) A significant amount of nascent chains are in stalled ribosomes. Cells were either untreated or pretreated with pactamycin for 5 or 10 min. to run off of actively translating ribosomes. Polysomes were isolated from these cells and incubated with Bio-Puro *in vitro* to label associated nascent chains. (C) CTU^S accounts for approximately one-third of CTU^T. Cells expressing FLAG-Ub were treated with pactamycin for 10 min. and polysome-associated nascent chains were labeled with Bio-Puro *in vitro* and then immunoprecipitated with anti-FLAG antibody. The immunoprecipitated products were subject to SDS-PAGE analysis, and the fluorescent streptavidin signal was quantitated relative to cells that were not treated with pactamycin. Error bars represent SEM of three independent experiments.

3.3.5 CTU is enhanced under conditions that promote protein misfolding or translational errors

I next determined how CTU^T was affected by agents that cause protein misfolding or translational stalling. Treatment with L-Azetidine-2-carboxylic acid (AZC), a proline analog that induces protein misfolding, enhanced CTU^T by approximately 1.5-fold (Figure 3.10A). The role of Hsp70 family chaperones in CTU was tested using Hsp70 inhibitors. VER155008 is an adenosine-derived inhibitor (Williamson *et al.* 2009) and 2-Phenylethanesulfonamide (Pifithrin- μ) disrupts the association of Hsp70 with several co-chaperones (*e.g.*, Hsp40, BAG-1L/1M) and substrate proteins (Leu *et al.* 2009). Both inhibitors led to an approximately 1.7-fold increase in CTU^T . Although Hsp70 is linked to co-translational protein folding, Hsp90 functions post-translationally (Hartl *et al.* 2011). Consistent with this, an inhibitor of Hsp90, 17-AGG, had no effect on CTU^T . Aminoglycoside antibiotics, such as hygromycin B and G418, affect translational fidelity and read-through of stop codons (Brodersen *et al.* 2000), and both agents increased CTU^T products to a similar degree (~1.4-fold). Eeyarestatin 1 (ES1), an inhibitor of Sec61-dependent translocation that prevents translation into the ER (Cross *et al.* 2009; McKibbin *et al.* 2012), led to an approximately 1.4-fold increase in CTU^T .

To discern whether the effects on CTU^T were due to increased CTU^S or CTU^A , we pre-treated cells with pactamycin (10 minutes) to run-off active translation complexes. Both hygromycin B and ES1 led to a substantial increase in CTU^S (approximately 42% and 37% of CTU^T , respectively, compared to 31% for untreated cells; Figure 3.10B) and an increase in total stalled nascent chains (Figure 3.10C), consistent with a model where

translational stalling triggers CTU^S. Cycloheximide, which results in nearly complete ribosome stalling, resulted in a 4-5-fold increase in stalled complexes and 3-fold increase in CTU^S (*i.e.*, nearly all CTU was CTU^S; Figure 3.11). AZC and Hsp70 inhibition did not lead to increased CTU^S and did not affect the fraction of stalled nascent chains, indicating that enhanced CTU^A accounted for the increased CTU^T induced by these agents. As the primary effects of AZC and Hsp70 are on protein folding, these results suggest that CTU^A represents a quality control pathway that ubiquitinates nascent chains in response to folding errors. Consistent with this, siRNA knockdown of the BTF3 subunit of the NAC (Nascent Polypeptide-Associated Complex) (Preissler & Deuerling 2012) resulted in a 1.5-fold enhancement of CTU^T (Figure 3.12) but did not affect accumulation of stalled ribosomes or CTU^S (Figure 3.12). Together, these results indicate that CTU^A is enhanced under conditions where folding of nascent polypeptides is impaired.

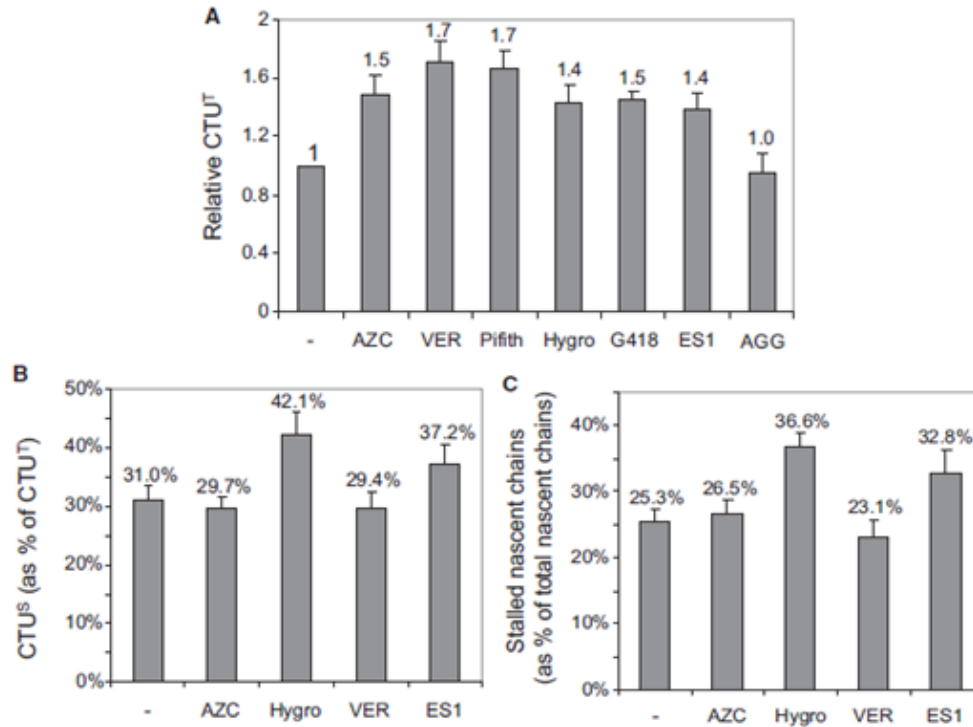


Figure 3.10: CTU was enhanced under conditions that promoted translational errors or protein misfolding.

(A) CTU^T was analyzed after treating cells for 60 min. with either AZC, the Hsp70 chaperone inhibitors VER155008 (VER) or Pifithrin (Pifith), hygromycin B (Hygro), G418, eeyarestatin 1 (ES1) or the Hsp90 inhibitor 17-AGG (AAG). CTU products were quantified by measuring fluorescent-streptavidin signal on blots, and relative signals were normalized in all panels to signal in the absence of inhibitor. Error bars indicate SEM of three independent experiments. (B) Cells expressing FLAG-Ub were treated with the indicated agents for 60 min., and CTU^S was quantitated as in Figure 3.10. Error bars indicate SEM of three independent experiments. (C) Cells were treated with the indicated agents for 60 min., and the stalled nascent chains were quantitated relative to total nascent chains. Error bars indicate SEM of three independent experiments.

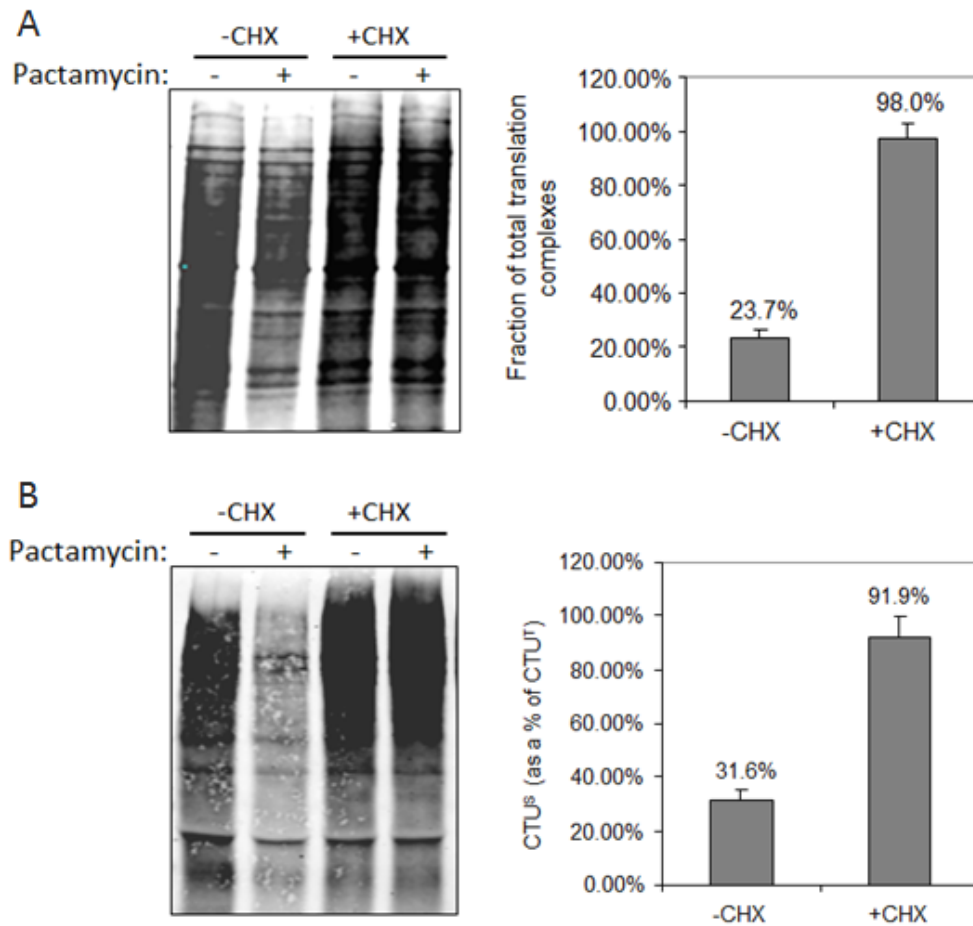


Figure 3.11: Cycloheximide triggers stalling and accumulation of ubiquitinated nascent chains.

(A) Cells expressing FLAG-Ub were treated with or without cycloheximide (CHX) for 10 min. and then with or without pactamycin for 10 min. (top), and nascent chains were quantitated as in Figure 3.10 (bottom). Error bars indicate SEM of three independent experiments. (B) The nascent chains from Figure 3.12A were subjected to FLAG immunoprecipitation (top), and CTU^S relative to CTU^T was determined by the method shown in Figure 3.9. Error bars indicate SEM of three independent experiments.

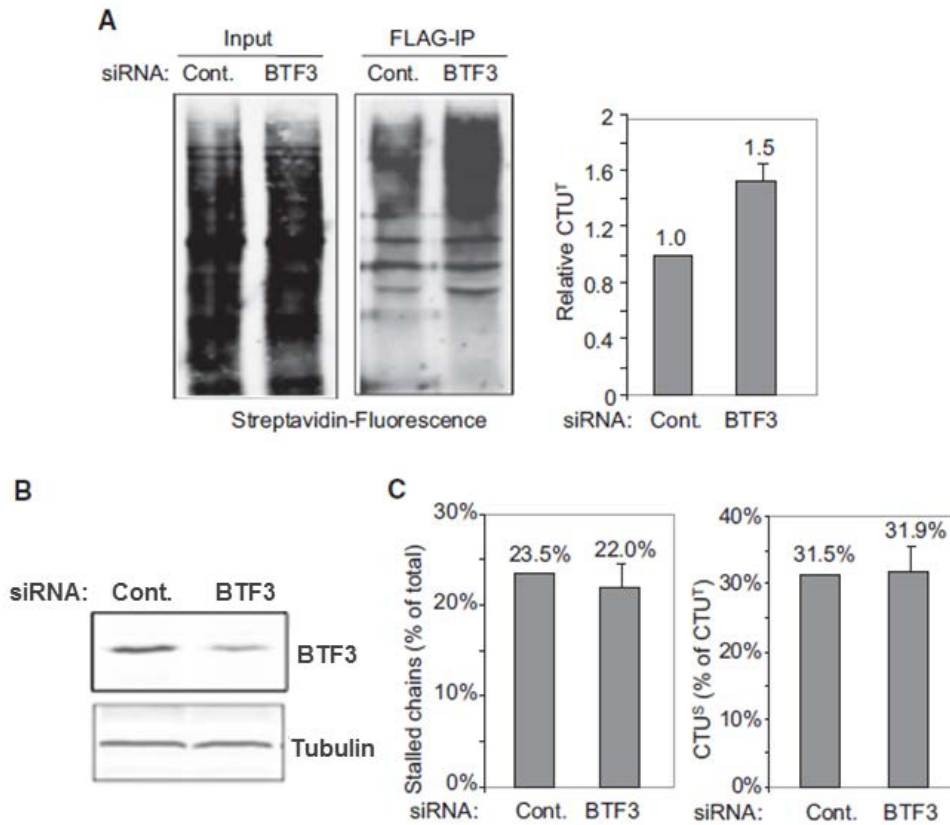


Figure 3.12: Depletion of NAC activity enhances CTU^T.

(A) 293T cells were transfected with siRNAs targeting the mRNA for BTF3 (the β subunit of the NAC) or a control siRNA, and the FLAG-Ub plasmid DNA was transfected 15 hours later. Cells were harvested 48 hours post-siRNA transfection, and CTU products were analyzed by anti-FLAG immunoprecipitation followed by quantitation of Bio-Puro incorporation with fluorescent-streptavidin. Signal was normalized in all panels to that of the control siRNA. Error bar indicates SEM of three independent experiments. (B) BTF3 siRNA knockdown was confirmed by immunoblotting, with tubulin probed as a loading control. (C) Total stalled nascent chains and CTU^S was analyzed in BTF3 or control siRNA-treated cells, using a 10 min. pactamycin treatment (as in Figure 3.10). Error bars indicate SEM of three independent replicates.

3.4 DISCUSSION

I have shown here that co-translational ubiquitination is a robust process in human cells, with 12-15% of all nascent polypeptides being ubiquitinated in a variety of cell lines and primary cells. CTU occurs in two contexts: in stalled complexes (CTU^S) and in active translation complexes (CTU^A). CTU^S has been described previously in the ubiquitination of stalled translation products arising from non-stop mRNAs (Dimitrova *et al.* 2009; Bengtson & Joazeiro 2010; Brandman *et al.* 2012). Stalling in this case is due to translation of the poly-A tail, generating a poly-lysine sequence that interacts strongly with the acidic ribosome exit tunnel. There are additional circumstances that CTU^S is likely to be activated, such as in clearing of translation products at internal stop codons (associated with nonsense-mediated mRNA decay) or other types of damaged mRNAs (Shoemaker & Green 2012). While we found that ~22-27% of all ribosomes were in stalled complexes, only a fraction of these stalled complexes (~15-18%) contained ubiquitinated nascent chains, suggesting that there are multiple types of stalled complexes and possibly multiple responses to stalled complexes. It should also be noted that various forms of proteotoxic stress have recently been reported to trigger translational pausing (Liu *et al.* 2013; Shalgi *et al.* 2013), which might, in turn, also trigger CTU^S.

CTU^A couples synthesis to protein degradation, suggesting that protein fate decisions are made in the narrow window of time between emergence of the nascent polypeptide from the exit tunnel and the release of the full-length protein from the ribosome. CTU^A was demonstrated in two ways. First, nascent chains that were ubiquitinated *in vivo* could be translated to completion *in vitro* when added to a

reticulocyte lysate system. Second, a short treatment with pactamycin was used to run-off active translation complexes *in vivo*, and this resulted in a loss of approximately two-thirds of all ubiquitinated nascent chains from polysomes. A link between CTU^A and protein folding quality control is suggested by the fact that Hsc/Hsp70 inhibitors, siRNA depletion of NAC subunits, and AZC, led to an increase in CTU^A. Both Hsc/Hsp70 and the NAC engage nascent polypeptides to initiate correct folding pathways before translation is complete (Hartl *et al.* 2011). In yeast, Hsp70 SSB associates with approximately 45% of nascent polypeptides (Willmund *et al.* 2013), consistent with the possibility that the relationship between nascent chain misfolding and ubiquitination may affect an incredibly broad range of cellular proteins.

The basis of recognition of nascent chains in both CTU^S and CTU^A remains unknown. I hypothesize that misfolding of the nascent chain is monitored and sensed by the CTU^A system. In addition to off-pathway folding errors, the rate of amino acid misincorporation during translation is relatively high, with amino acid substitutions estimated to occur between 1 in 10³-10⁴ codons translated (Drummond & Wilke 2009). It is conceivable that folding errors associated with mis-incorporations may account for a significant fraction of nascent chains that are subject to CTU^A (roughly 8-10% of all nascent chains). In contrast to CTU^A, CTU^S appears to be directly associated with stalling of the translational machinery, as CTU^S is induced by both drugs and polypeptide sequences (e.g., poly-lysine containing proteins) that promote stalling. It should also be noted that treatment of cells with cycloheximide leads to a transient accumulation of CTU products on polysomes. This effect should be considered in experimental designs

that include polysome isolation, as pre-treatment of cells with cycloheximide is a part of most polysome isolation protocols.

Two ubiquitin ligases have been implicated in ubiquitination of stalled nascent chains: Ltn1 and CCR4/Not complex (Dimitrova *et al.* 2009; Bengtson & Joazeiro 2010; Brandman *et al.* 2012). Additional factors - Tae2, Rqc1, and Cdc48 - have also recently been shown to function with Ltn1 in degradation of stalled nascent peptides (Bengtson & Joazeiro 2010; Brandman *et al.* 2012; Verma *et al.* 2013). As determined by siRNA knockdown, Ltn1 and CCR4/Not each accounted for less than 10% of total CTU activity in these assays (Figure 3.13A). The ligases for CTU^A have not yet been identified, but several reasonable additional candidates have been ruled out. CHIP is an Hsp70-associated RING E3 (Rosser *et al.* 2007), and the Ubr1 and Ubr2 ligases, have been shown to be involved in the co-translational degradation of artificial fusion proteins bearing destabilizing N-terminal residues (Turner & Varshavsky 2000). siRNA knockdown of CHIP had no effect on overall CTU, and Ubr1/Ubr2 double-knock out mouse embryo fibroblasts did not display diminished overall CTU (Figure 3.13B). Yeast Hul5 is a ubiquitin ligase that targets misfolded cytosolic proteins post-translationally (Fang *et al.* 2011), and siRNA knockdown of an apparent human ortholog (Ube3C) had no effect in our assays (Figure 3.13). Although the identity of the CTU^A ligase(s) remains to be determined, I envision that these ligases may function in one of two basic ways: either as ribosome-associated ligase(s) that monitor nascent polypeptides as they emerge from the ribosome, or as free cytosolic ligase(s) that monitor exposed nascent chains, either with or without the cooperation of chaperones. The first model is akin to the

modification of newly translated proteins by the ubiquitin-like modifier ISG15, an interferon-induced Ubl (Durfee *et al.* 2010). In this case, a single E3 (Herc5) mediates ISG15 conjugation, and Herc5 co-fractionates with polysomes. Herc5 co-fractionates with the 80S ribosome upon RNase treatment and with 60S subunit upon disruption of polysomes with EDTA. In the second model, features of defective or misfolded nascent chains might be recognized by the E3, independent of interaction with the ribosome itself.

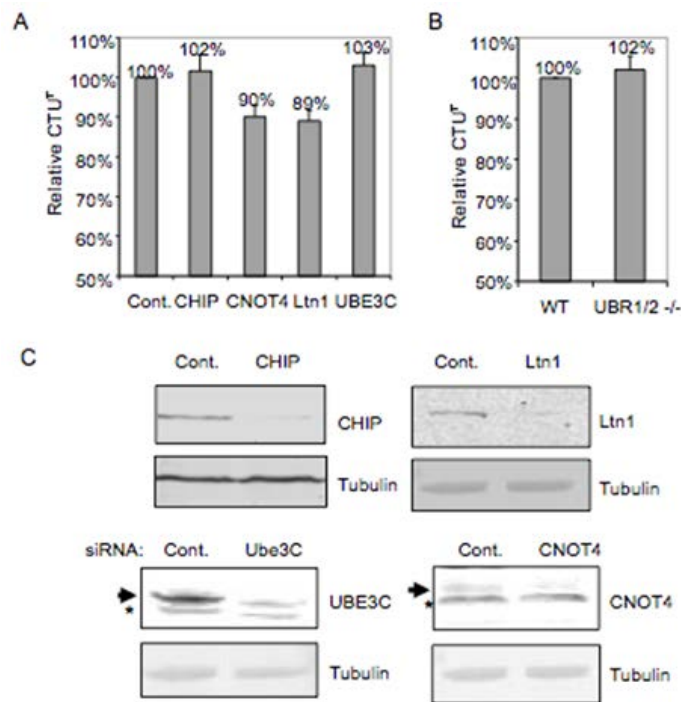


Figure 3.13: Role of Specific E3 Ligases in CTU^T.

(A) 293T cells were initially transfected with siRNAs targeting the mRNAs for the indicated E3 ligases or a control siRNA, and then transfected with FLAG-Ub plasmid DNA fifteen hours later. Cells were harvested 48 hours post-siRNA transfection, and CTU products were analyzed. (B) CTU^T was analyzed in wild-type and UBR1/2 double-knockout MEFs. CTU products were subjected to TUBE pulldown to isolate ubiquitinated nascent chains and CTU products were analyzed by quantitation of Bio-Puro incorporation with fluorescent-streptavidin. (C) The siRNA knockdowns were confirmed by immunoblotting with antibodies to the indicated ligases, with tubulin probed as a loading control. Asterisks mark background bands; arrows mark specific bands.

Our analyses of CTU products indicated that they are modified primarily with K48-linked polyubiquitin chains, and proteasome inhibition led to the accumulation of ubiquitinated nascent chains on cycloheximide-stalled polysomes in cells. Whether the proteasome can begin degrading CTU^A products before synthesis is complete (in the absence of cycloheximide-induced stalling) is not yet known. Our proteomic analysis preliminarily identified a set of ~130 CTU target proteins. These were mainly cytosolic or nuclear proteins, as opposed to membrane-associated proteins, consistent with our observation that less than 20% of CTU activity is associated with ribosomes at the ER. Further experimentation is required to distinguish between CTU^S and CTU^A targets in these analyses, and to determine whether subsets of CTU targets are ubiquitinated under different stress conditions.

Estimates of the fraction of newly synthesized proteins subject to rapid degradation in mammalian cells have varied from 6% to 30% (Wheatley *et al.* 1980; Schubert *et al.* 2000; Princiotta *et al.* 2003; Qian *et al.* 2005; Vabulas & Hartl 2005). Although this range illustrates the need for better techniques for assessing the turnover of newly synthesized proteins (Yewdell & Nicchitta 2006), these reports are generally consistent with our finding that CTU is a robust process in mammalian cells. Results presented here suggest that CTU^A is a component of a protein folding quality control system. The characteristics and recognition of nascent polypeptides with CTU^S and CTU^A complexes clearly require further definition. Key questions to be addressed concern the identification of the enzymes and degrons involved in CTU^S and CTU^A, how

the enzymes are localized to the translational machinery or nascent peptides, and, in the case of CTU^A, the basis for protein fate decisions being made in the course of translation.

Gene Name	Peptides	Annotation	Subcellular location
ABCD3	(3)3	ATP-binding cassette sub-family D member 3	Membrane
ACLY	(2)2	ATP-citrate synthase	Cytoplasm
ALB	(2)2	Putative uncharacterized protein ALB	Unknown
AP2B1	(2)3	AP-2 complex subunit beta	Cytoskeleton-associated
AP2M1	(5)6	AP-2 complex subunit mu	Cytoskeleton-associated
AP3D1	(1)1	AP-3 complex subunit delta-1	Cytoplasm
ATP1A1	(3)5	Sodium pump subunit alpha-1	Membrane
ATP1A2	(2)2	Sodium pump subunit alpha-2	Membrane
ATP5A1	(6)7	ATP synthase subunit alpha	Mitochondrial-associated
ATP6V0A1	(3)3	V-type proton ATPase 116 kDa subunit a isoform 1	Mitochondrial-associated
BAT1	(1)1	Spliceosome RNA helicase DDX39B	Nucleus
CAD	(20)25	CAD protein	Cytoplasm
CASP14	(1)1	CASP-14	Cytoplasm/Nucleus
CCBL2	(3)3	Kynurenine aminotransferase III	Mitochondrial-associated
CCT6A	(4)5	T-complex protein 1 subunit zeta	Cytoplasm
CCT7	(2)2	T-complex protein 1 subunit eta	Cytoplasm
CCT8	(1)1	T-complex protein 1 subunit theta	Cytoplasm
CHD4	(2)2	Chromodomain-helicase-DNA-binding protein 4	Nucleus
CLTC	(25)49	Clathrin heavy chain 1	Cytoskeleton-associated
CLTCL1	(11)20	Clathrin heavy chain 2	Cytoskeleton-associated
COPA	(21)31	Coatomer subunit alpha	Cytoplasm
CSDA	(2)2	DNA-binding protein A	Cytoplasm/Nucleus
DARS	(6)6	Aspartyl-tRNA synthetase	Cytoplasm
DDB2	(2)2	DNA damage-binding protein 2	Nucleus
DDX20	(3)3	ATP-dependent RNA helicase DDX20	Cytoplasm
DDX21	(8)12	Nucleolar RNA helicase 2	Nucleus
DDX5	(1)1	Probable ATP-dependent RNA helicase DDX5	Nucleus

Table 3.3

DHX30	(2)2	DEAH box protein 30	Mitochondrial-associated
DHX40	(1)1	Probable ATP-dependent RNA helicase DHX40	Unkown
DHX9	(13)22	ATP-dependent RNA helicase A	Cytoplasm/Nucleus
DYNC1H1	(8)9	Cytoplasmic dynein 1 heavy chain 1	Cytoskeleton-associated
EEF1A2	(3)3	Elongation factor 1-alpha 2	Ribosome-associated
EEF2	(9)14	Elongation factor 2	Ribosome-associated
EFTUD2	(9)14	Elongation factor Tu GTP-binding domain-containing protein 2	Nucleus
EIF2AK2	(2)2	Interferon-inducible RNA-dependent protein kinase	Cytoplasm
EIF2S3	(2)2	Eukaryotic translation initiation factor 2 subunit 3	Ribosome-associated
EIF3A	(30)42	Eukaryotic translation initiation factor 3 subunit A	Ribosome-associated
EIF3G	(3)3	Eukaryotic translation initiation factor 3 subunit G	Ribosome-associated
ENO1	(2)3	Alpha-enolase	Cytoplasm
EPRS	(17)22	Bifunctional aminoacyl-tRNA synthetase	Cytoplasm
ERLIN1	(2)2	Endoplasmic reticulum lipid raft-associated protein 1	ER-associated
ERLIN2	(1)1	Erlin-2	ER-associated
FAM115A	(4)5	Protein FAM115A	Unkown
FASN	(52)109	Fatty acid synthase	Cytoplasm
FLNA	(3)4	Filamin-A	Cytoskeleton-associated
FMR1	(2)3	Fragile X mental retardation protein 1	Cytoplasm
GNB2L1	(4)4	Receptor for activated C kinase	Ribosome-associated
GTF3C1	(1)1	General transcription factor 3C polypeptide 1	Nucleus
GTPBP4	(2)2	Nucleolar GTP-binding protein 1	Nucleus
HECTD3	(1)1	E3 ubiquitin-protein ligase HECTD3	Cytoplasm
HERC5	(2)2	E3 ISG15--protein ligase HERC5	Cytoplasm
HIST1H1C	(6)11	Histone H1d	Nucleus
HNRNPR	(4)7	Heterogeneous nuclear ribonucleoprotein R	Cytoplasm/Nucleus
HNRNPU	(20)43	Heterogeneous nuclear ribonucleoprotein U	Cytoplasm/Nucleus
HSPA1A	(3)4	Heat shock 70 kDa protein 1A/1B	Cytoplasm
HSPA1L	(2)2	Heat shock 70 kDa protein 1-like	Cytoplasm
HSPA8	(1)1	Heat shock 70 kDa protein 8	Cytoplasm
HSPCB	(4)5	Heat shock protein HSP 90-beta	Cytoplasm
HUWE1	(1)2	E3 ubiquitin-protein ligase HUWE1	Cytoplasm/Nucleus
IARS	(17)31	Isoleucyl-tRNA synthetase	Cytoplasm
IARS	(3)4	Isoleucyl-tRNA synthetase	Cytoplasm
IGF2BP1	(4)5	Insulin-like growth factor 2 mRNA-binding protein 1	Cytoplasm/Nucleus

Table 3.3 (continued)

IGF2BP3	(1)1	Insulin-like growth factor 2 mRNA-binding protein 3	Cytoplasm/Nucleus
IRS4	(12)15	Insulin receptor substrate 4	Cytoplasm
JAK1	(1)2	Tyrosine-protein kinase JAK1	Cytoplasm
KATNAL2	(1)1	Katanin p60 ATPase-containing subunit A-like 2	Cytoskeleton-associated
KIDINS220	(3)3	Kinase D-interacting substrate of 220 kDa	Cytoplasm
KTN1	(2)2	Kinectin	Cytoskeleton-associated
LARS	(7)11	Leucyl-tRNA synthetase	Cytoplasm
LAS1L	(1)2	Ribosomal biogenesis protein LAS1L	Nucleus
LBR	(3)3	Lamin-B receptor	Nucleus
LRP1	(3)3	Apolipoprotein E receptor	Cytoplasm
MARS	(6)8	Methionyl-tRNA synthetase	Cytoplasm
MCM5	(1)1	DNA replication licensing factor MCM5	Nucleus
MOV10	(10)12	Putative helicase MOV-10	Cytoskeleton-associated
MSH6	(1)1	DNA mismatch repair protein Msh6	Nucleus
MYCBP2	(7)9	Probable E3 ubiquitin-protein ligase MYCBP2	Nucleus
MYH14	(1)1	Myosin-14	Cytoskeleton-associated
MYH9	(3)3	Myosin-9	Cytoskeleton-associated
MYO1B	(2)2	Unconventional myosin-Ib	Cytoskeleton-associated
MYO1C	(1)2	Unconventional myosin-Ic	Cytoskeleton-associated
MYO5B	(3)3	Unconventional myosin-Vb	Cytoskeleton-associated
MYO6	(2)3	Unconventional myosin-VI	Cytoskeleton-associated
NCL	(5)8	Nucleolin	Nucleus
NCL3	(7)10	Calpain-5	Unkown
NXF1	(3)4	Nuclear RNA export factor 1	Cytoplasm/Nucleus
PA2G4	(3)4	Proliferation-associated protein 2G4	Cytoplasm/Nucleus
PABPC1	(18)28	Polyadenylate-binding protein 1	Cytoplasm/Nucleus
PABPC4	(7)10	Polyadenylate-binding protein 4	Cytoplasm
PARP1	(10)13	Poly [ADP-ribose] polymerase 1	Nucleus
PKM2	(2)2	Pyruvate kinase isozymes M1/M2	Cytoplasm
PRKDC	(11)14	DNA-dependent protein kinase catalytic subunit	Nucleus
PRPF8	(34)53	Pre-mRNA-processing-splicing factor 8	Nucleus
PSMD2	(6)8	26S proteasome regulatory subunit S2	Cytoplasm
PTPLAD1	(2)3	Protein tyrosine phosphatase-like protein PTPLAD1	ER-associated
RAD50	(2)2	DNA repair protein RAD50	Nucleus

Table 3.3 (continued)

RBM39	(1)1	RNA-binding protein 39	Nucleus
RBMXL2	(2)2	RNA-binding motif protein, X-linked-like-2	Nucleus
RFC1	(3)5	Replication factor C subunit 1	Nucleus
RPA1	(3)4	Replication protein A 70 kDa DNA-binding subunit	Nucleus
RPL6	(5)8	60S ribosomal protein L6	Ribosome-associated
RPL7A	(1)1	60S ribosomal protein L7a	Ribosome-associated
RPN2	(2)2	Ribophorin-2	ER-associated
RPS2	(4)5	40S ribosomal protein S2	Ribosome-associated
RPS3	(14)29	40S ribosomal protein S3	Ribosome-associated
RPS7	(2)3	40S ribosomal protein S7	Ribosome-associated
RPS8	(2)3	40S ribosomal protein S8	Ribosome-associated
SF3B3	(2)2	Splicing factor 3B subunit 3	Nucleus
SIN3A	(3)5	Paired amphipathic helix protein Sin3a	Nucleus
SLC16A1	(1)1	Monocarboxylate transporter 1	Membrane
SNRNP200	(9)11	U5 small nuclear ribonucleoprotein 200 kDa helicase	Nucleus
SSRP1	(2)2	FACT complex subunit SSRP1	Nucleus
SUPT16H	(6)7	FACT complex subunit SPT16	Nucleus
SYNCRIP	(1)1	Heterogeneous nuclear ribonucleoprotein Q	Nucleus
TARS	(3)3	Threonine--tRNA ligase	Cytoplasm
TCP1_	(3)4	T-complex protein 1 subunit alpha	Cytoplasm
TFRC	(1)2	Transferrin receptor protein 1	Membrane
TOP2A	(6)10	DNA topoisomerase 2-alpha	Nucleus
TOP2B	(9)12	DNA topoisomerase 2-beta	Cytoplasm/Nucleus
TRIP12	(2)2	Probable E3 ubiquitin-protein ligase TRIP12	Cytoplasm
TSR1	(1)1	Pre-rRNA-processing protein TSR1 homolog	Nucleus
TUBA1C	(3)6	Tubulin alpha-1C chain	Cytoskeleton-associated
TUBA4A	(2)2	Tubulin alpha-4A chain	Cytoskeleton-associated
USP9X	(1)1	Ubiquitin-specific protease 9	Cytoplasm
VCP	(8)13	TER ATPase	Cytoplasm
WDR33	(4)6	pre-mRNA 3' end processing protein WDR33	Nucleus
XRCC5	(2)3	DNA repair protein XRCC5	Nucleus
XRCC6	(3)4	DNA repair protein XRCC6	Nucleus
YBX1	(2)2	Nuclease-sensitive element-binding protein 1	Cytoplasm/Nucleus
ZNF281	(2)4	Zinc finger protein 281	Nucleus

Table 3.3 Identified CTU targets.

CTU products identified by LC/MS/MS. "Peptides" refers to number of unique peptides identified and number of assigned spectra.

Chapter 4: Potential role of CTU in against aging

4.1 INTRODUCTION

In the last decade, a strong connection has been established between protein translation and aging. Several findings indicate that reduced mRNA translation can significantly promote longevity of both invertebrate and vertebrate model organisms, including yeast, worms, flies, and mice (Hansen *et al.* 2007; Pan *et al.* 2007; Smith *et al.* 2008; Steffen *et al.* 2008; Selman *et al.* 2009; Zid *et al.* 2009; Johnson *et al.* 2013). However, the mechanism of how reduced protein translation can increase life span is unclear. Two major explanations have been proposed: 1) a subset of mRNAs encoding proteins that are beneficial for longevity and stress resistance are translated more efficiently when global translation is reduced (Steffen *et al.* 2008; Zid *et al.* 2009; Rogers *et al.* 2011), and 2) global reduction of protein synthesis allows the cellular protein repair and degradation system to maintain toxic proteins at a lower level (Kaeberlein & Kennedy 2007).

Loss of proteome homeostasis can be considered a hallmark of aging (Lopez-Otin *et al.* 2013). Onset of many age-related diseases is connected to the accumulation of damaged proteins and/or protein aggregates, such as Alzheimer's disease, Parkinson's disease, and cataracts (Balch *et al.* 2008; Douglas & Dillin 2010; Lopez-Otin *et al.* 2013). Successful maintenance of protein homeostasis requires collaboration between the protein synthesis machinery, chaperone systems, and proteolytic systems (ubiquitin-proteasome system (UPS) and autophagy-lysosomal system). Disruption of protein

synthesis fidelity or chronic expression of misfolded proteins has been shown to induce accumulation of protein aggregates and development of some age-associated diseases (Lee *et al.* 2006; Powers *et al.* 2009). In contrast, up-regulation of some chaperones, components of UPS, or autophagy has been reported to delay aging in many organisms (Walker & Lithgow 2003; Min *et al.* 2008; Kruegel *et al.* 2011; Liu *et al.* 2011; Rubinsztein *et al.* 2011; Chiang *et al.* 2012).

Newly synthesized proteins are prone to misfolding and aggregation (Ellis 2001), and this is compounded by errors in processes affecting transcription, mRNA processing, translation, and protein localization (Levine *et al.* 2005; Ogle & Ramakrishnan 2005; Pickrell *et al.* 2010). As a result, a significant fraction of newly synthesized proteins never attain their functional state. Timely and efficient clearance of misfolded proteins is crucial for maintaining cellular functions. Surprisingly, 6% - 30% of all eukaryotic newly synthesized proteins are very rapidly degraded by the UPS (Schubert *et al.* 2000; Qian *et al.* 2006), suggesting that the UPS plays an important role in quality control of newly synthesized proteins. In addressing the relationship between protein translation, ubiquitination, and degradation, I found that co-translational ubiquitination (CTU) is a conserved and robust pathway from yeast to mammals, with 5-6% of total nascent polypeptides being ubiquitinated in *S. cerevisiae*, and 12-15% in human cells. In addition, I showed that CTU is enhanced under conditions that promote protein misfolding or translational errors, indicating CTU is a pathway for the quality control of newly synthesized proteins. Given the connection between the protein translation and longevity, and the role of CTU in quality control of newly synthesized proteins, I have tested the

hypothesis that CTU may play a preventative role in cellular aging. The findings presented here provide preliminary evidence supporting this hypothesis.

4.2 MATERIALS AND METHODS

Strains: All *S. cerevisiae* strains except for the Mother Enrichment Program (MEP) strains used in this study are derivatives of BY4741 (*MATa*; *his3Δ1*; *leu2Δ*; *met15Δ*; *ura3Δ*). The BY4741 is referred to here as “wild type” relative to mutant derivatives, and all deletion mutants were obtained from the YKO MATa Strain Collection (Thermo Scientific), with the gene of interest was replaced by the KanMX4 cassette. MEP strains UCC5181 (*MATα ade2::hisG his3 leu2 trp1Δ63 ura3Δ0 met15Δ::ADE2 hoΔ::PSCW11-cre-EBD78-NATMX loxPUBC9-loxP-LEU2 loxP-CDC20-Intron-loxP-HPHMX*) and UCC5185 (*MATa/MATα ade2::hisG/ade2::hisG his3/his3 leu2/leu2 LYS2/lys2 ura3Δ0/ura3Δ0 trp1Δ63/trp1Δ63 MET15/met15Δ::ADE2 hoΔ::PSCW11-cre-EBD78-NATMX/hoΔ:: PSCW11-cre-EBD78-NATMX loxP-UBC9-loxP-LEU2/loxP-UBC9-loxP-LEU2 loxP-CDC20-Intron-loxPHPHMX/loxP-CDC20-Intron-loxP-HPHMX*) were kindly provided by Daniel Gottschling (Fred Hutchinson Cancer Research) (Lindstrom & Gottschling 2009).

Purification of Aged Cells (Magnetic Sorting Method): Mother enrichment program (MEP) cells were harvested from logarithmically growing YPD cultures (~OD₆₀₀=1.2), washed twice in phosphate-buffer saline (PBS), and resuspended in PBS at 1x10⁸ cells/ml (1OD₆₀₀≈1x10⁷ cells/ml). Sulfa-NHS-LC-biotin (Pierce) was added at a final concentration of 1 mg/ml and incubated at room temperature, protected from light, for 30 min. Cells were washed with YPD media for three times, and inoculated to a 1 L YPD culture at 2x10⁵ cells/ml. Cultures were incubated at 30°C for 2 hours and then treated with estradiol at a final concentration of 1 μM. At each time point, 500 ml of the culture was harvested and cells were resuspended in 8ml PBS and distributed to eight 1.5 ml microfuge tubes. Streptavidin-coated magnetic beads (Pierce) (100 μl) was added to each microfuge tube, and tubes were incubated for 30 min at room temperature. Cells

were then placed in a magnetic sorter (Promega), and after 15 min, the supernatants were carefully aspirated. Fresh YPD media (1 ml) was added to each tube, the mixtures were vortexed and cells again placed in the sorter for 10 min, and the process was repeated 3 times. Sorted cells were incubated in 25 ml pre-warmed YPD media for 20 min at 30°C, and then were pelleted and stored at -80 °C.

Yeast bud scar staining with calcofluor: Cells were collected by centrifugation, washed once with distilled deionized water (ddH₂O), resuspended in 1mg/ml calcofluor solution, and incubated at room temperature protected from light for 5 min. Cells were then washed 2-5 times with ddH₂O, and directly observed by fluorescence microscopy.

Replicative life span analysis by micromanipulation: Mother enrichment program (MEP) cells from exponentially growing YPD liquid cultures were diluted with fresh YPD medium, and then applied to YPD plates containing 1 μM estradiol. Individual cells (50-100) were separated on the plates using dissecting microscope and a micromanipulator, and selected for life span analysis. Selected cells were incubated at 30°C for 4 days to form microcolonies. As only mother cells can divide in the presence of estradiol, the number of cells in a microcolony represents the number of times a mother cell divided (referred to as the replicative life span).

4.3 RESULTS

4.3.1 Reduction of global protein translation leads to decreased CTU

CTU is a pathway for quality control of newly synthesized proteins, with the extent of CTU corresponding to the quality of ribosome-associated nascent chains (Duttler *et al.* 2013; Wang *et al.* 2013). To examine the possible effect of reduced translation on the quality of newly synthesized proteins, I determined the CTU level under conditions of lower protein translation rate. The mammalian target of rapamycin (mTOR) is a serine/threonine protein kinase that regulates protein synthesis, and inhibition of mTOR with rapamycin has been found to decrease protein translation and increase life span in many organisms (Powers *et al.* 2006; Medvedik *et al.* 2007; Harrison *et al.* 2009; Thoreen *et al.* 2009; Bjedov *et al.* 2010). I therefore treated 293T cells with rapamycin or Torin 1 (more potent mTOR inhibitor) (Thoreen *et al.* 2009) for 2 hours and then isolated polysomes from cell extracts by centrifugation using a 35% sucrose cushion. Ribosome-associated nascent chains were then labeled with biotinylated puromycin (Bio-Puro) *in vitro*. CTU products were isolated using TUBE-agarose beads and Bio-Puro-labeled nascent chains were detected with fluorescently tagged streptavidin. As shown in Figure 4.1B, both rapamycin and Torin 1 treatments led to a ~20% and ~40% decrease, respectively, in CTU. Meanwhile, S³⁵-Met-labeling showed that rapamycin and Torin1 inhibited overall translation by ~15% and ~50%, respectively (Figure 4.1A), consistent with previous studies (Thoreen *et al.* 2009; Thoreen *et al.* 2012). This result suggests that a reduction in translational load can lead to an increase in the quality of nascent chains in human cells.

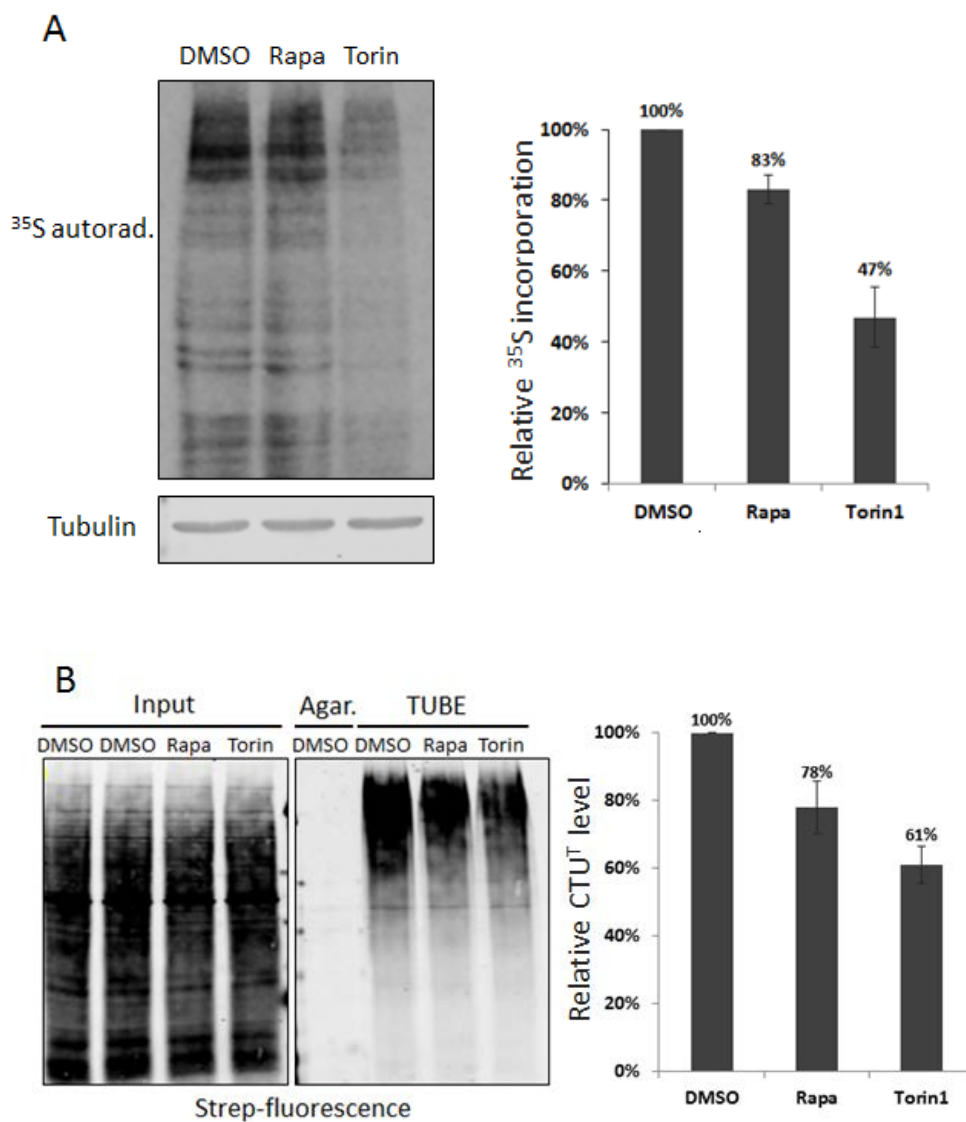


Figure 4.1: Rapamycin and Torin 1 treatments led to a decrease of global protein translation as well as CTU level in 293T cells.

(A) 293T cells were treated with DMSO, 250 nM rapamycin or 250 nM torin1 for 2 hours and then labeled with ³⁵S-methionine for 30 min. Cell lysates were analyzed by SDS-PAGE and autoradiography. Anti-tubulin blot shows proteins were loaded equally in each lane. Error bars indicate SEM of three independent experiments. (B) Polysomes were isolated from DMSO, rapamycin and Torin 1 treated cells and used for *in vitro* Bio-Puro conjugation assay to determine CTU levels. Error bars indicate SEM of three independent experiments.

CTU levels in yeast were also examined, using mutants that were predicted to decrease translational load. Several yeast deletion mutants were chosen, including $\Delta tif1$ (Tif1 is a translation initiation factor), $\Delta ssf1$ (Ssf1 is a 60S subunit maturation factor), $\Delta tor1$ (Tor 1 is a subunit of TORC1 kinase), $\Delta rpl21b$ and $\Delta rpl22a$ (Rpl21B and Rpl22A are two ribosomal proteins). All of these mutant strains have lower protein synthesis rates and extended replicative life spans (Steffen *et al.* 2008) (Figure 4.2A). Figure 4.2B shows that CTU level in all of these strains was 30%-50% lower than the wild-type strain, suggesting that reduction in protein synthesis increases the quality of translation products in yeast, as in human cells.

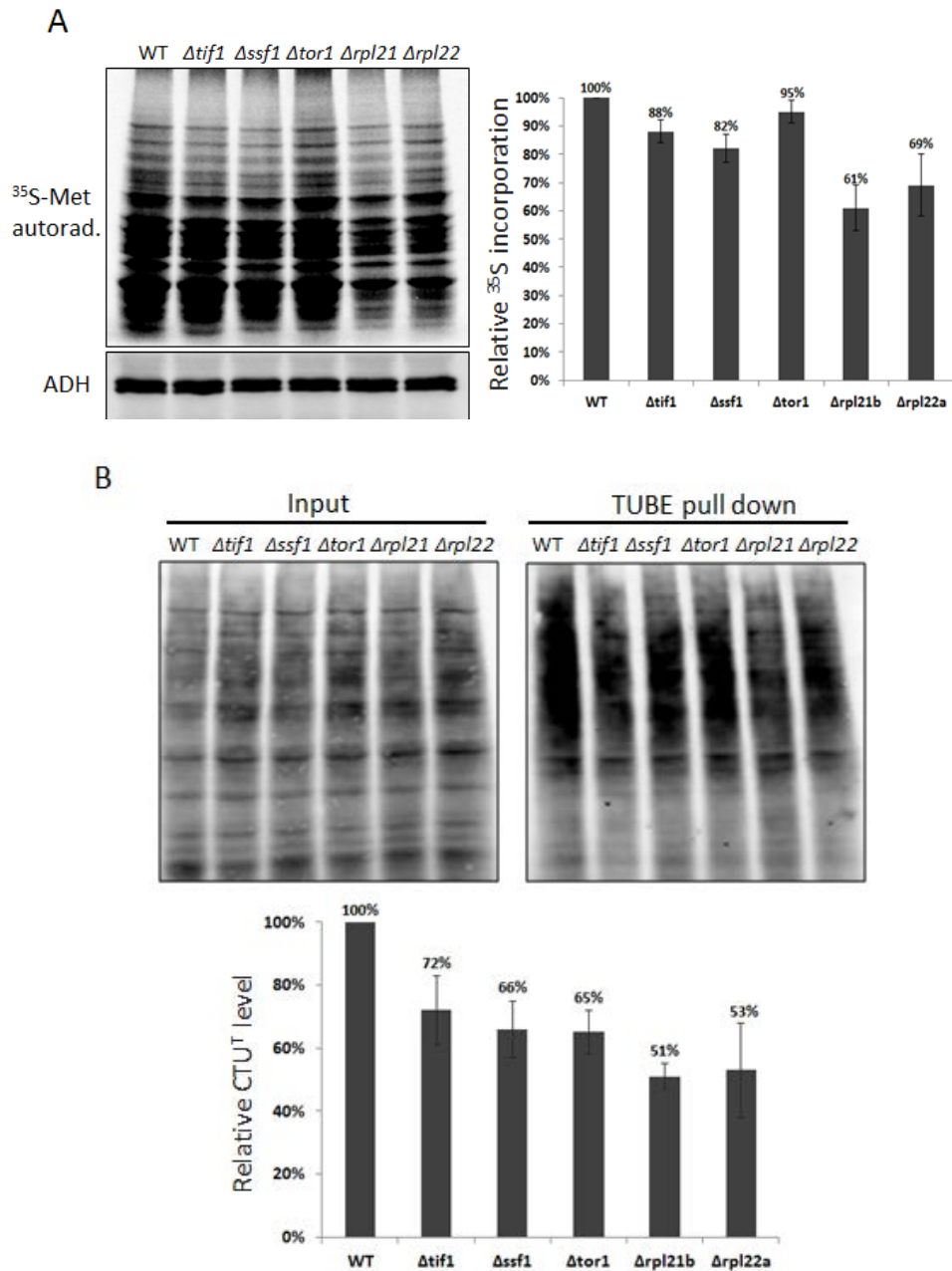


Figure 4.2: Yeast mutants with reduced protein synthesis rate show lower level of CTU.

(A) Selected yeast mutant strains showed reduced protein translation rate. All strains were labeled with ^{35}S -methionine for 30min, and then analyzed by SDS-PAGE and autoradiography. Error bars indicate SEM of three independent experiments. (B) CTU level was lower in mutant strains with reduced translation rate. The CTU level of all selected yeast strains was analyzed by polysome purification and *in vitro* Bio-Puro conjugation assays. Error bars indicate SEM of three independent experiments.

4.3.2 Newly synthesized proteins are a major source of proteasome substrates

A large fraction of newly synthesized proteins is rapidly degraded through a proteasome-dependent manner (Schubert *et al.* 2000). I therefore determined the fraction of total proteasome substrates that were derived from newly synthesized proteins. As expected, the total amount of ubiquitinated proteins in 293T cells increased about 60% after 2 hours of treatment with MG132, a proteasome inhibitor. Consistent with the findings of Kim *et al.* (Kim *et al.* 2011b), if cells were simultaneously treated with MG132 and cycloheximide (CHX), MG132 did not elicit a detectable increase of ubiquitinated proteins (Figure 4.3A). A similar result was observed when cells were co-treated with MG132 and harringtonine (Figure 4.3A), a translation initiation inhibitor, consistent with the notion that nearly all of the ubiquitinated proteins that accumulate in the presence of MG132 are derived from newly translated proteins. There was a slight decrease in total ubiquitination in samples only treated with CHX or harringtonine, representing the clearance of previously made newly synthesized proteins (Figure 4.3A). CHX also blocked the MG132-induced increase of ubiquitination in yeast cells (Figure 4.3B). Combined, these data indicate that newly synthesized proteins are a major source of proteasome substrates under unstressed conditions in both human and yeast cells.

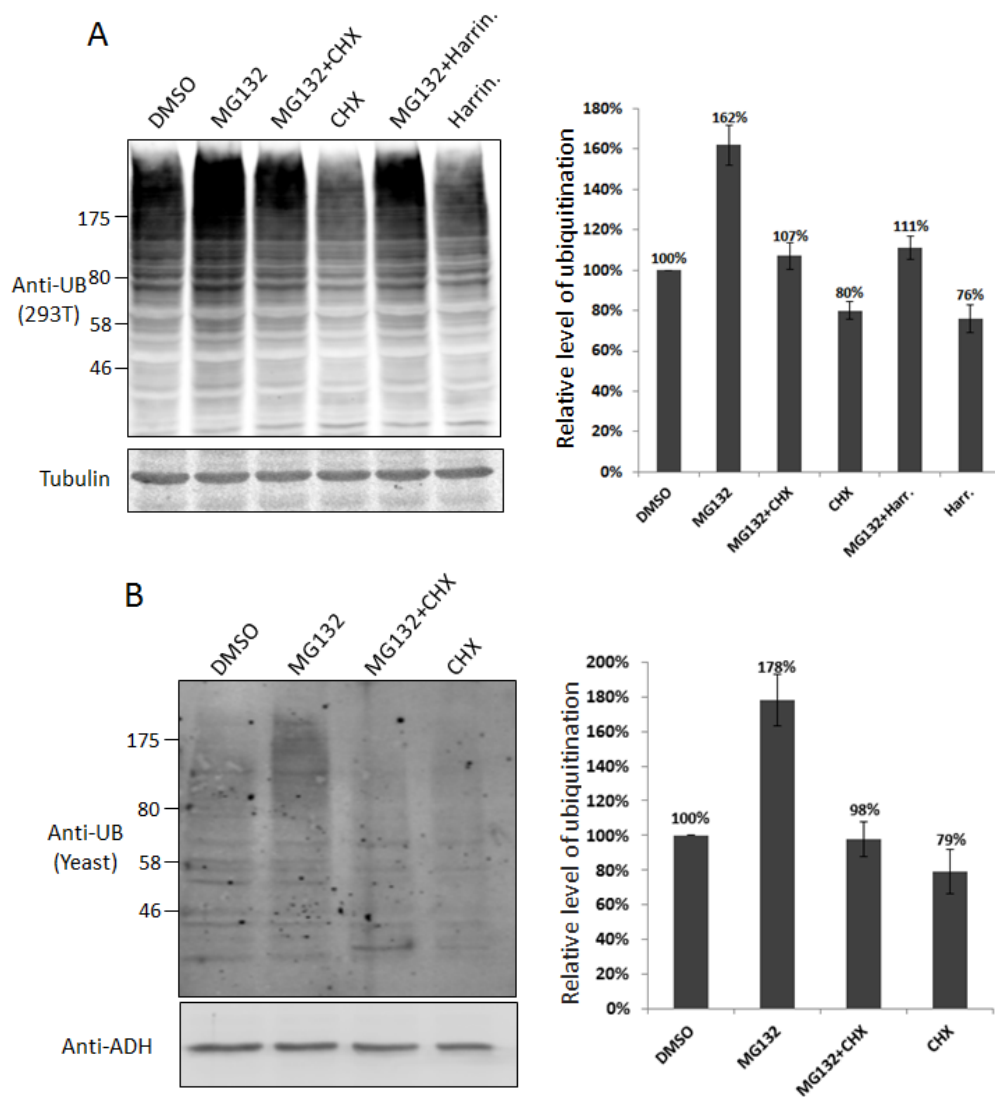


Figure 4.3: Newly synthesized proteins are the major source of proteasome substrates.

(A) 293T cells were treated with drugs as indicated, with final concentrations of 2 $\mu\text{g/ml}$ Harringtonine, 100 $\mu\text{g/ml}$ CHX and 50 μM MG132, for 2 h. Cell lysates were analyzed by SDS-PAGE and blotting with anti-ubiquitin. Anti-tubulin blot shows proteins were loaded equally in each lane. Error bars indicate SEM of three independent experiments. (B) Yeast cells were inoculated into a synthetic medium (0.17% yeast nitrogenous base without ammonium sulfate, 0.1% proline, appropriate amino acids, and 2% glucose). The culture grown overnight at 30°C was re-inoculated to a fresh media containing 0.003% SDS at 1:10 ratio. The cells were grown for another 3 h at 30°C, and then were added with 50 μM MG132 and/or 100 $\mu\text{g/ml}$ CHX. After 2.5 h incubation, cells were harvested and lysates were analyzed by SDS-PAGE and blotting with ubiquitin specific antibodies. Anti-ADH blot shows that proteins were loaded equally in each lane. Error bars indicate SEM of three independent experiments.

4.3.3 Transient proteasome inhibition decreases replicative life span (RLS), and this is suppressed by inhibition of translation.

Considering that decreased translational load is correlated with both decreased CTU and increased life span, I hypothesized that a transient accumulation of rapidly degraded newly synthesized proteins, including CTU products, might have a deleterious effect on replicative life span (RLS) in yeast. This was tested by treating mother enrichment program (MEP) yeast cells with MG132 for 2.5 hours, in the absence or presence of cycloheximide, followed by determination of replicative life span of 15 individual cells through micromanipulation. As shown in Figure 4.4, MG132 treatment led to around 25% decrease in RLS, with the median RLS decreased from 34 to 25 generations. Surprisingly, if the MG132-treated cells were simultaneously treated with CHX, the median RLS was restored back to 37 generations. These data indicate that accumulation of ubiquitinated newly synthesized proteins over a short period of time has long-term adverse effects of the yeast RLS. Given that the major source of proteasome substrates under unstressed conditions are newly synthesized proteins, this suggests that quality control of newly synthesized proteins might be an important determinant of aging under physiological conditions.

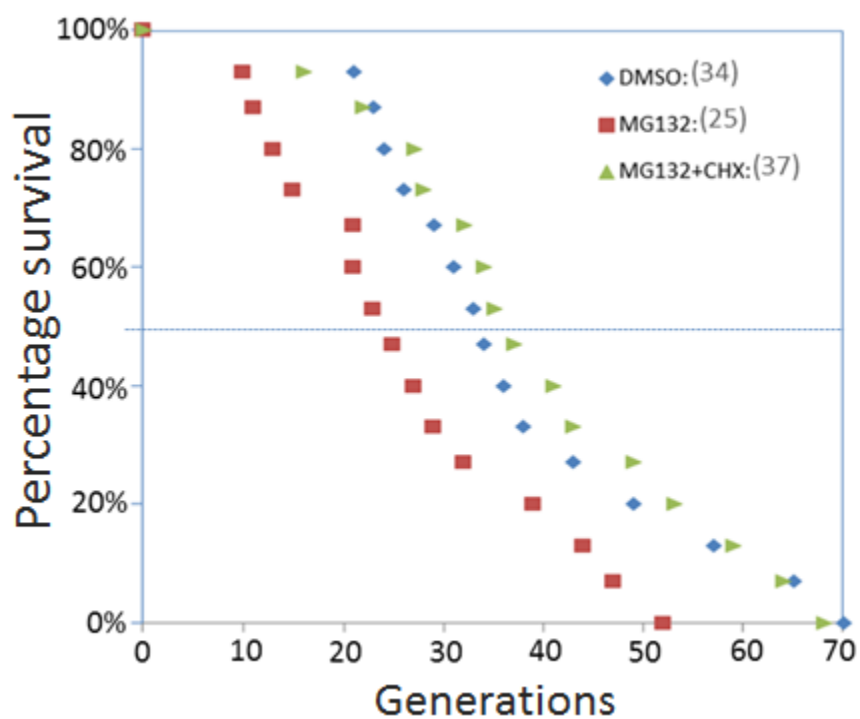


Figure 4.4: MG132 treatment led to a decrease of yeast RLS whereas co-treatment with CHX can restore it.

Yeast cells were inoculated into synthetic media as described in Figure 4.3B. The overnight culture was re-inoculated into the fresh synthetic media plus 0.003% SDS and grown for 3 more hours prior to addition of 50 μ M MG132 plus or minus of 100 μ g/ml CHX. Cells were incubated 2.5 h at 30 $^{\circ}$ C, and then washed 3 times with YPD media. The RLS of cells were then analyzed by micromanipulation.

4.3.4 CTU is increased in aged yeast

Aging is a process accompanied with the loss of proteasome homeostasis (proteostasis) (Lopez-Otin *et al.* 2013). One possible reason for loss of proteostasis is that production of misfolded/damaged proteins exceeds the capacity of proteolytic systems. With this in mind, I examined the CTU level in aged yeast cells. Aged yeast cells were enriched and isolated through a previously described magnetic sorting method (Smeal *et al.* 1996), as illustrated in Figure 4.5A. Briefly, the cell walls of exponentially growing yeast cells were first labeled with biotin (Sulfa-NHS0LC-biotin) in PBS, unincorporated biotin was washed away, and cells were returned to growth media for 24 hours. As the cell walls of daughter cells consist of only newly synthesized components, biotin-labeled molecules are only found on cell walls of mother cells. After 24 hours, mother cells were isolated from the total cell populations using streptavidin-coated magnetic beads. The average age of the mother cell population was estimated based on bud scars, as visualized by calcofluor white staining.

As shown in Figure 4.5B, the “aged” mother cells had greater than 10 bud scars. To enrich for “young” cells, the same procedure was followed, but cells were returned to growth media after biotin labeling for only 1 hour before collecting the biotin labeled cells. Importantly, although these were, by definition, mother cells, they were nevertheless “young” cells since an exponentially growing culture of yeast cells, as was used for the biotin labeling, consists primarily of daughter cells. This was confirmed again by calcofluor white staining, which showed that this “young” cell population had, on average, less than 2 bud scars. Polysomes were purified from both young and aged cells and the extent of CTU was determined using the *in vitro* Bio-Puromycin conjugation and TUBE pull-down approach. Figure 4.5C shows that CTU level of aged

cells was over 60% higher than the level of young cells, suggesting that the quality of newly synthesized proteins is lower in aged cells.

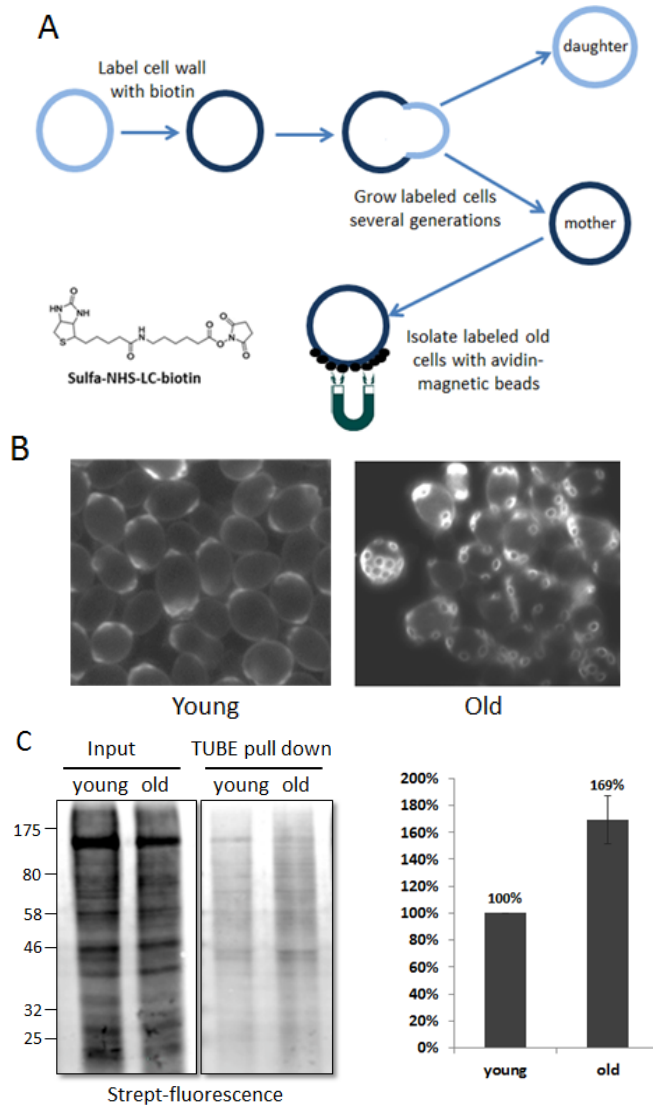


Figure 4.5 The CTU level is increased in old cells.

(A) Strategy for isolating old mother cells from total yeast populations. (B) Bud scar staining with calcofluor. Isolated cells were stained with calcofluor to determine the number of bud scars, which represent the age of the cell. (C) CTU level is increased with cell aging. Polysomes were isolated from both young and old cells, and used for the *in vitro* Bio-Puro conjugation assay to determine CTU level. Error bars indicate SEM of three independent experiments.

4.3.5 Deletion of Ltn1, the major E3 ligase for CTU^S, decreases RLS.

The results described above show that 1) decreased translational load decreases CTU and increases RLS, 2) transient accumulation of CTU products (via proteasome inhibition) has a deleterious effect on RLS, and 3) that CTU is higher in aged cells than in young cells. CTU is a combination of CTU^S and CTU^A (Wang *et al.* 2013). Although we do not know the ubiquitin ligases or other components involved in CTU^A, the majority of CTU^S is mediated by the Ltn1 ligase (Bengtson & Joazeiro 2010; Brandman *et al.* 2012; Shao *et al.* 2013).

To begin to evaluate the effect of Ltn1 on RLS, I first determined the contribution of Ltn1 to total CTU levels in yeast, which had not previously been reported. Polysomes were isolated from both wild type and $\Delta ltn1$ strains and incubated with Bio-Puro in test tubes to label nascent chains. CTU products were isolated with TUBE-beads and detected with fluorescent streptavidin. As shown in Figure 4.6A, deletion of Ltn1 led to over 50% decrease of CTU^T level, and the nearly complete elimination of CTU^S. Thus, Ltn1 is the major CTU^S ligase in yeast, and CTU^S accounts for approximately half of all CTU in yeast.

To evaluate the importance of CTU^S in RLS, the *ltn1* Δ mutation was created in the MEP yeast strain background. Figure 4.6B shows that deletion of Ltn1 caused a reduction of median RLS from 38 to 29 generations, suggesting that blocking the CTU^S pathway has an adverse effect on yeast RLS.

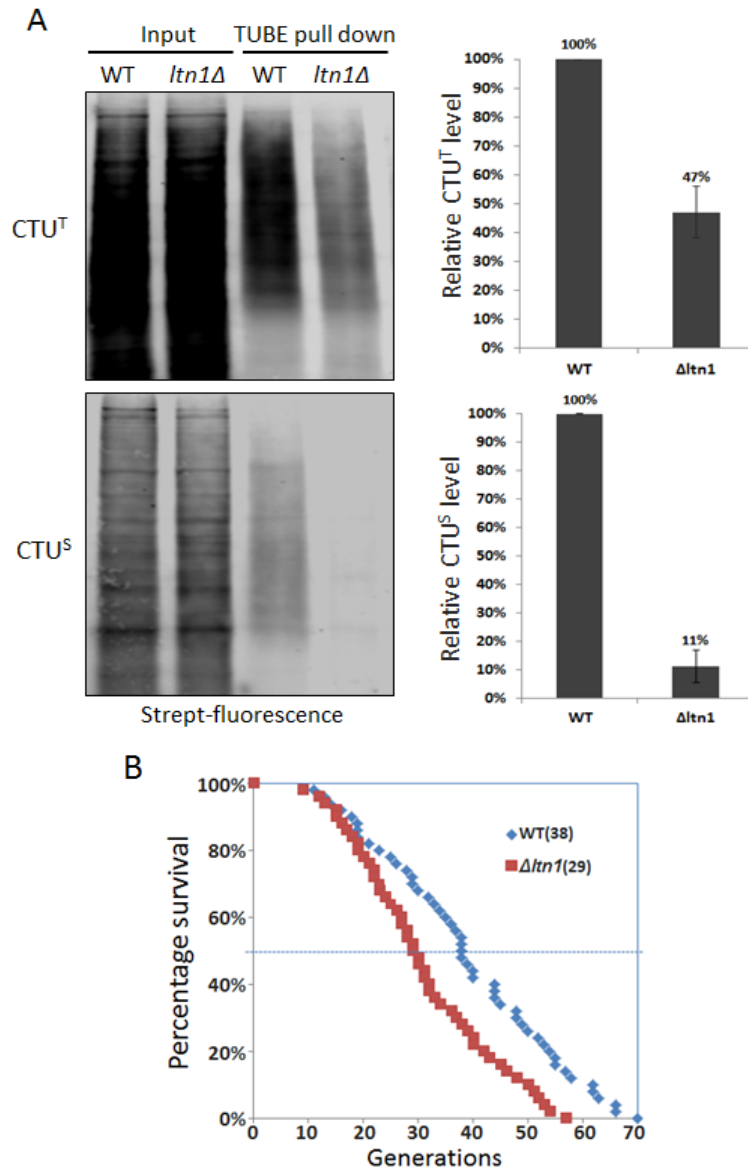


Figure 4.6: Deletion of *Ltn1* gene led to a decrease of RLS.

(A) Deletion of *Ltn1* led to ~50% decrease of CTU^T and ~90% decrease of CTU^S. Polysomes were purified from both wild type and *Δltn1* strains, and then used for *in vitro* Bio-Puro conjugation assay to determine the level of CTU. For CTU^S analysis, prior to polysome purification, cells were switched to YP media (YPD without glucose) and incubated at 30°C for 10 min to run-off active translation complexes (Ashe *et al.* 2000). Error bars indicate SEM of three independent experiments. (B) Deletion of *Ltn1* shortens the RLS of yeast. The RLS of both wild type and *Δltn1* strains were measured through micromanipulation as described in Materials and Methods. RLS of 50 individual cells were examined for each strain, with median RLS of wild type strain is 38 generations and median RLS of *Δltn1* strain is 29 generations.

4.4 DISCUSSION

The proteasome is the primary site for protein degradation, responsible for 80-90% of total intracellular protein turnover (Herrmann *et al.* 2010). In this study, I found that newly synthesized proteins are a major source of proteasome substrates in both yeast and human cells under physiological conditions, consistent with the previous finding that a very significant fraction of the ubiquitinated proteome represents the modification of newly synthesized proteins (Kim *et al.* 2011b). To test for a link between the degradation of newly synthesized proteins and longevity, I blocked the proteasome function to accumulate rapidly degraded newly made proteins (most are presumed to be due to folding failure) in yeast. Surprisingly, only two and half hours of proteasome inhibition by MG132 treatment shortened the RLS of yeast by 25%, with the median RLS decreased from 34 to 25 generations. Interestingly, if the MG132-treated cells were co-treated with CHX, their RLS was restored. These data indicate that accumulation of ubiquitinated newly synthesized proteins over a short period of time has long-term adverse effects of the yeast RLS. Given that the major source of proteasome substrates under unstressed conditions are newly synthesized proteins, this suggests that quality control of newly synthesized proteins might be an important determinant of aging under physiological conditions.

Reduced mRNA translation is believed to be beneficial for maintenance of proteome homeostasis, as the production of both normal and damaged proteins are reduced (Kaeberlein & Kennedy 2007). I have shown here that reduced translation can also increase the quality of newly synthesized proteins. For example, rapamycin treatment of 293T cells led to ~15% decrease of total protein translation and ~20% decrease of CTU (Figure 4.1). Therefore, if all CTU products represent misfolded/damaged proteins, the rapamycin treatment will result in ~35% reduction of

aberrant protein production from mRNA translation. A similar effect was also observed in yeast mutants with lower protein synthesis rates. As shown in Figure 4.2, all tested yeast mutants showed 5%-40% less protein translation, and meanwhile exhibited 30%-50% lower CTU levels, indicating that they only produce 30%-60% of misfolded proteins normally made from translation in wild-type yeast. Given that the major source of proteasome substrates under unstressed conditions are newly synthesized proteins (Figure 4.3), slight reductions of mRNA translation can significantly relieve the burden of the proteasome.

Levels of damaged/misfolded proteins and protein aggregates increase with age of various organisms, ranging from yeast to humans (Stadtman *et al.* 1992; Koga *et al.* 2011; Baraibar & Friguet 2012). Once these toxic proteins reach a critical level, a negative feedback loop is believed to further accelerate aging by exacerbating proteostatic decline (Andersson *et al.* 2013). Either increased production of damaged proteins or decreased capacity of protein quality control system can disrupt the protein homeostatic balance and lead to accumulation of toxic proteins. Indeed, the activity of the proteasome has been shown to decline during aging in many model organisms (Friguet *et al.* 2000; Shringarpure & Davies 2002; Baraibar & Friguet 2012). However, a recent study reported that the level and potential capacity of the proteasome is actually maintained in aged yeast, and proteasomes that cannot function properly are predominantly due to age-associated protein aggregates obstructing their function (Andersson *et al.* 2013). This observation raises an interesting question: Is the declined activity of proteasome a reason or a result of the accumulated damaged proteins in aged cells? In this study, I showed that the CTU level in aged cells (>10 generations) is ~70% higher than the level in young cells, supporting the hypothesis that increased production

of damaged proteins with age is a reason for disruption of the protein homeostatic balance.

CTU is a pathway for quality control of newly synthesized proteins (Duttler *et al.* 2013; Wang *et al.* 2013). Ltn1 has been confirmed as the major E3 ligase of CTU^S pathway in yeast in this study, since deletion of Ltn1 nearly eliminates all CTU^S products. In addition, I showed that deletion of Ltn1 resulted in ~25% decrease of yeast RLS. A previous study has reported that Ltn1 knockout mice exhibit extremely short life span, with ~90% death within 100 days (no wild-type mice died in this period of time). Moreover, the Ltn1^{-/-} mice showed profound early-onset and aged-dependent progressive neurological and motor dysfunction (Chu *et al.* 2009). Taken together, these data suggest that the CTU pathway plays a protective role during the aging process.

Chapter 5: Conclusion and future directions

5.1 CHARACTERIZATION OF THE CTU PATHWAY

In Chapter 3, I showed that CTU is a conserved and robust pathway from yeast to humans, with 5-6% of total nascent polypeptides being ubiquitinated in *S. cerevisiae*, and 12-15% in human cells. A preliminary set of CTU targets (~130) have been identified through my study. Several interesting findings were among this first set of targets. First, the mass spectrometry results showed strong evidence for K11 and K48 polyubiquitin chains on CTU targets, with no evidence of any other chain types. This result was confirmed by the experiment in which expression of R11/R48 ubiquitin led to a sharp decrease of the average molecular weight distribution of CTU products (Figure 3.5C). Second, most of the identified CTU targets are high molecular weight proteins, with the average length over 1000 amino acids, which is as twice long as the average length of total human proteins (~485 amino acids). Given the lower folding and higher aggregation propensity of the longer proteins (Ivankov *et al.* 2003; Wong *et al.* 2005; Kiraga *et al.* 2007; Ouyang & Liang 2008), this observation is consistent with the model that CTU is a quality control pathway for newly synthesized proteins. Although another group reported a similar finding in yeast (Duttler *et al.* 2013), we cannot rule out the possibility that this observation is a result of experimental bias. Since longer proteins normally contain more ubiquitination sites and are more likely to be highly ubiquitinated, the anti-ubiquitin pull down step in the purification of CTU products may tend to enrich those highly

ubiquitinated large proteins. Therefore, an unbiased strategy is required to isolate CTU targets for LC-MS/MS identification.

A recently developed technique by using an antibody that specifically recognizes the GG dipeptide “remnant” left on ubiquitinated lysine side chains after tryptic digestion would be a good choice to isolate CTU products in an unbiased manner (Xu *et al.* 2010). This approach has been successfully used by the Harper and Gygi labs to globally map ubiquitination sites (Kim *et al.* 2011b). Therefore, this approach is also able to identify the sites of CTU on the modified nascent polypeptides. This information could be important for at least two major reasons. Firstly, many proteins in our preliminary proteomic analysis were known in the Harper/Gygi study to contain many ubiquitination sites, in one case as many as 94 (PRKDC). It will be interesting if all of these sites, or only a subset, represent sites of co-translational ubiquitination, with another subset representing sites critical for post-translational ubiquitination. Secondly, the modification site results could be used to determine if there is a “code” for co-translational ubiquitination in terms of consensus recognition sites. Combining this technique with the approaches for separating stalled and active translation complexes, the targets of CTU^A and CTU^S, separately, can potentially be identified.

Although nascent chains have been previously shown to be ubiquitinated within stalled and defective translation complexes (referred to as CTU^S) (Bengtson & Joazeiro 2010; Brandman *et al.* 2012; Shao *et al.* 2013; Verma *et al.* 2013), I showed that nascent chain ubiquitination also occurred within active translation complexes (CTU^A). CTU^A accounted for approximately two-thirds of total CTU (CTU^T) in human cells and

approximately half of CTU^T in yeast cells. CTU^A and CTU^S may reflect two different mechanisms for recognition of defective proteins.

Translational stalling is thought to be the key determinant for substrate recognition in the CTU^S pathway (Bengtson & Joazeiro 2010). Since much of the ribosome stalling is due to translation of damaged/truncated mRNA, CTU^S is often coupled with mRNA quality control pathways: such as nonsense-mediated decay (NMD), no-go decay (NGD) and nonstop decay (NSD) (Shoemaker & Green 2012). By using a brief pactamycin treatment to run-off the nascent chains on active translation complexes, I found that approximately 20% of ribosomes are stalled or transiently paused complexes. Interestingly, only a fraction of these stalled/paused complexes (~15%-18%) contain ubiquitinated nascent chains. This is consistent with the model that a portion of translation stalling/pausing may provide a regulatory role of protein synthesis at a post-translation initiation level (those do not trigger ubiquitination) (Shalgi *et al.* 2013). This observation raised an important question: how does a cell distinguish ‘unnaturally’ stalled nascent chains needing to be disposed, from transient translation pausing with regulatory function? Although the exact mechanism of this discrimination remains unknown, a proposed model theorizes that the length of stalling time might be critical (Shoemaker & Green 2012).

Treatments that induced protein misfolding led to increased level of CTU^A (Figure 3.11), suggesting that misfolded nascent chains are the targets of CTU^A. The protein quality control system recognizes misfolded proteins based on their unique properties, such as exposure of long stretches of hydrophobic residues. However, since nascent

chains share the same properties with misfolded proteins, how the quality control system is able to discriminate misfolded nascent chains from normal nascent chains is an interesting question that needs to be addressed. Polypeptides normally cannot complete folding until they are fully synthesized and released from the ribosome, whereas protein domains are relatively independent folding units and usually can form stable and compact three-dimensional structures. A promising model is that polypeptides are undergoing a “domain-wise” co-translational quality surveillance, which corresponds to the “domain-wise” co-translational folding. In other words, a protein domain, but not the full length protein, is the minimal quality control unit. In this model, the nascent polypeptide containing at least one full length misfolded domain is the preferred target of the co-translational quality control pathway. Consistent with this hypothesis, large proteins with multiple domains are highly enriched among identified CTU targets; meanwhile proteins shorter than 300 amino acids are largely excluded (the length of a domain is between 50-300 amino acids) (Duttler *et al.* 2013).

Although the CTU pathway functions in quality control of newly synthesized proteins, whether the high basal level of CTU products all represents aberrant proteins requires further investigation. Besides misfolded nascent chains, short-lived regulatory proteins are a possible group of CTU targets. Many regulatory proteins are degraded very rapidly, with a half-life less than 10 min. For example, the protein HIF-1 α (hypoxia-inducible factor-1 alpha), which is a transcription factor that senses the availability of oxygen in the cellular environment and promotes the formation of blood vessels in hypoxic environments, is normally degraded with a half-life of 10 min (Salceda & Caro

1997). Rapid elimination of short-lived regulatory proteins is critical for the regulation of transcription, metabolism and growth. However, regulatory proteins are normally low abundance proteins, so deeper proteomic identification with high substrate coverage is required to identify this possible type of CTU targets.

The E3 ligase(s) that are responsible for CTU^A and CTU^S pathways remain to be identified. The ribosome-associated E3 ligase, Ltn1, has been reported to be involved in the CTU^S pathway (Bengtson & Joazeiro 2010; Brandman *et al.* 2012). I showed here that deletion of Ltn1 in yeast eliminated nearly all CTU^S products and led to ~50% decrease of CTU^T. However, knocking down Ltn1 in human cells by siRNA showed only a minor decrease of CTU^T level (~10% decrease). These data indicate that Ltn1 is the major E3 ligase of CTU^S pathway in yeast, but how important is Ltn1 in mammalian CTU^S pathway requires further evaluation. The issue with the siRNA experiment in mammalian cells is that it cannot knock down Ltn1 completely, so the more accurate way to test the role of Ltn1 in mammalian cells is by using the Ltn1^{-/-} mouse cell line which is available (Chu *et al.* 2009).

Hel2 is another ribosome-associated E3 ligase that has been proposed to function upstream of Ltn1 for clearance of stalled nascent chains (Brandman *et al.* 2012). My result revealed that deletion of Hel2 only caused a moderate decrease of CTU^S level (~15% decrease), suggesting that Hel2 is not a prerequisite of Ltn1-mediated degradation of stalled nascent chains. The exact function of Hel2 in the CTU^S pathway needs further evaluation. Little is known about what E3 ligase(s) are involved in the CTU^A process. Several E3 ligases, which are known to function in protein quality control, have been

tested, but none of them seems to play a major role in the CTU^A pathway (Duttler *et al.* 2013; Wang *et al.* 2013). One possible model is that there are multiple E3 ligases functioning in the CTU^A pathway, with each of them recognizing a subset of CTU^A substrates.

5.2 PROTEIN TRANSLATION AND CTU IN LONGEVITY AND AGING

Newly synthesized proteins contribute a consistent stream of misfolded proteins to the cellular quality control system. In Chapter 4, I showed that newly synthesized proteins are the major source of proteasome substrates under non-stressed conditions (Figure. 4.3), consistent with a previous finding that a very significant fraction of the ubiquitinated proteasome is represented by newly synthesized proteins (Kim *et al.* 2011b). It is interesting to consider the impact of rapidly degraded newly made proteins, including CTU products, on overall cellular homeostasis. Since the number of ribosomes is several fold higher than the number of proteasomes in eukaryotic cells, and a large fraction of newly made proteins need to be disposed rapidly, the damaged/misfolded newly synthesized proteins should represent a substantial burden for the proteasome pathway. Now the questions are: what percentage of proteasome capacity is occupied by rapidly degraded newly synthesized proteins under non-stressed conditions, and more importantly, what capacity of the proteasome system is left for possible stress-induced misfolded proteins?

The capacity of the proteasome can be represented as the degradation rate of a given substrate. The load of proteasome substrates can be depleted by inhibition of protein

translation (as newly synthesized proteins are the major sources of proteasome substrates). Therefore, the full capacity of the proteasome system can be represented as the time required for degradation of a certain amount of a given substrate in cells, when endogenous proteasome substrates are pre-cleared by inhibition of translation. Likewise, the un-occupied proteasome capacity can be estimated when endogenous proteasome substrates are not pre-cleared.

Reduced protein translation has been shown to increase the life span of various organisms. One possible reason is that it is a benefit for maintenance of proteome homeostasis, because the production of both normal and aberrant proteins is reduced, leading to less influx of misfolded proteins to the quality control system. I showed that reduction of protein translation is actually more beneficial to proteostasis than had been previously thought. I found that reduced protein translation leads to a lower level of CTU. As the extent of CTU corresponds to the quality of nascent polypeptides (Figure 3.11), it suggests that reduced protein translation can increase the quality of newly synthesized proteins, possibly by relieving the burden of chaperone systems. Further evidence is required to verify this hypothesis. Increased quality of newly synthesized proteins should be accompanied with reduced production of aberrant proteins by translation. Therefore, it is important to measure the fraction of rapidly degraded newly synthesized proteins, under conditions with a lower protein translation rate. Furthermore, it is also important to test whether reduction of protein translation retards the accumulation of protein aggregates in aged cells. Protein aggregates can be detected by expression of the GFP-

fused HSP104 chaperone, which normally co-localizes with protein aggregates *in vivo* (Erjavec *et al.* 2007).

It is interesting to note that aged yeast cells contain higher level of CTU. This might be a consequence of accumulated cellular damage that occurs with age, which can impair the accuracy of protein synthesis. This is consistent with the findings that aged cells have accumulated DNA damage and show less RNA-processing fidelity, both of which could decrease the accuracy of protein synthesis (Moskalev *et al.* 2013).

The potential role of CTU in aging was also tested in Chapter 4. Deletion of Ltn1, the major E3 ligase of CTU^S pathway, led to an approximate 25% decrease of yeast RLS. To further confirm the role of Ltn1 in aging, it will be important to test whether loss of Ltn1 accelerates the disruption of proteome homeostasis, a hallmark of aging. A previous study has reported that Ltn1 knockout mice exhibit an extremely short life span, with ~90% of them dying within 100 days, and moreover, the mutant mice showed profound early-onset and aged-dependent progressive neurological and motor dysfunction (Chu *et al.* 2009). These data support the idea that the CTU pathway, at least CTU^S pathway, has a potential role in retarding aging. However, the role of the CTU^A pathway in aging remains unknown. A method that can specifically block the CTU^A pathway is required for testing the role of CTU^A in aging progression.

References

- AGASHE, V.R., GUHA, S., CHANG, H.C., GENEVAUX, P., HAYER-HARTL, M., STEMPEL, M., GEORGOPOULOS, C., HARTL, F.U. & BARRAL, J.M. 2004. Function of trigger factor and DnaK in multidomain protein folding: increase in yield at the expense of folding speed. *Cell* **117**: 199-209.
- AGUILANIU, H., GUSTAFSSON, L., RIGOLET, M. & NYSTROM, T. 2003. Asymmetric inheritance of oxidatively damaged proteins during cytokinesis. *Science* **299**: 1751-3.
- AKERFELT, M., MORIMOTO, R.I. & SISTONEN, L. 2010. Heat shock factors: integrators of cell stress, development and lifespan. *Nat Rev Mol Cell Biol* **11**: 545-55.
- ALBANESE, V., YAM, A.Y., BAUGHMAN, J., PARNOT, C. & FRYDMAN, J. 2006. Systems analyses reveal two chaperone networks with distinct functions in eukaryotic cells. *Cell* **124**: 75-88.
- ANAN, T., NAGATA, Y., KOGA, H., HONDA, Y., YABUKI, N., MIYAMOTO, C., KUWANO, A., MATSUDA, I., ENDO, F., SAYA, H. & NAKAO, M. 1998. Human ubiquitin-protein ligase Nedd4: expression, subcellular localization and selective interaction with ubiquitin-conjugating enzymes. *Genes Cells* **3**: 751-63.
- ANDERSSON, V., HANZEN, S., LIU, B., MOLIN, M. & NYSTROM, T. 2013. Enhancing protein disaggregation restores proteasome activity in aged cells. *Aging (Albany NY)* **5**: 802-12.
- ANFINSEN, C.B. 1973. Principles that govern the folding of protein chains. *Science* **181**: 223-30.
- ARIAS, E. & CUERVO, A.M. 2011. Chaperone-mediated autophagy in protein quality control. *Curr Opin Cell Biol* **23**: 184-9.
- ARNDT, V., ROGON, C. & HOHFELD, J. 2007. To be, or not to be--molecular chaperones in protein degradation. *Cell Mol Life Sci* **64**: 2525-41.
- ASHE, M.P., DE LONG, S.K. & SACHS, A.B. 2000. Glucose depletion rapidly inhibits translation initiation in yeast. *Mol Biol Cell* **11**: 833-48.
- ASHERIE, N. 2004. Protein crystallization and phase diagrams. *Methods* **34**: 266-72.
- BAILLY, V., LAUDER, S., PRAKASH, S. & PRAKASH, L. 1997. Yeast DNA repair proteins Rad6 and Rad18 form a heterodimer that has ubiquitin conjugating, DNA binding, and ATP hydrolytic activities. *J Biol Chem* **272**: 23360-5.
- BALCH, W.E., MORIMOTO, R.I., DILLIN, A. & KELLY, J.W. 2008. Adapting proteostasis for disease intervention. *Science* **319**: 916-9.
- BARAIBAR, M.A. & FRIGUET, B. 2012. Changes of the proteasomal system during the aging process. *Prog Mol Biol Transl Sci* **109**: 249-75.
- BECK, F., UNVERDORFEN, P., BOHN, S., SCHWEITZER, A., PFEIFER, G., SAKATA, E., NICKELL, S., PLITZKO, J.M., VILLA, E., BAUMEISTER, W. & FORSTER, F. 2012. Near-atomic resolution structural model of the yeast 26S proteasome. *Proc Natl Acad Sci U S A* **109**: 14870-5.

- BEHREND, C. & HARPER, J.W. 2011. Constructing and decoding unconventional ubiquitin chains. *Nat Struct Mol Biol* **18**: 520-8.
- BENAROUDJ, N., ZWICKL, P., SEEMULLER, E., BAUMEISTER, W. & GOLDBERG, A.L. 2003. ATP hydrolysis by the proteasome regulatory complex PAN serves multiple functions in protein degradation. *Mol Cell* **11**: 69-78.
- BENCSATH, K.P., PODGORSKI, M.S., PAGALA, V.R., SLAUGHTER, C.A. & SCHULMAN, B.A. 2002. Identification of a multifunctional binding site on Ubc9p required for Smt3p conjugation. *J Biol Chem* **277**: 47938-45.
- BENGTSON, M.H. & JOAZEIRO, C.A. 2010. Role of a ribosome-associated E3 ubiquitin ligase in protein quality control. *Nature* **467**: 470-3.
- BENNETT, E.J. & HARPER, J.W. 2008. DNA damage: ubiquitin marks the spot. *Nat Struct Mol Biol* **15**: 20-2.
- BJEDOV, I., TOIVONEN, J.M., KERR, F., SLACK, C., JACOBSON, J., FOLEY, A. & PARTRIDGE, L. 2010. Mechanisms of life span extension by rapamycin in the fruit fly *Drosophila melanogaster*. *Cell Metab* **11**: 35-46.
- BOGUNOVIC, D., BYUN, M., DURFEE, L.A., ABHYANKAR, A., SANAL, O., MANSOURI, D., SALEM, S., RADOVANOVIC, I., GRANT, A.V., ADIMI, P., MANSOURI, N., OKADA, S., BRYANT, V.L., KONG, X.F., KREINS, A., VELEZ, M.M., BOISSON, B., KHALILZADEH, S., OZCELIK, U., DARAZAM, I.A., SCHOGGINS, J.W., RICE, C.M., AL-MUHSEN, S., BEHR, M., VOGT, G., PUEL, A., BUSTAMANTE, J., GROS, P., HUIBREGTSE, J.M., ABEL, L., BOISSON-DUPUIS, S. & CASANOVA, J.L. 2012. Mycobacterial disease and impaired IFN-gamma immunity in humans with inherited ISG15 deficiency. *Science* **337**: 1684-8.
- BRADLEY, M.O., HAYFLICK, L. & SCHIMKE, R.T. 1976. Protein degradation in human fibroblasts (WI-38). Effects of aging, viral transformation, and amino acid analogs. *J Biol Chem* **251**: 3521-9.
- BRANDMAN, O., STEWART-ORNSTEIN, J., WONG, D., LARSON, A., WILLIAMS, C.C., LI, G.W., ZHOU, S., KING, D., SHEN, P.S., WEIBEZAHN, J., DUNN, J.G., ROUSKIN, S., INADA, T., FROST, A. & WEISSMAN, J.S. 2012. A ribosome-bound quality control complex triggers degradation of nascent peptides and signals translation stress. *Cell* **151**: 1042-54.
- BRANDT, F., ETCHELLS, S.A., ORTIZ, J.O., ELCOCK, A.H., HARTL, F.U. & BAUMEISTER, W. 2009. The native 3D organization of bacterial polysomes. *Cell* **136**: 261-71.
- BRODERSEN, D.E., CLEMONS, W.M., JR., CARTER, A.P., MORGAN-WARREN, R.J., WIMBERLY, B.T. & RAMAKRISHNAN, V. 2000. The structural basis for the action of the antibiotics tetracycline, pactamycin, and hygromycin B on the 30S ribosomal subunit. *Cell* **103**: 1143-54.
- BULTEAU, A.L., LUNDBERG, K.C., HUMPHRIES, K.M., SADEK, H.A., SZWEDA, P.A., FRIGUET, B. & SZWEDA, L.I. 2001. Oxidative modification and inactivation of the proteasome during coronary occlusion/reperfusion. *J Biol Chem* **276**: 30057-63.
- CABRITA, L.D., HSU, S.T., LAUNAY, H., DOBSON, C.M. & CHRISTODOULOU, J. 2009. Probing ribosome-nascent chain complexes produced in vivo by NMR spectroscopy. *Proc Natl Acad Sci U S A* **106**: 22239-44.

- CARRARD, G., DIEU, M., RAES, M., TOUSSAINT, O. & FRIGUET, B. 2003. Impact of ageing on proteasome structure and function in human lymphocytes. *Int J Biochem Cell Biol* **35**: 728-39.
- CHAN, H.S. & DILL, K.A. 1998. Protein folding in the landscape perspective: chevron plots and non-Arrhenius kinetics. *Proteins* **30**: 2-33.
- CHASTAGNER, P., ISRAEL, A. & BROU, C. 2006. Itch/AIP4 mediates Deltex degradation through the formation of K29-linked polyubiquitin chains. *EMBO Rep* **7**: 1147-53.
- CHEN, B., RETZLAFF, M., ROOS, T. & FRYDMAN, J. 2011. Cellular strategies of protein quality control. *Cold Spring Harb Perspect Biol* **3**: a004374.
- CHIANG, W.C., CHING, T.T., LEE, H.C., MOUSIGIAN, C. & HSU, A.L. 2012. HSF-1 regulators DDL-1/2 link insulin-like signaling to heat-shock responses and modulation of longevity. *Cell* **148**: 322-34.
- CHONDROGIANNI, N., STRATFORD, F.L., TROUGAKOS, I.P., FRIGUET, B., RIVETT, A.J. & GONOS, E.S. 2003. Central role of the proteasome in senescence and survival of human fibroblasts: induction of a senescence-like phenotype upon its inhibition and resistance to stress upon its activation. *J Biol Chem* **278**: 28026-37.
- CHU, J., HONG, N.A., MASUDA, C.A., JENKINS, B.V., NELMS, K.A., GOODNOW, C.C., GLYNNE, R.J., WU, H., MASLIAH, E., JOAZEIRO, C.A. & KAY, S.A. 2009. A mouse forward genetics screen identifies LISTERIN as an E3 ubiquitin ligase involved in neurodegeneration. *Proc Natl Acad Sci U S A* **106**: 2097-103.
- CIECHANOVER, A., HELLER, H., ELIAS, S., HAAS, A.L. & HERSHKO, A. 1980. ATP-dependent conjugation of reticulocyte proteins with the polypeptide required for protein degradation. *Proc Natl Acad Sci U S A* **77**: 1365-8.
- CIECHANOVER, A., HELLER, H., KATZ-ETZION, R. & HERSHKO, A. 1981. Activation of the heat-stable polypeptide of the ATP-dependent proteolytic system. *Proc Natl Acad Sci U S A* **78**: 761-5.
- CIECHANOVER, A., HOD, Y. & HERSHKO, A. 1978. A heat-stable polypeptide component of an ATP-dependent proteolytic system from reticulocytes. *Biochem Biophys Res Commun* **81**: 1100-5.
- CLEMENTZ, M.A., CHEN, Z., BANACH, B.S., WANG, Y., SUN, L., RATIA, K., BAEZ-SANTOS, Y.M., WANG, J., TAKAYAMA, J., GHOSH, A.K., LI, K., MESECAR, A.D. & BAKER, S.C. 2010. Deubiquitinating and interferon antagonism activities of coronavirus papain-like proteases. *J Virol* **84**: 4619-29.
- CROSS, B.C., MCKIBBIN, C., CALLAN, A.C., ROBOTI, P., PIACENTI, M., RABU, C., WILSON, C.M., WHITEHEAD, R., FLITSCH, S.L., POOL, M.R., HIGH, S. & SWANTON, E. 2009. Eeyarestatin I inhibits Sec61-mediated protein translocation at the endoplasmic reticulum. *J Cell Sci* **122**: 4393-400.
- CUERVO, A.M., BERGAMINI, E., BRUNK, U.T., DROGE, W., FFRENCH, M. & TERMAN, A. 2005. Autophagy and aging: the importance of maintaining "clean" cells. *Autophagy* **1**: 131-40.
- CUERVO, A.M. 2008. Autophagy and aging: keeping that old broom working. *Trends Genet* **24**: 604-12.

- DA FONSECA, P.C., HE, J. & MORRIS, E.P. 2012. Molecular model of the human 26S proteasome. *Mol Cell* **46**: 54-66.
- DASTUR, A., BEAUDENON, S., KELLEY, M., KRUG, R.M. & HUIBREGTSE, J.M. 2006. Herc5, an interferon-induced HECT E3 enzyme, is required for conjugation of ISG15 in human cells. *J Biol Chem* **281**: 4334-8.
- DAVID, A., DOLAN, B.P., HICKMAN, H.D., KNOWLTON, J.J., CLAVARINO, G., PIERRE, P., BENNINK, J.R. & YEWDELL, J.W. 2012. Nuclear translation visualized by ribosome-bound nascent chain puromycylation. *J Cell Biol* **197**: 45-57.
- DENZEL, M.S., STORM, N.J., GUTSCHMIDT, A., BADDI, R., HINZE, Y., JAROSCH, E., SOMMER, T., HOPPE, T. & ANTEBI, A. 2014. Hexosamine pathway metabolites enhance protein quality control and prolong life. *Cell* **156**: 1167-78.
- DEPRISTO, M.A., WEINREICH, D.M. & HARTL, D.L. 2005. Missense meanderings in sequence space: a biophysical view of protein evolution. *Nat Rev Genet* **6**: 678-87.
- DESHAIES, R.J. & JOAZEIRO, C.A. 2009. RING domain E3 ubiquitin ligases. *Annu Rev Biochem* **78**: 399-434.
- DIMITROVA, L.N., KUROHA, K., TATEMATSU, T. & INADA, T. 2009. Nascent peptide-dependent translation arrest leads to Not4p-mediated protein degradation by the proteasome. *J Biol Chem* **284**: 10343-52.
- DOUGLAS, P.M. & DILLIN, A. 2010. Protein homeostasis and aging in neurodegeneration. *J Cell Biol* **190**: 719-29.
- DRUMMOND, D.A. & WILKE, C.O. 2009. The evolutionary consequences of erroneous protein synthesis. *Nat Rev Genet* **10**: 715-24.
- DUNKER, A.K., SILMAN, I., UVERSKY, V.N. & SUSSMAN, J.L. 2008. Function and structure of inherently disordered proteins. *Curr Opin Struct Biol* **18**: 756-64.
- DURFEE, L.A., LYON, N., SEO, K. & HUIBREGTSE, J.M. The ISG15 conjugation system broadly targets newly synthesized proteins: implications for the antiviral function of ISG15. *Mol Cell* **38**: 722-32.
- DURFEE, L.A., KELLEY, M.L. & HUIBREGTSE, J.M. 2008. The basis for selective E1-E2 interactions in the ISG15 conjugation system. *J Biol Chem* **283**: 23895-902.
- DURFEE, L.A. 2010. The Enzymology and Substrate Selectivity of the ISG15 Conjugation System. *PhD Dissertation*.
- DURFEE, L.A., LYON, N., SEO, K. & HUIBREGTSE, J.M. 2010. The ISG15 conjugation system broadly targets newly synthesized proteins: implications for the antiviral function of ISG15. *Mol Cell* **38**: 722-32.
- DUTTLER, S., PECHMANN, S. & FRYDMAN, J. 2013. Principles of cotranslational ubiquitination and quality control at the ribosome. *Mol Cell* **50**: 379-93.
- EHRENFRIED, J.A., EVERS, B.M., CHU, K.U., TOWNSEND, C.M., JR. & THOMPSON, J.C. 1996. Caloric restriction increases the expression of heat shock protein in the gut. *Ann Surg* **223**: 592-7; discussion 597-9.
- EICHMANN, C., PREISSLER, S., RIEK, R. & DEUERLING, E. 2010. Cotranslational structure acquisition of nascent polypeptides monitored by NMR spectroscopy. *Proc Natl Acad Sci U S A* **107**: 9111-6.

- EISENBERG, T., KNAUER, H., SCHAUER, A., BUTTNER, S., RUCKENSTUHL, C., CARMONA-GUTIERREZ, D., RING, J., SCHROEDER, S., MAGNES, C., ANTONACCI, L., FUSSI, H., DESZCZ, L., HARTL, R., SCHRAML, E., CRIOLLO, A., MEGALOU, E., WEISKOPF, D., LAUN, P., HEEREN, G., BREITENBACH, M., GRUBECK-LOEBENSTEIN, B., HERKER, E., FAHRENKROG, B., FROHLICH, K.U., SINNER, F., TAVERNARAKIS, N., MINOIS, N., KROEMER, G. & MADEO, F. 2009. Induction of autophagy by spermidine promotes longevity. *Nat Cell Biol* **11**: 1305-14.
- ELETR, Z.M., HUANG, D.T., DUDA, D.M., SCHULMAN, B.A. & KUHLMAN, B. 2005. E2 conjugating enzymes must disengage from their E1 enzymes before E3-dependent ubiquitin and ubiquitin-like transfer. *Nat Struct Mol Biol* **12**: 933-4.
- ELETR, Z.M. & KUHLMAN, B. 2007. Sequence determinants of E2-E6AP binding affinity and specificity. *J Mol Biol* **369**: 419-28.
- ELLIS, R.J. 2001. Macromolecular crowding: obvious but underappreciated. *Trends Biochem Sci* **26**: 597-604.
- ELLIS, R.J. & MINTON, A.P. 2006. Protein aggregation in crowded environments. *Biol Chem* **387**: 485-97.
- ERJAVEC, N., LARSSON, L., GRANTHAM, J. & NYSTROM, T. 2007. Accelerated aging and failure to segregate damaged proteins in Sir2 mutants can be suppressed by overproducing the protein aggregation-remodeling factor Hsp104p. *Genes Dev* **21**: 2410-21.
- ESCUSA-TORET, S., VONK, W.I. & FRYDMAN, J. 2013. Spatial sequestration of misfolded proteins by a dynamic chaperone pathway enhances cellular fitness during stress. *Nat Cell Biol* **15**: 1231-43.
- ETLINGER, J.D. & GOLDBERG, A.L. 1977. A soluble ATP-dependent proteolytic system responsible for the degradation of abnormal proteins in reticulocytes. *Proc Natl Acad Sci U S A* **74**: 54-8.
- FANG, N.N., NG, A.H., MEASDAY, V. & MAYOR, T. 2011. Hul5 HECT ubiquitin ligase plays a major role in the ubiquitylation and turnover of cytosolic misfolded proteins. *Nat Cell Biol* **13**: 1344-52.
- FARGNOLI, J., KUNISADA, T., FORNACE, A.J., JR., SCHNEIDER, E.L. & HOLBROOK, N.J. 1990. Decreased expression of heat shock protein 70 mRNA and protein after heat treatment in cells of aged rats. *Proc Natl Acad Sci U S A* **87**: 846-50.
- FARRELL, P.J., BROEZE, R.J. & LENGYEL, P. 1979. Accumulation of an mRNA and protein in interferon-treated Ehrlich ascites tumour cells. *Nature* **279**: 523-5.
- FERRINGTON, D.A., HUSOM, A.D. & THOMPSON, L.V. 2005. Altered proteasome structure, function, and oxidation in aged muscle. *FASEB J* **19**: 644-6.
- FINLEY, D., BARTEL, B. & VARSHAVSKY, A. 1989. The tails of ubiquitin precursors are ribosomal proteins whose fusion to ubiquitin facilitates ribosome biogenesis. *Nature* **338**: 394-401.
- FINLEY, D., ULRICH, H.D., SOMMER, T. & KAISER, P. 2012. The ubiquitin-proteasome system of *Saccharomyces cerevisiae*. *Genetics* **192**: 319-60.
- FRIAS-STAHIELI, N., GIANNAKOPOULOS, N.V., KIKKERT, M., TAYLOR, S.L., BRIDGEN, A., PARAGAS, J., RICHT, J.A., ROWLAND, R.R., SCHMALJOHN, C.S., LENSCHOW, D.J.,

- SNIJDER, E.J., GARCIA-SASTRE, A. & VIRGIN, H.W.T. 2007. Ovarian tumor domain-containing viral proteases evade ubiquitin- and ISG15-dependent innate immune responses. *Cell Host Microbe* **2**: 404-16.
- FRIGUET, B., BULTEAU, A.L., CHONDROGIANNI, N., CONCONI, M. & PETROPOULOS, I. 2000. Protein degradation by the proteasome and its implications in aging. *Ann N Y Acad Sci* **908**: 143-54.
- FRYDMAN, J., ERDJUMENT-BROMAGE, H., TEMPST, P. & HARTL, F.U. 1999. Co-translational domain folding as the structural basis for the rapid de novo folding of firefly luciferase. *Nat Struct Biol* **6**: 697-705.
- FUJIWARA, K., ISHIHAMA, Y., NAKAHIGASHI, K., SOGA, T. & TAGUCHI, H. 2010. A systematic survey of in vivo obligate chaperonin-dependent substrates. *EMBO J* **29**: 1552-64.
- GIANNAKOPOULOS, N.V., LUO, J.K., PAPOV, V., ZOU, W., LENSCHOW, D.J., JACOBS, B.S., BORDEN, E.C., LI, J., VIRGIN, H.W. & ZHANG, D.E. 2005. Proteomic identification of proteins conjugated to ISG15 in mouse and human cells. *Biochem Biophys Res Commun* **336**: 496-506.
- GIANNAKOPOULOS, N.V., ARUTYUNOVA, E., LAI, C., LENSCHOW, D.J., HAAS, A.L. & VIRGIN, H.W. 2009. ISG15 Arg151 and the ISG15-conjugating enzyme Ube1L are important for innate immune control of Sindbis virus. *J Virol* **83**: 1602-10.
- GOLDBERG, A.L. & ST JOHN, A.C. 1976. Intracellular protein degradation in mammalian and bacterial cells: Part 2. *Annu Rev Biochem* **45**: 747-803.
- GOLDKNOPF, I.L. & BUSCH, H. 1977. Isopeptide linkage between nonhistone and histone 2A polypeptides of chromosomal conjugate-protein A24. *Proc Natl Acad Sci U S A* **74**: 864-8.
- GOLDSTEIN, G., SCHEID, M., HAMMERLING, U., SCHLESINGER, D.H., NIALL, H.D. & BOYSE, E.A. 1975. Isolation of a polypeptide that has lymphocyte-differentiating properties and is probably represented universally in living cells. *Proc Natl Acad Sci U S A* **72**: 11-5.
- GOLL, D.E., NETI, G., MARES, S.W. & THOMPSON, V.F. 2008. Myofibrillar protein turnover: the proteasome and the calpains. *J Anim Sci* **86**: E19-35.
- GROLL, M., DITZEL, L., LOWE, J., STOCK, D., BOCHTLER, M., BARTUNIK, H.D. & HUBER, R. 1997. Structure of 20S proteasome from yeast at 2.4 Å resolution. *Nature* **386**: 463-71.
- GUERRA, S., CACERES, A., KNOBELOCH, K.P., HORAK, I. & ESTEBAN, M. 2008. Vaccinia virus E3 protein prevents the antiviral action of ISG15. *PLoS Pathog* **4**: e1000096.
- HAAS, A.L., WARMS, J.V., HERSHKO, A. & ROSE, I.A. 1982. Ubiquitin-activating enzyme. Mechanism and role in protein-ubiquitin conjugation. *J Biol Chem* **257**: 2543-8.
- HAAS, A.L. & WILKINSON, K.D. 2008. DeTEKting ubiquitination of APC/C substrates. *Cell* **133**: 570-2.
- HALLER, O., STAEHEL, P. & KOCHS, G. 2007. Interferon-induced Mx proteins in antiviral host defense. *Biochimie* **89**: 812-8.

- HANSEN, M., TAUBERT, S., CRAWFORD, D., LIBINA, N., LEE, S.J. & KENYON, C. 2007. Lifespan extension by conditions that inhibit translation in *Caenorhabditis elegans*. *Aging Cell* **6**: 95-110.
- HANSON, P.I. & WHITEHEART, S.W. 2005. AAA+ proteins: have engine, will work. *Nat Rev Mol Cell Biol* **6**: 519-29.
- HARMAN, D. 1956. Aging: a theory based on free radical and radiation chemistry. *J Gerontol* **11**: 298-300.
- HARRISON, D.E., STRONG, R., SHARP, Z.D., NELSON, J.F., ASTLE, C.M., FLURKEY, K., NADON, N.L., WILKINSON, J.E., FRENKEL, K., CARTER, C.S., PAHOR, M., JAVORS, M.A., FERNANDEZ, E. & MILLER, R.A. 2009. Rapamycin fed late in life extends lifespan in genetically heterogeneous mice. *Nature* **460**: 392-5.
- HARTL, F.U., BRACHER, A. & HAYER-HARTL, M. Molecular chaperones in protein folding and proteostasis. *Nature* **475**: 324-32.
- HARTL, F.U. & HAYER-HARTL, M. 2009. Converging concepts of protein folding in vitro and in vivo. *Nat Struct Mol Biol* **16**: 574-81.
- HARTL, F.U., BRACHER, A. & HAYER-HARTL, M. 2011. Molecular chaperones in protein folding and proteostasis. *Nature* **475**: 324-32.
- HAYDEN, M.S. & GHOSH, S. 2008. Shared principles in NF-kappaB signaling. *Cell* **132**: 344-62.
- HERRMANN, J., LERMAN, L.O. & LERMAN, A. 2010. On to the road to degradation: atherosclerosis and the proteasome. *Cardiovasc Res* **85**: 291-302.
- HERSHKO, A., CIECHANOVER, A., HELLER, H., HAAS, A.L. & ROSE, I.A. 1980. Proposed role of ATP in protein breakdown: conjugation of protein with multiple chains of the polypeptide of ATP-dependent proteolysis. *Proc Natl Acad Sci U S A* **77**: 1783-6.
- HERSHKO, A., CIECHANOVER, A. & ROSE, I.A. 1981. Identification of the active amino acid residue of the polypeptide of ATP-dependent protein breakdown. *J Biol Chem* **256**: 1525-8.
- HERSHKO, A., HELLER, H., ELIAS, S. & CIECHANOVER, A. 1983. Components of ubiquitin-protein ligase system. Resolution, affinity purification, and role in protein breakdown. *J Biol Chem* **258**: 8206-14.
- HERSHKO, A., LESHINSKY, E., GANOTH, D. & HELLER, H. 1984. ATP-dependent degradation of ubiquitin-protein conjugates. *Proc Natl Acad Sci U S A* **81**: 1619-23.
- HEYDARI, A.R., YOU, S., TAKAHASHI, R., GUTSMANN-CONRAD, A., SARGE, K.D. & RICHARDSON, A. 2000. Age-related alterations in the activation of heat shock transcription factor 1 in rat hepatocytes. *Exp Cell Res* **256**: 83-93.
- HIPP, M.S., KALVERAM, B., RAASI, S., GROETTRUP, M. & SCHMIDTKE, G. 2005. FAT10, a ubiquitin-independent signal for proteasomal degradation. *Mol Cell Biol* **25**: 3483-91.
- HIRSCH, C., GAUSS, R., HORN, S.C., NEUBER, O. & SOMMER, T. 2009. The ubiquitylation machinery of the endoplasmic reticulum. *Nature* **458**: 453-60.

- HOLCIK, M. & SONENBERG, N. 2005. Translational control in stress and apoptosis. *Nat Rev Mol Cell Biol* **6**: 318-27.
- HORWICH, A.L. & FENTON, W.A. 2009. Chaperonin-mediated protein folding: using a central cavity to kinetically assist polypeptide chain folding. *Q Rev Biophys* **42**: 83-116.
- HOTOKEZAKA, Y., VAN LEYEN, K., LO, E.H., BEATRIX, B., KATAYAMA, I., JIN, G. & NAKAMURA, T. 2009. alphaNAC depletion as an initiator of ER stress-induced apoptosis in hypoxia. *Cell Death Differ* **16**: 1505-14.
- HOUGH, R., PRATT, G. & RECHSTEINER, M. 1987. Purification of two high molecular weight proteases from rabbit reticulocyte lysate. *J Biol Chem* **262**: 8303-13.
- HSIANG, T.Y., ZHAO, C. & KRUG, R.M. 2009. Interferon-induced ISG15 conjugation inhibits influenza A virus gene expression and replication in human cells. *J Virol* **83**: 5971-7.
- HUANG, D.T., PAYDAR, A., ZHUANG, M., WADDELL, M.B., HOLTON, J.M. & SCHULMAN, B.A. 2005. Structural basis for recruitment of Ubc12 by an E2 binding domain in NEDD8's E1. *Mol Cell* **17**: 341-50.
- HUANG, L., KINNUCAN, E., WANG, G., BEAUDENON, S., HOWLEY, P.M., HUIBREGTSE, J.M. & PAVLETICH, N.P. 1999. Structure of an E6AP-UbcH7 complex: insights into ubiquitination by the E2-E3 enzyme cascade. *Science* **286**: 1321-6.
- HUIBREGTSE, J.M., SCHEFFNER, M. & HOWLEY, P.M. 1991. A cellular protein mediates association of p53 with the E6 oncoprotein of human papillomavirus types 16 or 18. *EMBO J* **10**: 4129-35.
- HUIBREGTSE, J.M., SCHEFFNER, M., BEAUDENON, S. & HOWLEY, P.M. 1995. A family of proteins structurally and functionally related to the E6-AP ubiquitin-protein ligase. *Proc Natl Acad Sci U S A* **92**: 5249.
- IVANKOV, D.N., GARBUZYNSKIY, S.O., ALM, E., PLAXCO, K.W., BAKER, D. & FINKELSTEIN, A.V. 2003. Contact order revisited: influence of protein size on the folding rate. *Protein Sci* **12**: 2057-62.
- IWAI, K. & TOKUNAGA, F. 2009. Linear polyubiquitination: a new regulator of NF-kappaB activation. *EMBO Rep* **10**: 706-13.
- JAGANNATHAN, S., NWOSU, C. & NICCHITTA, C.V. 2011. Analyzing mRNA localization to the endoplasmic reticulum via cell fractionation. *Methods Mol Biol* **714**: 301-21.
- JAHNGEN, J.H., LIPMAN, R.D., EISENHAUER, D.A., JAHNGEN, E.G., JR. & TAYLOR, A. 1990. Aging and cellular maturation cause changes in ubiquitin-eye lens protein conjugates. *Arch Biochem Biophys* **276**: 32-7.
- JAISWAL, H., CONZ, C., OTTO, H., WOLFLE, T., FITZKE, E., MAYER, M.P. & ROSPERT, S. 2011. The chaperone network connected to human ribosome-associated complex. *Mol Cell Biol* **31**: 1160-73.
- JENTSCH, S. & RUMPF, S. 2007. Cdc48 (p97): a "molecular gearbox" in the ubiquitin pathway? *Trends Biochem Sci* **32**: 6-11.
- JIN, J., LI, X., GYGI, S.P. & HARPER, J.W. 2007. Dual E1 activation systems for ubiquitin differentially regulate E2 enzyme charging. *Nature* **447**: 1135-8.

- JIN, L., WILLIAMSON, A., BANERJEE, S., PHILIPP, I. & RAPE, M. 2008. Mechanism of ubiquitin-chain formation by the human anaphase-promoting complex. *Cell* **133**: 653-65.
- JOAZEIRO, C.A., WING, S.S., HUANG, H., LEVERSON, J.D., HUNTER, T. & LIU, Y.C. 1999. The tyrosine kinase negative regulator c-Cbl as a RING-type, E2-dependent ubiquitin-protein ligase. *Science* **286**: 309-12.
- JOHNSON, S.C., RABINOVITCH, P.S. & KAEBERLEIN, M. 2013. mTOR is a key modulator of ageing and age-related disease. *Nature* **493**: 338-45.
- KAEBERLEIN, M. & KENNEDY, B.K. 2007. Protein translation, 2007. *Aging Cell* **6**: 731-4.
- KAGANOVICH, D., KOPITO, R. & FRYDMAN, J. 2008. Misfolded proteins partition between two distinct quality control compartments. *Nature* **454**: 1088-95.
- KAMADA, Y., FUNAKOSHI, T., SHINTANI, T., NAGANO, K., OHSUMI, M. & OHSUMI, Y. 2000. Tor-mediated induction of autophagy via an Apg1 protein kinase complex. *J Cell Biol* **150**: 1507-13.
- KAMPINGA, H.H. & CRAIG, E.A. 2010. The HSP70 chaperone machinery: J proteins as drivers of functional specificity. *Nat Rev Mol Cell Biol* **11**: 579-92.
- KAUL, S.C., YAGUCHI, T., TAIRA, K., REDDEL, R.R. & WADHWA, R. 2003. Overexpressed mortalin (mot-2)/mthsp70/GRP75 and hTERT cooperate to extend the in vitro lifespan of human fibroblasts. *Exp Cell Res* **286**: 96-101.
- KELKAR, D.A., KHUSHOO, A., YANG, Z. & SKACH, W.R. 2012. Kinetic analysis of ribosome-bound fluorescent proteins reveals an early, stable, cotranslational folding intermediate. *J Biol Chem* **287**: 2568-78.
- KELLER, J.N., HUANG, F.F. & MARKESBERY, W.R. 2000. Decreased levels of proteasome activity and proteasome expression in aging spinal cord. *Neuroscience* **98**: 149-56.
- KELLEY, M.L., KEIGER, K.E., LEE, C.J. & HUIBREGTSE, J.M. 2005. The global transcriptional effects of the human papillomavirus E6 protein in cervical carcinoma cell lines are mediated by the E6AP ubiquitin ligase. *J Virol* **79**: 3737-47.
- KERNER, M.J., NAYLOR, D.J., ISHIHAMA, Y., MAIER, T., CHANG, H.C., STINES, A.P., GEORGOPOULOS, C., FRISHMAN, D., HAYER-HARTL, M., MANN, M. & HARTL, F.U. 2005. Proteome-wide analysis of chaperonin-dependent protein folding in *Escherichia coli*. *Cell* **122**: 209-20.
- KETSCHER, L., BASTERS, A., PRINZ, M. & KNOBELOCH, K.P. 2012. mHERC6 is the essential ISG15 E3 ligase in the murine system. *Biochem Biophys Res Commun* **417**: 135-40.
- KIM, H.C. & HUIBREGTSE, J.M. 2009. Polyubiquitination by HECT E3s and the determinants of chain type specificity. *Mol Cell Biol* **29**: 3307-18.
- KIM, H.C., STEFFEN, A.M., OLDHAM, M.L., CHEN, J. & HUIBREGTSE, J.M. 2011a. Structure and function of a HECT domain ubiquitin-binding site. *EMBO Rep* **12**: 334-41.
- KIM, W., BENNETT, E.J., HUTTLIN, E.L., GUO, A., LI, J., POSSEMATO, A., SOWA, M.E., RAD, R., RUSH, J., COMB, M.J., HARPER, J.W. & GYGI, S.P. 2011b. Systematic

- and quantitative assessment of the ubiquitin-modified proteome. *Mol Cell* **44**: 325-40.
- KIM, Y.E., HIPPEL, M.S., BRACHER, A., HAYER-HARTL, M. & HARTL, F.U. 2013. Molecular chaperone functions in protein folding and proteostasis. *Annu Rev Biochem* **82**: 323-55.
- KIMURA, Y. & TANAKA, K. 2010. Regulatory mechanisms involved in the control of ubiquitin homeostasis. *J Biochem* **147**: 793-8.
- KIRAGA, J., MACKIEWICZ, P., MACKIEWICZ, D., KOWALCZUK, M., BIECEK, P., POLAK, N., SMOLARCZYK, K., DUDEK, M.R. & CEBRAT, S. 2007. The relationships between the isoelectric point and: length of proteins, taxonomy and ecology of organisms. *BMC Genomics* **8**: 163.
- KISSELEV, A.F., AKOPIAN, T.N., WOO, K.M. & GOLDBERG, A.L. 1999. The sizes of peptides generated from protein by mammalian 26 and 20 S proteasomes. Implications for understanding the degradative mechanism and antigen presentation. *J Biol Chem* **274**: 3363-71.
- KLASS, M.R. 1983. A method for the isolation of longevity mutants in the nematode *Caenorhabditis elegans* and initial results. *Mech Ageing Dev* **22**: 279-86.
- KLIONSKY, D.J., BAEHRECKE, E.H., BRUMELL, J.H., CHU, C.T., CODOGNO, P., CUERVO, A.M., DEBNATH, J., DERETIC, V., ELAZAR, Z., ESKELINEN, E.L., FINKBEINER, S., FUEYO-MARGARETO, J., GEWIRTZ, D., JAATTELA, M., KROEMER, G., LEVINE, B., MELIA, T.J., MIZUSHIMA, N., RUBINSZTEIN, D.C., SIMONSEN, A., THORBURN, A., THUMM, M. & TOOZE, S.A. 2011. A comprehensive glossary of autophagy-related molecules and processes (2nd edition). *Autophagy* **7**: 1273-94.
- KNOBELOCH, K.P., UTERMÖHLEN, O., KISSER, A., PRINZ, M. & HORAK, I. 2005. Reexamination of the role of ubiquitin-like modifier ISG15 in the phenotype of UBP43-deficient mice. *Mol Cell Biol* **25**: 11030-4.
- KNOWLES, S.E. & BALLARD, F.J. 1976. Selective control of the degradation of normal and aberrant proteins in Reuber H35 hepatoma cells. *Biochem J* **156**: 609-17.
- KOGA, H., KAUSHIK, S. & CUERVO, A.M. 2011. Protein homeostasis and aging: The importance of exquisite quality control. *Ageing Res Rev* **10**: 205-15.
- KOMANDER, D., CLAGUE, M.J. & URBE, S. 2009. Breaking the chains: structure and function of the deubiquitinases. *Nat Rev Mol Cell Biol* **10**: 550-63.
- KOMATSU, M., WAGURI, S., UENO, T., IWATA, J., MURATA, S., TANIDA, I., EZAKI, J., MIZUSHIMA, N., OHSUMI, Y., UCHIYAMA, Y., KOMINAMI, E., TANAKA, K. & CHIBA, T. 2005. Impairment of starvation-induced and constitutive autophagy in Atg7-deficient mice. *J Cell Biol* **169**: 425-34.
- KRUEGEL, U., ROBISON, B., DANGE, T., KAHLERT, G., DELANEY, J.R., KOTIREDDY, S., TSUCHIYA, M., TSUCHIYAMA, S., MURAKAMI, C.J., SCHLEIT, J., SUTPHIN, G., CARR, D., TAR, K., DITTMAR, G., KAEBERLEIN, M., KENNEDY, B.K. & SCHMIDT, M. 2011. Elevated proteasome capacity extends replicative lifespan in *Saccharomyces cerevisiae*. *PLoS Genet* **7**: e1002253.
- KUSUMAWIDJAJA, G., KAYED, H., GIESE, N., BAUER, A., ERKAN, M., GIESE, T., HOHEISE, J.D., FRIESS, H. & KLEEFF, J. 2007. Basic transcription factor 3 (BTF3) regulates

- transcription of tumor-associated genes in pancreatic cancer cells. *Cancer Biol Ther* **6**: 367-76.
- LAI, C., STRUCKHOFF, J.J., SCHNEIDER, J., MARTINEZ-SOBRIDO, L., WOLFF, T., GARCIA-SASTRE, A., ZHANG, D.E. & LENSCHOW, D.J. 2009. Mice lacking the ISG15 E1 enzyme Ube1L demonstrate increased susceptibility to both mouse-adapted and non-mouse-adapted influenza B virus infection. *J Virol* **83**: 1147-51.
- LAKE, M.W., WUEBBENS, M.M., RAJAGOPALAN, K.V. & SCHINDELIN, H. 2001. Mechanism of ubiquitin activation revealed by the structure of a bacterial MoeB-MoaD complex. *Nature* **414**: 325-9.
- LANDER, G.C., ESTRIN, E., MATYSKIELA, M.E., BASHORE, C., NOGALES, E. & MARTIN, A. 2012. Complete subunit architecture of the proteasome regulatory particle. *Nature* **482**: 186-91.
- LEE, J., GIORDANO, S. & ZHANG, J. 2012. Autophagy, mitochondria and oxidative stress: cross-talk and redox signalling. *Biochem J* **441**: 523-40.
- LEE, J.W., BEEBE, K., NANGLE, L.A., JANG, J., LONGO-GUESS, C.M., COOK, S.A., DAVISSON, M.T., SUNDBERG, J.P., SCHIMMEL, P. & ACKERMAN, S.L. 2006. Editing-defective tRNA synthetase causes protein misfolding and neurodegeneration. *Nature* **443**: 50-5.
- LEIDEL, S., PEDRIOLI, P.G., BUCHER, T., BROST, R., COSTANZO, M., SCHMIDT, A., AEBERSOLD, R., BOONE, C., HOFMANN, K. & PETER, M. 2009. Ubiquitin-related modifier Urm1 acts as a sulphur carrier in thiolation of eukaryotic transfer RNA. *Nature* **458**: 228-32.
- LEIMKUHNER, S., WUEBBENS, M.M. & RAJAGOPALAN, K.V. 2001. Characterization of Escherichia coli MoeB and its involvement in the activation of molybdopterin synthase for the biosynthesis of the molybdenum cofactor. *J Biol Chem* **276**: 34695-701.
- LENSCHOW, D.J., GIANNAKOPOULOS, N.V., GUNN, L.J., JOHNSTON, C., O'GUIN, A.K., SCHMIDT, R.E., LEVINE, B. & VIRGIN, H.W.T. 2005. Identification of interferon-stimulated gene 15 as an antiviral molecule during Sindbis virus infection in vivo. *J Virol* **79**: 13974-83.
- LEU, J.I., PIMKINA, J., FRANK, A., MURPHY, M.E. & GEORGE, D.L. 2009. A small molecule inhibitor of inducible heat shock protein 70. *Mol Cell* **36**: 15-27.
- LEVINE, C.G., MITRA, D., SHARMA, A., SMITH, C.L. & HEGDE, R.S. 2005. The efficiency of protein compartmentalization into the secretory pathway. *Mol Biol Cell* **16**: 279-91.
- LINDNER, H.A., LYTUVYN, V., QI, H., LACHANCE, P., ZIOMEK, E. & MENARD, R. 2007. Selectivity in ISG15 and ubiquitin recognition by the SARS coronavirus papain-like protease. *Arch Biochem Biophys* **466**: 8-14.
- LINDSTROM, D.L. & GOTTSCHLING, D.E. 2009. The mother enrichment program: a genetic system for facile replicative life span analysis in Saccharomyces cerevisiae. *Genetics* **183**: 413-22, 1SI-13SI.
- LIU, B., HAN, Y. & QIAN, S.B. 2013. Cotranslational response to proteotoxic stress by elongation pausing of ribosomes. *Mol Cell* **49**: 453-63.

- LIU, G., ROGERS, J., MURPHY, C.T. & RONGO, C. 2011. EGF signalling activates the ubiquitin proteasome system to modulate *C. elegans* lifespan. *EMBO J* **30**: 2990-3003.
- LOPEZ-OTIN, C., BLASCO, M.A., PARTRIDGE, L., SERRANO, M. & KROEMER, G. 2013. The hallmarks of aging. *Cell* **153**: 1194-217.
- LOWE, J., STOCK, D., JAP, B., ZWICKL, P., BAUMEISTER, W. & HUBER, R. 1995. Crystal structure of the 20S proteasome from the archaeon *T. acidophilum* at 3.4 Å resolution. *Science* **268**: 533-9.
- LU, G., REINERT, J.T., PITHA-ROWE, I., OKUMURA, A., KELLUM, M., KNOBELOCH, K.P., HASSEL, B. & PITHA, P.M. 2006. ISG15 enhances the innate antiviral response by inhibition of IRF-3 degradation. *Cell Mol Biol (Noisy-le-grand)* **52**: 29-41.
- MAKDE, R.D., ENGLAND, J.R., YENNAWAR, H.P. & TAN, S. 2010. Structure of RCC1 chromatin factor bound to the nucleosome core particle. *Nature* **467**: 562-6.
- MALAKHOV, M.P., MALAKHOVA, O.A., KIM, K.I., RITCHIE, K.J. & ZHANG, D.E. 2002. UBP43 (USP18) specifically removes ISG15 from conjugated proteins. *J Biol Chem* **277**: 9976-81.
- MALAKHOV, M.P., KIM, K.I., MALAKHOVA, O.A., JACOBS, B.S., BORDEN, E.C. & ZHANG, D.E. 2003. High-throughput immunoblotting. Ubiquitin-like protein ISG15 modifies key regulators of signal transduction. *J Biol Chem* **278**: 16608-13.
- MALAKHOVA, O.A., KIM, K.I., LUO, J.K., ZOU, W., KUMAR, K.G., FUCHS, S.Y., SHUAI, K. & ZHANG, D.E. 2006. UBP43 is a novel regulator of interferon signaling independent of its ISG15 isopeptidase activity. *EMBO J* **25**: 2358-67.
- MCCLELLAN, A.J., TAM, S., KAGANOVICH, D. & FRYDMAN, J. 2005. Protein quality control: chaperones culling corrupt conformations. *Nat Cell Biol* **7**: 736-41.
- MCKIBBIN, C., MARES, A., PIACENTI, M., WILLIAMS, H., ROBOTI, P., PUUMALAINEN, M., CALLAN, A.C., LESIAK-MIECZKOWSKA, K., LINDER, S., HARANT, H., HIGH, S., FLITSCH, S.L., WHITEHEAD, R.C. & SWANTON, E. 2012. Inhibition of protein translocation at the endoplasmic reticulum promotes activation of the unfolded protein response. *Biochem J* **442**: 639-48.
- MEDVEDIK, O., LAMMING, D.W., KIM, K.D. & SINCLAIR, D.A. 2007. MSN2 and MSN4 link calorie restriction and TOR to sirtuin-mediated lifespan extension in *Saccharomyces cerevisiae*. *PLoS Biol* **5**: e261.
- MIN, J.N., WHALEY, R.A., SHARPLESS, N.E., LOCKYER, P., PORTBURY, A.L. & PATTERSON, C. 2008. CHIP deficiency decreases longevity, with accelerated aging phenotypes accompanied by altered protein quality control. *Mol Cell Biol* **28**: 4018-25.
- MOGENSEN, T.H. 2009. Pathogen recognition and inflammatory signaling in innate immune defenses. *Clin Microbiol Rev* **22**: 240-73, Table of Contents.
- MOORE, S.A., LOPEZ, A., RICHARDSON, A. & PAHLAVANI, M.A. 1998. Effect of age and dietary restriction on expression of heat shock protein 70 in rat alveolar macrophages. *Mech Ageing Dev* **104**: 59-73.
- MORETT, E. & BORK, P. 1999. A novel transactivation domain in parkin. *Trends Biochem Sci* **24**: 229-31.

- MORIMOTO, R.I. 2008. Proteotoxic stress and inducible chaperone networks in neurodegenerative disease and aging. *Genes Dev* **22**: 1427-38.
- MOSKALEV, A.A., SHAPOSHNIKOV, M.V., PLYUSNINA, E.N., ZHAVORONKOV, A., BUDOVSKY, A., YANAI, H. & FRAIFELD, V.E. 2013. The role of DNA damage and repair in aging through the prism of Koch-like criteria. *Ageing Res Rev* **12**: 661-84.
- MUNOZ, M.J. 2003. Longevity and heat stress regulation in *Caenorhabditis elegans*. *Mech Ageing Dev* **124**: 43-8.
- MURROW, L. & DEBNATH, J. 2013. Autophagy as a stress-response and quality-control mechanism: implications for cell injury and human disease. *Annu Rev Pathol* **8**: 105-37.
- NAKASATO, N., IKEDA, K., URANO, T., HORIE-INOUE, K., TAKEDA, S. & INOUE, S. 2006. A ubiquitin E3 ligase Efp is up-regulated by interferons and conjugated with ISG15. *Biochem Biophys Res Commun* **351**: 540-6.
- NARASIMHAN, J., WANG, M., FU, Z., KLEIN, J.M., HAAS, A.L. & KIM, J.J. 2005. Crystal structure of the interferon-induced ubiquitin-like protein ISG15. *J Biol Chem* **280**: 27356-65.
- NEFF, N.T., DEMARTINO, G.N. & GOLDBERG, A.L. 1979. The effect of protease inhibitors and decreased temperature on the degradation of different classes of proteins in cultured hepatocytes. *J Cell Physiol* **101**: 439-57.
- NETZER, W.J. & HARTL, F.U. 1997. Recombination of protein domains facilitated by co-translational folding in eukaryotes. *Nature* **388**: 343-9.
- NOMA, A., SAKAGUCHI, Y. & SUZUKI, T. 2009. Mechanistic characterization of the sulfur-relay system for eukaryotic 2-thiouridine biogenesis at tRNA wobble positions. *Nucleic Acids Res* **37**: 1335-52.
- NUSS, J.E., CHOKSI, K.B., DEFORD, J.H. & PAPACONSTANTINOU, J. 2008. Decreased enzyme activities of chaperones PDI and BiP in aged mouse livers. *Biochem Biophys Res Commun* **365**: 355-61.
- NUSSBAUM, A.K., DICK, T.P., KEILHOLZ, W., SCHIRLE, M., STEVANOVIC, S., DIETZ, K., HEINEMEYER, W., GROLL, M., WOLF, D.H., HUBER, R., RAMMENSEE, H.G. & SCHILD, H. 1998. Cleavage motifs of the yeast 20S proteasome beta subunits deduced from digests of enolase 1. *Proc Natl Acad Sci U S A* **95**: 12504-9.
- O'ROURKE, E.J., KUBALLA, P., XAVIER, R. & RUVKUN, G. 2013. omega-6 Polyunsaturated fatty acids extend life span through the activation of autophagy. *Genes Dev* **27**: 429-40.
- OGLE, J.M. & RAMAKRISHNAN, V. 2005. Structural insights into translational fidelity. *Annu Rev Biochem* **74**: 129-77.
- OKUMURA, A., LU, G., PITHA-ROWE, I. & PITHA, P.M. 2006. Innate antiviral response targets HIV-1 release by the induction of ubiquitin-like protein ISG15. *Proc Natl Acad Sci U S A* **103**: 1440-5.
- OKUMURA, A., PITHA, P.M. & HARTY, R.N. 2008. ISG15 inhibits Ebola VP40 VLP budding in an L-domain-dependent manner by blocking Nedd4 ligase activity. *Proc Natl Acad Sci U S A* **105**: 3974-9.

- OLZSCHA, H., SCHERMANN, S.M., WOERNER, A.C., PINKERT, S., HECHT, M.H., TARTAGLIA, G.G., VENDRUSCOLO, M., HAYER-HARTL, M., HARTL, F.U. & VABULAS, R.M. 2011. Amyloid-like aggregates sequester numerous metastable proteins with essential cellular functions. *Cell* **144**: 67-78.
- ORLOWSKI, M. & ROSS, J.F. 1981. Relationship of internal cyclic AMP levels, rates of protein synthesis and mucor dimorphism. *Arch Microbiol* **129**: 353-6.
- OUDSHOORN, D., VAN BOHEEMEN, S., SANCHEZ-APARICIO, M.T., RAJSBAUM, R., GARCIA-SASTRE, A. & VERSTEEG, G.A. 2012. HERC6 is the main E3 ligase for global ISG15 conjugation in mouse cells. *PLoS One* **7**: e29870.
- OUELLET, J. & BARRAL, Y. 2012. Organelle segregation during mitosis: lessons from asymmetrically dividing cells. *J Cell Biol* **196**: 305-13.
- OUYANG, Z. & LIANG, J. 2008. Predicting protein folding rates from geometric contact and amino acid sequence. *Protein Sci* **17**: 1256-63.
- PAHLAVANI, M.A., HARRIS, M.D., MOORE, S.A., WEINDRUCH, R. & RICHARDSON, A. 1995. The expression of heat shock protein 70 decreases with age in lymphocytes from rats and rhesus monkeys. *Exp Cell Res* **218**: 310-8.
- PAN, K.Z., PALTER, J.E., ROGERS, A.N., OLSEN, A., CHEN, D., LITHGOW, G.J. & KAPAH, P. 2007. Inhibition of mRNA translation extends lifespan in *Caenorhabditis elegans*. *Aging Cell* **6**: 111-9.
- PANDEY, U.B., NIE, Z., BATLEVI, Y., MCCRAY, B.A., RITSON, G.P., NEDELSKY, N.B., SCHWARTZ, S.L., DIPROSPERO, N.A., KNIGHT, M.A., SCHULDINER, O., PADMANABHAN, R., HILD, M., BERRY, D.L., GARZA, D., HUBBERT, C.C., YAO, T.P., BAEHRECKE, E.H. & TAYLOR, J.P. 2007. HDAC6 rescues neurodegeneration and provides an essential link between autophagy and the UPS. *Nature* **447**: 859-63.
- PASSMORE, L.A. & BARFORD, D. 2004. Getting into position: the catalytic mechanisms of protein ubiquitylation. *Biochem J* **379**: 513-25.
- PECHMANN, S., WILLMUND, F. & FRYDMAN, J. 2013. The ribosome as a hub for protein quality control. *Mol Cell* **49**: 411-21.
- PESTKA, S. 1971. Inhibitors of ribosome functions. *Annu Rev Microbiol* **25**: 487-562.
- PETROSKI, M.D. & DESHAIES, R.J. 2005. Function and regulation of cullin-RING ubiquitin ligases. *Nat Rev Mol Cell Biol* **6**: 9-20.
- PICKART, C.M. 2001. Mechanisms underlying ubiquitination. *Annu Rev Biochem* **70**: 503-33.
- PICKRELL, J.K., PAI, A.A., GILAD, Y. & PRITCHARD, J.K. 2010. Noisy splicing drives mRNA isoform diversity in human cells. *PLoS Genet* **6**: e1001236.
- POOLE, B. & WIBO, M. 1973. Protein degradation in cultured cells. The effect of fresh medium, fluoride, and iodoacetate on the digestion of cellular protein of rat fibroblasts. *J Biol Chem* **248**: 6221-6.
- POOLE, B., OHKUMA, S. & WARBURTON, M.J. 1977. The accumulation of weakly basic substances in lysosomes and the inhibition of intracellular protein degradation. *Acta Biol Med Ger* **36**: 1777-88.

- POTU, H., SGORBISSA, A. & BRANCOLINI, C. 2010. Identification of USP18 as an important regulator of the susceptibility to IFN-alpha and drug-induced apoptosis. *Cancer Res* **70**: 655-65.
- POWERS, E.T., MORIMOTO, R.I., DILLIN, A., KELLY, J.W. & BALCH, W.E. 2009. Biological and chemical approaches to diseases of proteostasis deficiency. *Annu Rev Biochem* **78**: 959-91.
- POWERS, R.W., 3RD, KAEBERLEIN, M., CALDWELL, S.D., KENNEDY, B.K. & FIELDS, S. 2006. Extension of chronological life span in yeast by decreased TOR pathway signaling. *Genes Dev* **20**: 174-84.
- PREISSLER, S. & DEUERLING, E. 2012. Ribosome-associated chaperones as key players in proteostasis. *Trends Biochem Sci* **37**: 274-83.
- PRINCIOTTA, M.F., FINZI, D., QIAN, S.B., GIBBS, J., SCHUCHMANN, S., BUTTGEREIT, F., BENNINK, J.R. & YEWDELL, J.W. 2003. Quantitating protein synthesis, degradation, and endogenous antigen processing. *Immunity* **18**: 343-54.
- QIAN, S.B., BENNINK, J.R. & YEWDELL, J.W. 2005. Quantitating defective ribosome products. *Methods Mol Biol* **301**: 271-81.
- QIAN, S.B., PRINCIOTTA, M.F., BENNINK, J.R. & YEWDELL, J.W. 2006. Characterization of rapidly degraded polypeptides in mammalian cells reveals a novel layer of nascent protein quality control. *J Biol Chem* **281**: 392-400.
- RANI, N., AICHEM, A., SCHMIDTKE, G., KREFT, S.G. & GROETTRUP, M. 2012. FAT10 and NUB1L bind to the VWA domain of Rpn10 and Rpn1 to enable proteasome-mediated proteolysis. *Nat Commun* **3**: 749.
- RAPE, M. 2009. Ubiquitin, infinitely seductive: symposium on the many faces of ubiquitin. *EMBO Rep* **10**: 558-62.
- REITS, E.A., VOS, J.C., GROMME, M. & NEEFJES, J. 2000. The major substrates for TAP in vivo are derived from newly synthesized proteins. *Nature* **404**: 774-8.
- ROGERS, A.N., CHEN, D., MCCOLL, G., CZERWIENIEC, G., FELKEY, K., GIBSON, B.W., HUBBARD, A., MELOV, S., LITHGOW, G.J. & KAPAHI, P. 2011. Life span extension via eIF4G inhibition is mediated by posttranscriptional remodeling of stress response gene expression in *C. elegans*. *Cell Metab* **14**: 55-66.
- ROSPERT, S., DUBAQUIE, Y. & GAUTSCHI, M. 2002. Nascent-polypeptide-associated complex. *Cell Mol Life Sci* **59**: 1632-9.
- ROSS, J.F. & ORLOWSKI, M. 1982. Growth-rate-dependent adjustment of ribosome function in chemostat-grown cells of the fungus *Mucor racemosus*. *J Bacteriol* **149**: 650-3.
- ROSSER, M.F., WASHBURN, E., MUCHOWSKI, P.J., PATTERSON, C. & CYR, D.M. 2007. Chaperone functions of the E3 ubiquitin ligase CHIP. *J Biol Chem* **282**: 22267-77.
- RUBINSZTEIN, D.C., MARINO, G. & KROEMER, G. 2011. Autophagy and aging. *Cell* **146**: 682-95.
- RUOTOLO, R., GRASSI, F., PERCUDANI, R., RIVETTI, C., MARTORANA, D., MARAINI, G. & OTTONELLO, S. 2003. Gene expression profiling in human age-related nuclear cataract. *Mol Vis* **9**: 538-48.

- SALCEDA, S. & CARO, J. 1997. Hypoxia-inducible factor 1alpha (HIF-1alpha) protein is rapidly degraded by the ubiquitin-proteasome system under normoxic conditions. Its stabilization by hypoxia depends on redox-induced changes. *J Biol Chem* **272**: 22642-7.
- SATO, S., WARD, C.L. & KOPITO, R.R. 1998. Cotranslational ubiquitination of cystic fibrosis transmembrane conductance regulator in vitro. *J Biol Chem* **273**: 7189-92.
- SAUER, R.T. & BAKER, T.A. 2011. AAA+ proteases: ATP-fueled machines of protein destruction. *Annu Rev Biochem* **80**: 587-612.
- SCHEFFNER, M., HUIBREGTSE, J.M., VIERSTRA, R.D. & HOWLEY, P.M. 1993. The HPV-16 E6 and E6-AP complex functions as a ubiquitin-protein ligase in the ubiquitination of p53. *Cell* **75**: 495-505.
- SCHEFFNER, M., NUBER, U. & HUIBREGTSE, J.M. 1995. Protein ubiquitination involving an E1-E2-E3 enzyme ubiquitin thioester cascade. *Nature* **373**: 81-3.
- SCHEFFNER, M. & KUMAR, S. 2014. Mammalian HECT ubiquitin-protein ligases: biological and pathophysiological aspects. *Biochim Biophys Acta* **1843**: 61-74.
- SCHMIDTKE, G., KALVERAM, B. & GROETTRUP, M. 2009. Degradation of FAT10 by the 26S proteasome is independent of ubiquitylation but relies on NUB1L. *FEBS Lett* **583**: 591-4.
- SCHOGGINS, J.W. & RICE, C.M. 2011. Interferon-stimulated genes and their antiviral effector functions. *Curr Opin Virol* **1**: 519-25.
- SCHUBERT, U., ANTON, L.C., GIBBS, J., NORBURY, C.C., YEWDELL, J.W. & BENNINK, J.R. 2000. Rapid degradation of a large fraction of newly synthesized proteins by proteasomes. *Nature* **404**: 770-4.
- SCHULMAN, B.A. & HARPER, J.W. 2009. Ubiquitin-like protein activation by E1 enzymes: the apex for downstream signalling pathways. *Nat Rev Mol Cell Biol* **10**: 319-31.
- SEBASTIAN, S. & LUBAN, J. 2005. TRIM5alpha selectively binds a restriction-sensitive retroviral capsid. *Retrovirology* **2**: 40.
- SELMAN, C., TULLET, J.M., WIESER, D., IRVINE, E., LINGARD, S.J., CHOUDHURY, A.I., CLARET, M., AL-QASSAB, H., CARMIGNAC, D., RAMADANI, F., WOODS, A., ROBINSON, I.C., SCHUSTER, E., BATTERHAM, R.L., KOZMA, S.C., THOMAS, G., CARLING, D., OKKENHAUG, K., THORNTON, J.M., PARTRIDGE, L., GEMS, D. & WITHERS, D.J. 2009. Ribosomal protein S6 kinase 1 signaling regulates mammalian life span. *Science* **326**: 140-4.
- SEN, G.C. & SARKAR, S.N. 2007. The interferon-stimulated genes: targets of direct signaling by interferons, double-stranded RNA, and viruses. *Curr Top Microbiol Immunol* **316**: 233-50.
- SHA, Z., BRILL, L.M., CABRERA, R., KLEIFELD, O., SCHELIGA, J.S., GLICKMAN, M.H., CHANG, E.C. & WOLF, D.A. 2009. The eIF3 interactome reveals the translatasome, a supercomplex linking protein synthesis and degradation machineries. *Mol Cell* **36**: 141-52.

- SHALGI, R., HURT, J.A., KRYKBAEVA, I., TAIPALE, M., LINDQUIST, S. & BURGE, C.B. 2013. Widespread regulation of translation by elongation pausing in heat shock. *Mol Cell* **49**: 439-52.
- SHAO, S., VON DER MALSBERG, K. & HEGDE, R.S. 2013. Listerin-dependent nascent protein ubiquitination relies on ribosome subunit dissociation. *Mol Cell* **50**: 637-48.
- SHOEMAKER, C.J. & GREEN, R. 2012. Translation drives mRNA quality control. *Nat Struct Mol Biol* **19**: 594-601.
- SHRINGARPURE, R. & DAVIES, K.J. 2002. Protein turnover by the proteasome in aging and disease. *Free Radic Biol Med* **32**: 1084-9.
- SINGH, R., KOLVRAA, S., BROSS, P., JENSEN, U.B., GREGERSEN, N., TAN, Q., KNUDSEN, C. & RATTAN, S.I. 2006. Reduced heat shock response in human mononuclear cells during aging and its association with polymorphisms in HSP70 genes. *Cell Stress Chaperones* **11**: 208-15.
- SKAUG, B. & CHEN, Z.J. 2010. Emerging role of ISG15 in antiviral immunity. *Cell* **143**: 187-90.
- SMEAL, T., CLAUS, J., KENNEDY, B., COLE, F. & GUARENTE, L. 1996. Loss of transcriptional silencing causes sterility in old mother cells of *S. cerevisiae*. *Cell* **84**: 633-42.
- SMIT, J.J. & SIXMA, T.K. 2014. RBR E3-ligases at work. *EMBO Rep* **15**: 142-54.
- SMITH, E.D., TSUCHIYA, M., FOX, L.A., DANG, N., HU, D., KERR, E.O., JOHNSTON, E.D., TCHAO, B.N., PAK, D.N., WELTON, K.L., PROMISLOW, D.E., THOMAS, J.H., KAEBERLEIN, M. & KENNEDY, B.K. 2008. Quantitative evidence for conserved longevity pathways between divergent eukaryotic species. *Genome Res* **18**: 564-70.
- SONTAG, E.M., VONK, W.I. & FRYDMAN, J. 2014. Sorting out the trash: the spatial nature of eukaryotic protein quality control. *Curr Opin Cell Biol* **26**: 139-46.
- SPRIGGS, K.A., BUSHELL, M. & WILLIS, A.E. 2010. Translational regulation of gene expression during conditions of cell stress. *Mol Cell* **40**: 228-37.
- STADTMAN, E.R., STARKE-REED, P.E., OLIVER, C.N., CARNEY, J.M. & FLOYD, R.A. 1992. Protein modification in aging. *EXS* **62**: 64-72.
- STEFFEN, K.K., MACKAY, V.L., KERR, E.O., TSUCHIYA, M., HU, D., FOX, L.A., DANG, N., JOHNSTON, E.D., OAKES, J.A., TCHAO, B.N., PAK, D.N., FIELDS, S., KENNEDY, B.K. & KAEBERLEIN, M. 2008. Yeast life span extension by depletion of 60s ribosomal subunits is mediated by Gcn4. *Cell* **133**: 292-302.
- STEVENS, T.J. & ARKIN, I.T. 2000. Do more complex organisms have a greater proportion of membrane proteins in their genomes? *Proteins* **39**: 417-20.
- STEWART, M.L., GROLLMAN, A.P. & HUANG, M.T. 1971. Aurintricarboxylic acid: inhibitor of initiation of protein synthesis. *Proc Natl Acad Sci U S A* **68**: 97-101.
- STREMLAU, M., OWENS, C.M., PERRON, M.J., KIESSLING, M., AUTISSIER, P. & SODROSKI, J. 2004. The cytoplasmic body component TRIM5alpha restricts HIV-1 infection in Old World monkeys. *Nature* **427**: 848-53.

- STREMLAU, M., PERRON, M., LEE, M., LI, Y., SONG, B., JAVANBAKHT, H., DIAZ-GRIFFERO, F., ANDERSON, D.J., SUNDQUIST, W.I. & SODROSKI, J. 2006. Specific recognition and accelerated uncoating of retroviral capsids by the TRIM5alpha restriction factor. *Proc Natl Acad Sci U S A* **103**: 5514-9.
- TAKEUCHI, T., INOUE, S. & YOKOSAWA, H. 2006. Identification and Herc5-mediated ISGylation of novel target proteins. *Biochem Biophys Res Commun* **348**: 473-7.
- TALIS, A.L., HUIBREGTSE, J.M. & HOWLEY, P.M. 1998. The role of E6AP in the regulation of p53 protein levels in human papillomavirus (HPV)-positive and HPV-negative cells. *J Biol Chem* **273**: 6439-45.
- TANAKA, K., WAXMAN, L. & GOLDBERG, A.L. 1983. ATP serves two distinct roles in protein degradation in reticulocytes, one requiring and one independent of ubiquitin. *J Cell Biol* **96**: 1580-5.
- TATAR, M., KHAZAELI, A.A. & CURTSINGER, J.W. 1997. Chaperoning extended life. *Nature* **390**: 30.
- TAYLOR, S.V., KELLEHER, N.L., KINSLAND, C., CHIU, H.J., COSTELLO, C.A., BACKSTROM, A.D., MCLAFFERTY, F.W. & BEGLEY, T.P. 1998. Thiamin biosynthesis in Escherichia coli. Identification of ThiS thiocarboxylate as the immediate sulfur donor in the thiazole formation. *J Biol Chem* **273**: 16555-60.
- THOREEN, C.C., KANG, S.A., CHANG, J.W., LIU, Q., ZHANG, J., GAO, Y., REICHLING, L.J., SIM, T., SABATINI, D.M. & GRAY, N.S. 2009. An ATP-competitive mammalian target of rapamycin inhibitor reveals rapamycin-resistant functions of mTORC1. *J Biol Chem* **284**: 8023-32.
- THOREEN, C.C., CHANTRANUPONG, L., KEYS, H.R., WANG, T., GRAY, N.S. & SABATINI, D.M. 2012. A unifying model for mTORC1-mediated regulation of mRNA translation. *Nature* **485**: 109-13.
- TURNER, G.C. & VARSHAVSKY, A. 2000. Detecting and measuring cotranslational protein degradation in vivo. *Science* **289**: 2117-20.
- VABULAS, R.M. & HARTL, F.U. 2005. Protein synthesis upon acute nutrient restriction relies on proteasome function. *Science* **310**: 1960-3.
- VAN DER REIJDEN, B.A., ERPELINCK-VERSCHUEREN, C.A., LOWENBERG, B. & JANSEN, J.H. 1999. TRIADs: a new class of proteins with a novel cysteine-rich signature. *Protein Sci* **8**: 1557-61.
- VAN DER VEEN, A.G. & PLOEGH, H.L. 2012. Ubiquitin-like proteins. *Annu Rev Biochem* **81**: 323-57.
- VAN WIJK, S.J. & TIMMERS, H.T. 2010. The family of ubiquitin-conjugating enzymes (E2s): deciding between life and death of proteins. *FASEB J* **24**: 981-93.
- VAYDA, M.E. 1995. Assessment of translational regulation by run-off translation of polysomes in vitro. *Methods Cell Biol* **50**: 349-59.
- VERMA, R., ARAVIND, L., OANIA, R., McDONALD, W.H., YATES, J.R., 3RD, KOONIN, E.V. & DESHAIES, R.J. 2002. Role of Rpn11 metalloprotease in deubiquitination and degradation by the 26S proteasome. *Science* **298**: 611-5.

- VERMA, R., OANIA, R.S., KOLAWA, N.J. & DESHAIES, R.J. 2013. Cdc48/p97 promotes degradation of aberrant nascent polypeptides bound to the ribosome. *Elife* **2**: e00308.
- VERNACE, V.A., ARNAUD, L., SCHMIDT-GLENEWINKEL, T. & FIGUEIREDO-PEREIRA, M.E. 2007. Aging perturbs 26S proteasome assembly in *Drosophila melanogaster*. *FASEB J* **21**: 2672-82.
- VERSTEEG, G.A., HALE, B.G., VAN BOHEEMEN, S., WOLFF, T., LENSCHOW, D.J. & GARCIA-SASTRE, A. 2010. Species-specific antagonism of host ISGylation by the influenza B virus NS1 protein. *J Virol* **84**: 5423-30.
- VOISINE, C., PEDERSEN, J.S. & MORIMOTO, R.I. 2010. Chaperone networks: tipping the balance in protein folding diseases. *Neurobiol Dis* **40**: 12-20.
- WALKER, G.A. & LITHGOW, G.J. 2003. Lifespan extension in *C. elegans* by a molecular chaperone dependent upon insulin-like signals. *Aging Cell* **2**: 131-9.
- WANG, F., DURFEE, L.A. & HUIBREGTSE, J.M. 2013. A cotranslational ubiquitination pathway for quality control of misfolded proteins. *Mol Cell* **50**: 368-78.
- WANG, L., DONG, H., SOROKA, C.J., WEI, N., BOYER, J.L. & HOCHSTRASSER, M. 2008. Degradation of the bile salt export pump at endoplasmic reticulum in progressive familial intrahepatic cholestasis type II. *Hepatology* **48**: 1558-69.
- WAXMAN, L., FAGAN, J.M. & GOLDBERG, A.L. 1987. Demonstration of two distinct high molecular weight proteases in rabbit reticulocytes, one of which degrades ubiquitin conjugates. *J Biol Chem* **262**: 2451-7.
- WELCHMAN, R.L., GORDON, C. & MAYER, R.J. 2005. Ubiquitin and ubiquitin-like proteins as multifunctional signals. *Nat Rev Mol Cell Biol* **6**: 599-609.
- WENZEL, D.M., LISSOUNOV, A., BRZOVIC, P.S. & KLEVIT, R.E. 2011. UBC7 reactivity profile reveals parkin and HHARI to be RING/HECT hybrids. *Nature* **474**: 105-8.
- WERNEKE, S.W., SCHILTE, C., ROHATGI, A., MONTE, K.J., MICHAULT, A., ARENZANA-SEISDEDOS, F., VANLANDINGHAM, D.L., HIGGS, S., FONTANET, A., ALBERT, M.L. & LENSCHOW, D.J. 2011. ISG15 is critical in the control of Chikungunya virus infection independent of Ube1L mediated conjugation. *PLoS Pathog* **7**: e1002322.
- WHEATLEY, D.N., GIDDINGS, M.R. & INGLIS, M.S. 1980. Kinetics of degradation of "short-" and "long-lived" proteins in cultured mammalian cells. *Cell Biol Int Rep* **4**: 1081-90.
- WILLIAMSON, D.S., BORGOGNONI, J., CLAY, A., DANIELS, Z., DOKURNO, P., DRYSDALE, M.J., FOLOPPE, N., FRANCIS, G.L., GRAHAM, C.J., HOWES, R., MACIAS, A.T., MURRAY, J.B., PARSONS, R., SHAW, T., SURGENOR, A.E., TERRY, L., WANG, Y., WOOD, M. & MASSEY, A.J. 2009. Novel adenosine-derived inhibitors of 70 kDa heat shock protein, discovered through structure-based design. *J Med Chem* **52**: 1510-3.
- WILLMUND, F., DEL ALAMO, M., PECHMANN, S., CHEN, T., ALBANESE, V., DAMMER, E.B., PENG, J. & FRYDMAN, J. 2013. The cotranslational function of ribosome-associated hsp70 in eukaryotic protein homeostasis. *Cell* **152**: 196-209.

- WOLF, D.H. & HILT, W. 2004. The proteasome: a proteolytic nanomachine of cell regulation and waste disposal. *Biochim Biophys Acta* **1695**: 19-31.
- WOLFF, S., WEISSMAN, J.S. & DILLIN, A. 2014. Differential scales of protein quality control. *Cell* **157**: 52-64.
- WONG, P., FRITZ, A. & FRISHMAN, D. 2005. Designability, aggregation propensity and duplication of disease-associated proteins. *Protein Eng Des Sel* **18**: 503-8.
- XU, G., PAIGE, J.S. & JAFFREY, S.R. 2010. Global analysis of lysine ubiquitination by ubiquitin remnant immunoaffinity profiling. *Nat Biotechnol* **28**: 868-73.
- XU, P., DUONG, D.M., SEYFRIED, N.T., CHENG, D., XIE, Y., ROBERT, J., RUSH, J., HOCHSTRASSER, M., FINLEY, D. & PENG, J. 2009. Quantitative proteomics reveals the function of unconventional ubiquitin chains in proteasomal degradation. *Cell* **137**: 133-45.
- YAO, T. & COHEN, R.E. 2002. A cryptic protease couples deubiquitination and degradation by the proteasome. *Nature* **419**: 403-7.
- YE, Y. 2006. Diverse functions with a common regulator: ubiquitin takes command of an AAA ATPase. *J Struct Biol* **156**: 29-40.
- YE, Y. & RAPE, M. 2009. Building ubiquitin chains: E2 enzymes at work. *Nat Rev Mol Cell Biol* **10**: 755-64.
- YEWDELL, J.W., ANTON, L.C. & BENNINK, J.R. 1996. Defective ribosomal products (DRiPs): a major source of antigenic peptides for MHC class I molecules? *J Immunol* **157**: 1823-6.
- YEWDELL, J.W. & NICCHITTA, C.V. 2006. The DRiP hypothesis decennial: support, controversy, refinement and extension. *Trends Immunol* **27**: 368-73.
- YUAN, W. & KRUG, R.M. 2001. Influenza B virus NS1 protein inhibits conjugation of the interferon (IFN)-induced ubiquitin-like ISG15 protein. *EMBO J* **20**: 362-71.
- ZENG, W., SUN, L., JIANG, X., CHEN, X., HOU, F., ADHIKARI, A., XU, M. & CHEN, Z.J. 2010. Reconstitution of the RIG-I pathway reveals a signaling role of unanchored polyubiquitin chains in innate immunity. *Cell* **141**: 315-30.
- ZHANG, G. & IGNATOVA, Z. 2009. Generic algorithm to predict the speed of translational elongation: implications for protein biogenesis. *PLoS One* **4**: e5036.
- ZHAO, C., BEAUDENON, S.L., KELLEY, M.L., WADDELL, M.B., YUAN, W., SCHULMAN, B.A., HUIBREGTSE, J.M. & KRUG, R.M. 2004. The UbcH8 ubiquitin E2 enzyme is also the E2 enzyme for ISG15, an IFN-alpha/beta-induced ubiquitin-like protein. *Proc Natl Acad Sci U S A* **101**: 7578-82.
- ZHAO, C., DENISON, C., HUIBREGTSE, J.M., GYGI, S. & KRUG, R.M. 2005. Human ISG15 conjugation targets both IFN-induced and constitutively expressed proteins functioning in diverse cellular pathways. *Proc Natl Acad Sci U S A* **102**: 10200-5.
- ZHAO, C., HSIANG, T.Y., KUO, R.L. & KRUG, R.M. 2010. ISG15 conjugation system targets the viral NS1 protein in influenza A virus-infected cells. *Proc Natl Acad Sci U S A* **107**: 2253-8.
- ZHAO, C., COLLINS, M.N., HSIANG, T.Y. & KRUG, R.M. 2013. Interferon-induced ISG15 pathway: an ongoing virus-host battle. *Trends Microbiol* **21**: 181-6.

- ZHENG, N., WANG, P., JEFFREY, P.D. & PAVLETICH, N.P. 2000. Structure of a c-Cbl-UbcH7 complex: RING domain function in ubiquitin-protein ligases. *Cell* **102**: 533-9.
- ZHOU, M., FISHER, E.A. & GINSBERG, H.N. 1998. Regulated Co-translational ubiquitination of apolipoprotein B100. A new paradigm for proteasomal degradation of a secretory protein. *J Biol Chem* **273**: 24649-53.
- ZID, B.M., ROGERS, A.N., KATEWA, S.D., VARGAS, M.A., KOLIPINSKI, M.C., LU, T.A., BENZER, S. & KAPAHI, P. 2009. 4E-BP extends lifespan upon dietary restriction by enhancing mitochondrial activity in *Drosophila*. *Cell* **139**: 149-60.
- ZOU, W. & ZHANG, D.E. 2006. The interferon-inducible ubiquitin-protein isopeptide ligase (E3) EFP also functions as an ISG15 E3 ligase. *J Biol Chem* **281**: 3989-94.

Vita

Feng Wang was born in Guilin, People's Republic of China. He is the son of Fuqiang Wang and Jinyu Bai. In Jun. 2005, he graduated from Xiamen University, China, with a Bachelor of Science degree in Biology. He received his Master of Science degree in 2008 in Dr. Xiang Xiao's lab at the same university. In 2008, he came to U.S for his graduate education in Microbiology program in the University of Texas at Austin. In 2009, he joined Dr. Jon Huibregtse's lab for his doctoral studies.

Permanent email: fengwang@utexas.edu

This dissertation was typed by Feng Wang.